

**PLASMA ENHANCED CHEMICAL VAPOUR DEPOSITION OF**  
**THIN CARBON FILMS**

**Author Patrick Carey, B Sc ,**

**Submitted for the award of**  
**Master of Engineering**

**Supervisor**  
**David Cameron, Ph.D**

**School of Electronic Engineering,**  
**Dublin City University**

**September 1989**

I hereby declare that the contents of this thesis are based  
on my own research

Signed,

A handwritten signature in black ink that reads "Patrick Carey". The signature is written in a cursive style with a long horizontal flourish at the end.

**Patrick Carey**

## **ABSTRACT**

There have been considerable developments in the field of hard carbon thin film deposition in the past decade. The films show properties of extreme hardness, chemical inertness and optical transparency and their use has been suggested for wear protective coatings. The results presented here concern the use of Plasma Enhanced Chemical Vapour Deposition (PECVD) to produce these films. Details of the effects of the important deposition parameters on their mechanical properties are presented.

The deposition system design and implementation are described. The resultant film characteristics are presented graphically as a function of the deposition variables. Films were produced which exhibited extreme hardness of up to 3000 Vickers. Their deposition rate was found to decrease with substrate temperature and increase with induced bias and pressure. The intrinsic stress and wear resistance were found to increase with the induced bias and substrate temperature but decreased as the pressure was increased. The film adhesion was found to improve at higher temperature and bias and also at higher pressure but films in this region were found to be of reduced hardness.

The intrinsic stress and poor adhesion of carbon films were identified as the main difficulties in the application of these films as wear protective coatings. Possible ways of improving these film characteristics were investigated.

The main deposition variables of substrate temperature, induced bias and pressure were identified, along with the possible optimisation of carbon thin film characteristics by control of the deposition environment.

## ACKNOWLEDGEMENTS

I would like to thank the following people

To David Cameron, my supervisor, for his advice and enthusiasm

To Michael Ahern, of Donnelly Mirrors Ltd, for his cooperation and friendship

To Collette Nugent, my typist, for her patience and time

To my colleagues and friends in the university, especially Martin Collier, for their support and encouragement.

And a special thanks to my Parents and Doretta, for all their love

## CONTENTS

### **Chapter One – Introduction**

1 1	Introduction	1
1 2	Plasma Assisted Deposition Processes	1
1 3	Thin Films	3
1 4	Categorisation of Films	3
1 5	Historical Background to Thin Film Preparation	6
1 6	Review of Literature	8
1 7	Possible Areas of Development	
	Identified from the Literature Review	11

### **Chapter Two – Plasma Theory**

2 1	Origin of Plasmas	12
2 2	Glow Discharge Plasma	13
2 3	Events which occur at the Cathode	18
2 4	Events which occur in the Dark Space	19
2 5	The Negative Glow	21
2 6	Radio Frequency Gas Discharge	28

### **Chapter Three – Theory of Film Deposition**

3 1	Introduction to Film Deposition	35
3 1 1	Vacuum Technology	35
3 1 2	Physical Vapour Deposition	35
3 1 3	PVD Processes	37
3 1 4	Chemical Vapour Deposition	39
3 2	Plasma Enhanced Chemical Vapour Deposition	39
3 2 1	Introduction	39
3 2 2	General Features of Plasma Deposition	43
3 2 3	Deposition Variables	44
3 2 4	Plasma Volume Reactions	45

### **Chapter Four – Nature of Thin Films**

4 1	The Free Surface	49
4 2	Film Growth	50
4 2 1	Adsorption and Nucleation Processes	50
4 2 2	The Four Stages of Film Growth	53
4 3	Surface Reactions	55
4 3 1	Ion Bombardment	55
4 3 2	Electron Bombardment	57
4 3 3	Preferential Sputtering and Initial Etching	

in an R F Plasma	57
4 3 4 Role of Hydrogen	60
4 4 Structures of Carbon Forms	62
4 4 1 Introduction	62
4 4 2 The Carbon Atom and the Nature of the Carbon–Carbon Bond	62
4 4 3 Structure of Carbons	63
4 4 4 Structure of Polymers	65
4 5 Structure of Thin Films	67
4 5 1 Deposition Rate	67
4 5 2 Pressure, Temperature, and Surface Roughness	67
4 5 3 Influence of Substrate Bias	69
4 6 Stresses in Thin Films	71
4 7 Adhesion of Thin Films	74
4 7 1 Control of Adhesion	75

## **Chapter Five – Design and Implementation of Plasma Deposition System**

5 1 Types of Deposition Reactors	76
5 2 Components of PECVD System	78
5 3 Design Criteria for Deposition System	81
5 4 Initial Trial Reactor	82
5 4 1 Deposition Apparatus	83
5 5 R F Power Generator	84
5 5 1 Specifications	84
5 5 2 Impedance Matching	85
5 5 3 Complex Loads	86
5 5 4 Matching to Coaxial Feedlines	87
5 6 Design of Components in Carbon Film Deposition System	88
5 6 1 R F Shielding	88
5 6 2 Pumping System	89
5 6 3 Inlet Gas Control and Mixing	89
5 6 4 Chamber Geometry	90
5 6 5 Substrate Holder and Heater	91
5 6 6 Gas Inlet Nozzle	92
5 6 7 Parameter Control and Monitoring	92
5 7 Substrate Preparation	94
5 7 1 Introduction	94
5 7 2 Thermal and Mechanical Considerations	94
5 7 3 Choice of Substrates	94
5 7 4 Substrate Cleaning	95

<b>Chapter Six – Results</b>	
6 1	Growth Rate of Films 97
6 2	Stress of Thin Films 100
6 3	Adhesion of Films 104
6 4	Effect of Deposition Parameters on the Mechanical Properties of Thin Carbon Films 108
6 5	Summary of Results on the Mechanical Properties of Thin Carbon Films 112
6 6	Composition and Structure of Carbon Films 113
6 6 1	Infra-Red Spectroscopy 113
6 6 2	X-Ray Diffraction 118
6 7	Plasma Gas Species 119
 <b>Chapter Seven – Discussions</b>	
7 1	Introduction 121
7 2	Effect of Substrate Temperature 121
7 3	Effect of Induced Bias 123
7 4	Effect of Total Pressure 124
7 5	Chamber Geometry 125
7 6	Formation of Carbides 126
7 7	Optimum Conditions 126
 <b>Chapter Eight – Conclusions</b>	
8 1	Conclusions 127
 <b>Chapter Nine – Recommendations</b>	
9 1	Introduction 130
9 2	Deposition System 130
9 3	Deposition Process 131
9 4	Film Analysis 131
 <b>References</b>	 133
 <b>Appendix A</b>	 140
<p style="text-align: center;">Paper Presented to the 6<sup>th</sup> Irish Manufacturing Conference  August 1989 entitled  "Plasma Deposition of Hard Carbon Films as Wear Protective Coatings"</p>	

# CHAPTER 1

## INTRODUCTION

### 1.1 Introduction

Thin films can be used to protect or enhance the properties of the underlying material called the substrate. They can be used for a variety of reasons either decorative, mechanical, electrical, optical or chemical [1-3].

The particular area of interest is in the plasma deposition of hard carbon films as wear protective coatings. Due to the increasing costs of raw materials, ways of prolonging the life of material or attributing to cheap materials the characteristics of an expensive bulk material is becoming increasingly important. Researchers have produced carbon films of hardness exceeding 3000 HV. Abrasive wear rate is inversely proportional to the hardness of the material, so these films would make excellent wear protective coatings. The unusual combination of density, hardness, chemical inertness, optical transparency and electrical characteristics make carbon films a very interesting area of study as wear protective coatings and other applications [4-7].

The aims of this project are to design and build a system capable of depositing these films. Together with the deposition system there must also be a film evaluation procedure to relate the film qualities with system parameter settings.

Carbon thin films have been produced by researchers on a limited basis using various methods such as Plasma Enhanced Chemical Vapour Deposition (PECVD) [8-14], Direct Current (DC) and Radio Frequency (RF) plasmas [15-17], Laser induced plasma [18], Electron beam assisted [19-20], Ion beam methods [21-28] and Microwave plasma [29]. It is the intention to produce "state of the art" films and identify the influence of the most important deposition parameters on the resultant film properties.

### 1.2 Plasma-Enhanced Deposition Processes

A plasma is defined as an ionised gas. It is often described as the fourth state of matter. Plasma Enhanced Chemical Vapour Deposition [30] facilitates the deposition of many types of films at much lower temperatures than would be possible with chemical vapour deposition alone.

Plasma-enhanced deposition processing is done using electric discharge plasmas in which the energy to sustain the ionised state is supplied by an externally applied electric field. Most of the applications involve the use of low pressure (glow

discharge) plasmas. The energetic species in these plasmas are the free electrons. They gain energy from the electric field faster than the ions do and are thermally isolated from the atoms and molecules, as far as elastic collisions are concerned, by the mass difference. Consequently, the electrons accumulate sufficient kinetic energy to undergo inelastic collisions and to sustain the ionisation, while the heavy particle (molecule) temperature remains low.

In PECVD reactant gases are passed through an active glow discharge plasma. A typical deposition arrangement [31] is shown in figure 1.1 which is a parallel plate type. This is most frequently used because of its ease of construction and good film properties i.e. coverage, uniformity, etc. The voltage division between the plasma and the rf driven electrodes depends to first order on their relative sizes, the voltage is largest for the smaller electrode. Plasma bombardment can have an important influence on the properties of the growing coatings.

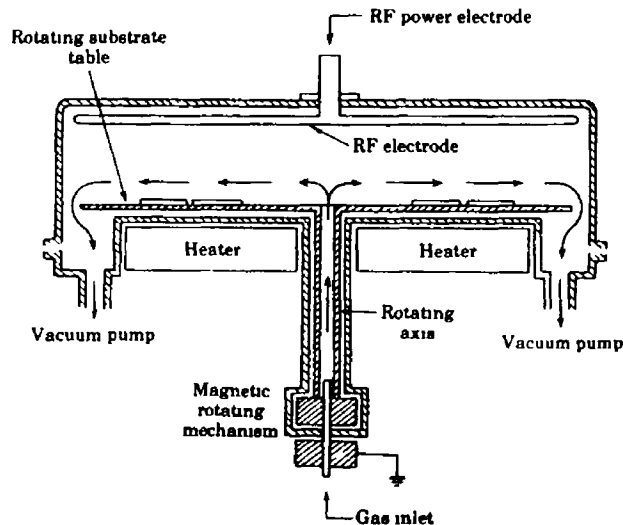


Figure 1.1 Capacitive Coupling Type

The deposition process for carbon films can be divided into two categories: those that use hydrocarbon gases as a source of carbon and those that use solid carbon itself. The latter involves a sputtering technique utilizing high energy ion beams, lasers, pulsed discharges etc. The former technique is by far more common and is the one that concerns us.

Dense films have been grown from hydrocarbon gases using a variety of rf and dc discharge reactors. The hydrocarbon source gases that have been used are methane, ethane, butane, propane, acetylene, ethylene, propylene, cyclohexane, octane, decane, benzene, xylene, naphthalene, and probably others. Very little analysis has been made of the plasma products. Most researchers take the black box approach to the

reaction, concentrating on the variables and relating the resultant films to their selection of parameters. The substrate is generally placed on the small electrically powered electrode where it acquires a negative d.c. self-bias, and so preferentially attracts positive ions and molecules [32].

### 1.3 Thin Films

The first evaporated thin films are often attributed to Faraday [33] in 1857, when he exploded metal wires in an inert atmosphere. Since then thin film technology has become one of the fastest growing areas of technology. Thin film applications can be found in optical, electronics, chemical, and mechanical areas.

Advantages of using a film on a substrate are either to protect the substrate from external forces or attribute to the substrate properties of a more precious or rare material. The particular area of interest for this project is in materials science. It is estimated that in the United States 100 billion dollars worth of damage is done to equipment annually by wear alone [34]. Diamond-like films are extremely hard, resistant to wear, waterproof and transparent. Machine tools, razor blades and bearings coated with a thin layer of harder material have lasted up to a hundred times longer than ones without [35]. Diamond-coated glass in windows or optical instruments would not get scratched or degrade. Diamond coatings have already been applied to magnetic storage media to prevent damage from the reading head [1]. Thin films are typically of the order of tens of angstroms up to tens of microns with average thicknesses for wear protective coatings being typically 5  $\mu\text{m}$ .

### 1.4 Categorisation of Films

The extremely varied methods of preparation have produced, as might be expected, films with a very broad spectrum of properties. This variation reflects differences in structure and elemental composition, which in turn depend upon the details of the method of preparation.

Some authors such as Angus [36] proposed that carbon films be classed according to their gram atom number densities,  $\rho_n$  and their atomic composition. The gram atom number densities,  $\rho_n$  is just the total number of gram atoms per unit volume

$$\rho_n = \rho_m / \sum X_i A_i \quad (1.1)$$

where  $\rho_m$  is the mass density,  $X_i$  the atom fraction and  $A_i$  the atomic mass of

element 1. In figure 1.2  $\rho_n$  is plotted as a function of the atom fraction of hydrogen for a variety of carbonaceous solids. The materials on the upper part of figure 1.2 represent those films of number densities greater than 0.2 g-atom per  $\text{cm}^3$  and show the spread in densities from various researchers.

The position of diamond (D) and adamantane (AD) should be noted in figure 1.2. Adamantane is a fully hydrogen-saturated microcrystal of diamond containing ten carbon atoms. The dense carbon and hydrocarbon films fall in the region between these two extreme cases. The graph illustrates just how unusual this is. There are no other carbon or hydrocarbon structures with such high number densities.

The position of conventional "plasma polymers" hydrocarbon films (PP) is also of interest. These appear to have a greater number density than conventional hydrocarbon polymers and may be considered to be part of the dense hydrocarbon grouping. The other solid carbon phases, which are based either on a graphitic, trigonal structure or completely unsaturated carbon chains, all fall at number densities well below 0.2 g atom per  $\text{cm}^3$ . The aromatic hydrocarbons (e.g. benzene, naphthalene, and anthracene), the linear saturated hydrocarbons (e.g. polyethylene and dodecane) and the unsaturated hydrocarbons (e.g. polyacetylene, hexatriene, and butadiene) fall together in groupings at number densities significantly less than 0.2 g-atoms per  $\text{cm}^3$ .

There has been no consistent nomenclature for describing these unusual hydrocarbon and carbon films. A variety of names have been used e.g. diamond-like films, hard carbonaceous films, hard carbon, a-C:H, and 1-carbon. Often different names have been used to describe very similar materials and conversely, the same name used to describe very different materials.

The figure 1.2 provides a rational basis for the naming of the films. Films with  $\rho_n > 0.2$  are designated "dense carbonaceous films". Films containing significant amounts of hydrogen are called "dense hydrocarbon films". The abbreviation a-C:H will also be used to describe these latter films when it is clear that they are amorphous. Films that are essentially pure carbon will be called "dense carbon" if  $\rho_n > 0.2$  g-atom per  $\text{cm}^3$ .

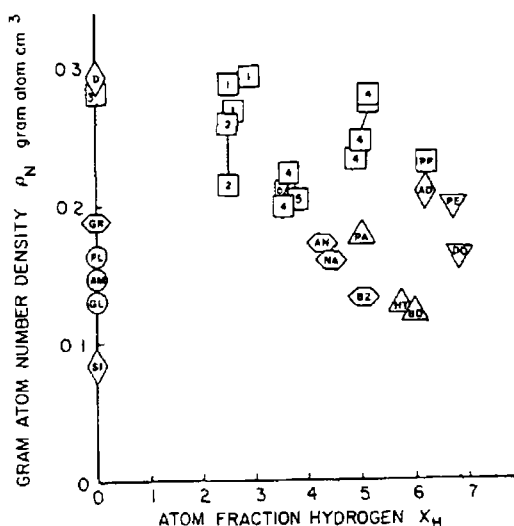


Figure 12 Gram atom number density vs atom fraction of hydrogen [36]

In the above figure the numbers 1-6 represent the spread of "Diamond-like" solids found by researchers. Other phases: AD, adamantane, AM, amorphous carbon, DO, dodecane, AN, anthracene, BD, butadiene, BZ, benzene, D, diamond, GL, glassy polyethylene, PL, polyene, PP, plasma polymers, Si, silicon. The numbers correspond to the spread in results from various researchers.

The term "diamond-like" has been widely used by many authors because of the obvious similarities in properties between the films and diamond. If it is applied, it clearly should be restricted to films of  $\rho_N > 0.2$  g-atom per  $\text{cm}^3$ .

The term "i-carbon" or "i-C" has been suggested by Weissmantel [37]. The i refers to the fact that the films are usually made by deposition of accelerated ions. This nomenclature appears somewhat less appropriate. For example, in sputter deposition the impacting species are largely neutral. Also, many authors claim processes which do not involve significant numbers of ionised species.

The term "hard carbonaceous" has also been suggested and used widely. The designation, while appropriate in many cases, could also apply to the hard, trigonally bonded films produced by evaporation. Also hardness is difficult to quantify, especially, for thin films.

## 1.5 Historical Background To Thin Film Preparation

Man has always tried ways of improving the physical properties of the materials [38] he works with or just to enhance their appearance. In an age of ever increasing prices for raw materials and the search to push technology to its limit, new materials must be found so that the continued expansion of the human empire is possible.

As mentioned, Faraday is claimed to have deposited the first film by evaporating a tungsten wire in an inert atmosphere. Thin film technology has expanded rapidly in the past 100 years. Chemical Vapor Deposition (CVD) has been around for many years. The process whereby gases are heated to very high temperatures, dissociating and forming a solid phase which condenses onto a targeted area or substrate. Physical Vapour Deposition (PVD) is a process whereby a solid or liquid is vapourised.

Both of these thin film processes have limitations and advantages as will be discussed in section 3.1. PECVD is a hybrid process taking the advantages of both processes.

Although the quest for diamond growth [39] from a low pressure vapour started at least as far back as 1911, in Germany, by W. Von Bolton [40], it was not until 1955 that this effort intensified. During that year the General Electric [41] process for making industrial diamonds at high pressures and high temperatures was announced, and Bridgman soon followed with an article in *Scientific American* [42], speculating that diamond powders and films should be equally achievable at low pressures during deposition.

The first attempts by Eversole [43] in 1958 of Union Carbide were extremely slow and impractical and the evidence for diamond film growth was meager. This process was studied in detail in the 1960's and 1970's by Angus [44] and co-workers at Case Western Reserve University. Eversole's findings were fully confirmed but the low growth rates ( $0.001 \mu\text{m h}^{-1}$ ) were not substantially increased. The various techniques developed relied on a two-step process of first producing a layer with a small percentage (less than 1%) of diamond bonds and second removing the much larger percentage of graphitically bonded material by a selective hydrogen reduction process at a high temperature and pressure. The process was repeated many times to produce a single film (on diamond powder) with enough material for analysis.

Derjaguin, Fedoseen, Spitsyn and co-workers [45] at the Institute of Physical Chemistry in Moscow also heeded the work of Eversole in conjunction with some

earlier predictions of growing diamonds by Lejnunskij and Frank-kameneckij. During the course of their studies starting in the mid-1950's, they investigated the kinetics of the pyrolysis of various hydrocarbon-hydrogen gas mixtures, including methane-hydrogen, and the mechanisms of nucleation and growth of diamond on diamond seed crystals.

During their research, the Russian workers began to realise the importance of atomic hydrogen as a selective etchant, for removing graphite but not diamond, and its utility to dissolve continuously any graphite that forms during deposition. It became clear that to accelerate diamond growth, it was necessary to introduce even higher concentrations of atomic hydrogen than the equilibrium concentration related to the thermal dissociation of hydrocarbon-hydrogen gases. This important breakthrough came about 1976 by Derjaguin and Fedoseen. They published a book entitled "Growth of Diamond and Graphite from the Gas Phase" in which they outlined three different methods for producing a superequilibrium of atomic hydrogen: catalytic, electric discharge, and heated tungsten filament (HF).

They used a chemical vapour transport process in a closed tube to which an unspecified electric discharge was used to generate the necessary atomic hydrogen. They produced scanning electron micrographs of large crystals (up to 30  $\mu\text{m}$ ) and highly faceted thick continuous films were seen alongside the confirming electron diffraction data. This was followed immediately by an a.c. plasma discharge technique in a flowing gas system used by Mania et al [46], and the HF chemical vapour deposition (HF CVD) approach was taken by Matsumoto [15,47] and co-workers in Japan. He showed in detail that the concentration of methane in the methane-hydrogen gas mixture must be about 1% to get optimum diamond growth. Most subsequent work confirms this curious result: use copious amounts of hydrogen to produce diamond with very little, if any, hydrogen. This group of researchers have published many papers in areas of HF CVD, microwave plasma CVD and r.f. PECVD.

The term "diamond-like-carbon" was coined by Aisenberg and Chabot [48] in 1971, it covers a wide range of materials including both amorphous and microcrystalline atomic structures and containing anywhere from 0% to more than 30% hydrogen. True diamond can only be considered when the hydrogen content is less than 1%. This has recently been achieved by Spencer et al [21], which showed TEM micrographs of fine grained diamond structure.

There is a huge amount of interest in  $\text{r}$ -carbon in the Soviet Union. One claim is to have produced diamond film up to a centimeter thick [2]. This would seem impossible due to internal stress limitations.

## 1 6 Review of Literature

In the past twenty years the interest in so-called diamond like carbon or i-C films has grown enormously, at least 5,000 articles published in the past ten years alone [3-5]. These films are produced by ionizing a hydrocarbon compound, which is possibly dissociated and accelerated in an electric field towards the substrate where the film is grown. The deposition takes place at a moderately low pressure. Carbon films grown in this way have some remarkable properties: they are insulating ( $10^7$ - $10^{14}$   $\Omega$  cm) and have a negative temperature coefficient of conductivity ( $10^{-2}$   $^{\circ}\text{C}^{-1}$ ) [49], a high dielectric strength (breakdown voltage of about  $10^6$   $\text{Vcm}^{-1}$ ), a dielectric constant of 8 - 12 [50], extreme hardness (a microhardness of 3000 HV or more, chemical inertness towards acids and organic solvents [51], an optical bandgap of 1-2 eV [52], the possibility of being doped with either n-type or p-type dopants [53], a density of about  $2 \text{ g cm}^{-3}$  and a refractive index of 2 - 2.8 [54].

Such films have found applications as dielectrics in the electronics industry and as protective coatings for metals, for other surfaces such as silicon and for silicon devices. Hard coatings with a low coefficient of friction have become increasingly interesting in mechanical devices where high wear resistance and dry lubricating properties make them well suited in applications where oils and greases cannot be used. Depending on the fabrication process, the properties of the film will vary from ones similar to those of bulk diamond to ones similar to those of amorphous carbon. The reader is referred to several excellent reviews namely that by Lars-Peter Anderson [4]. The various properties of the films are outlined by Enke [55], with particular reference to their use as metallurgical and protective coatings.

The main area of literature searching was concentrated on the deposition process and the film properties dependence on experimental parameters. Along with the process, evaluating the resultant films properties is critical in establishing the best parameter setting for an ideal film. So, a large amount of papers have been written on thin film evaluation both structurally and characteristically i.e. adhesion, stress, hardness.

Most researchers use the two parallel plates arrangement and capacitively couple the rf power into the chamber. A detailed reasoning for choosing this method will be given later. Rf power, bias voltage of the powered electrode, gas pressure and deposition temperature can all be measured and controlled independently. These properties and additional parameters that are fixed for a given system (geometry, frequency), determine the deposition process and the film properties. The reactor geometry, i.e. basically the ratio of capacitively coupled electrode surface area (Cathode

Ac) to the grounded part of the system (Anode Aa), is of importance for potential distribution. The ratio of the sheath potentials over the cathode and anode hard space ( $V_{sc}$  and  $V_{sa}$  respectively) depends on electrode [30] areas as will be shown in Section 2.6.

This electrode area geometry develops an asymmetric voltage distribution between the plates, which is important for the sheath potential between plasma and the powered electrode, and is given by measuring the negative self-bias. The plasma is "focussed" onto the small powered electrode, therefore deposition is almost totally onto this electrode. Due to the high negative self-bias, the acceleration potential is lower for the electrons in comparison to the positive ions. Therefore, the electron contribution to the power dissipated on the substrate is negligible. Larger particles such as dust charge up negatively and so are repelled from the substrate, thus preventing pin-holes developing in the film.

There has been a wide spectrum of hydrocarbon gases used as a precursor material. Anderson and Berg [56] used alkanes,  $C_mH_{2m+2}$ , from methane to butane and found an almost linear increase of the deposition rate with  $m$ . Methane has been suggested because it can dissociate into only a few types of radicals. Also, since no double C bonds are present it will not form polymers so readily. Two factors appear to be responsible for this dependence. With increasing molecular weight the ionization probability increases. Together with the larger carbon content per ion, this leads to an increased carbon flux towards the substrate.

D. Nir and R. Walsh [57] tried ways of reducing the hydrogen content of the films which they said was the main cause of stress. Since, graphite oxidises at 400 °C and diamond at 800 °C, they heated the sample to greater than 400 °C, and added oxygen in the form of  $CO_2$  to preferentially burn out the graphite which replaced some of the hydrogen with oxygen. Hydrogen was also added to the reaction to achieve low hydrogen content films.

The impact energy is physically the most important parameter in the deposition of dense hydrocarbon films. It is normally lower than the sheath potential. Thus bias potentials around 1000 eV are needed to provide the optimum impact energy for dense hydrocarbon formation.

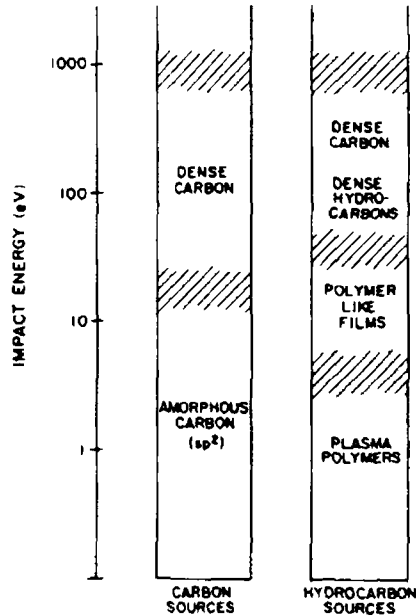


Figure 13 Influence of impact energy on type of film produced.

Bubenzner et al [58] demonstrated the dependence of the mean impact energy on both bias potential and pressure. In their benzene rf discharge the proportionality was found to be,

$$E \sim V_B P^{-1/2} \quad (12)$$

where

E = mean impact energy

$V_B$  = bias voltage

P = overall pressure

Since the ion energy is not directly measurable in rf systems, most workers used the discharge power and hydrocarbon pressure to control the deposition process and the film properties. In fact, the negative bias voltage and pressure have been shown to effect film properties such as density, hydrogen content, and refractive index. Parameter and film properties have an intricate interdependency.

A possible area of development is in finding an optimum parameter level for the best film. Enke [55], carried out extensive tests on parameter interdependence.

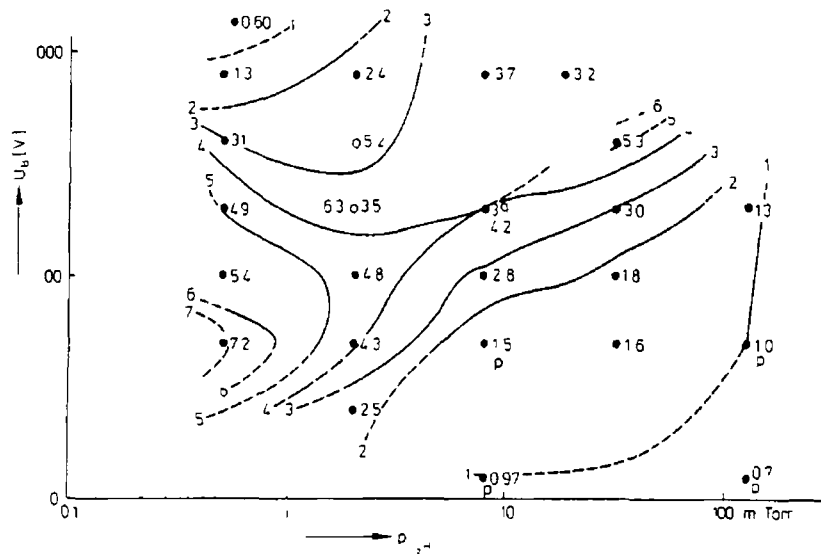


Figure 14 Curves of equal compressive stress of 1-carbon layers

From Enke's results, he concludes that the decrease in stress towards the graphite like region can be explained as due to the incorporation of less hydrogen, which is of course always present in the plasma. The original motivation for the stress measurements was the hope that a region within the parameter space could exist where the stress changes sign to become tensile, so that it would be possible to deposit nearly stress-free carbon layers of any desired thickness.

### 1.7 Possible Areas of Development Identified from the Literature Review

It is evident from the vast amount of research papers on carbon films, that these films can be produced by various techniques and exhibit very unusual properties as discussed previously. Why then is there not a range of commercial products available with carbon coatings? The answer would seem to be in identifying the main problems with carbon films, namely the high internal stress and poor adhesion of these films.

These two factors are the limiting criteria in the production of hard carbon films. Poor adhesion and highly stressed films are related in that stress forces can be so great as to cause delamination of the film from the substrate, hence leading to poor adhesion results. Primary objectives would be to deposit hard carbon films and investigate the deposition parameters effect upon the film characteristics. Reduction in the film stress and improved adhesion are essential for the development of carbon films into the areas of wear protective coatings.

## CHAPTER 2

### PLASMA THEORY

#### 2.1 Origin of Plasmas

Plasmas have been studied for many years, with the result that there are very many excellent reference works on plasma theory [30,59]. In 1879 it was well established that a plasma [38], the state of ionised gases, described by Crookes as "a world where matter may exist in a fourth state" had attained an important and more recently a crucial place in research and industry world wide.

Crookes developed the "glow discharge tube". In this tube an electrical current flows between the two electrodes, causing the gas to break down into positively charged ions and electrons.

Thomson [60] in 1897 identified electrons as an inherent part of the atom, freed under those conditions from its parent atom. Man had at last opened up the atom.

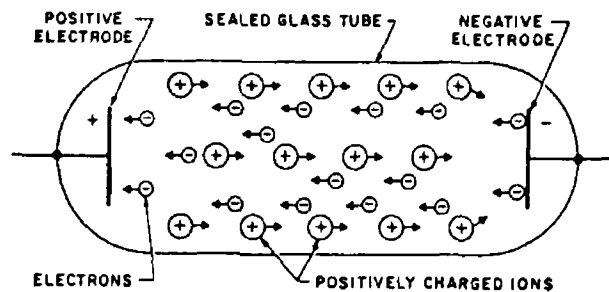


Figure 2.1 Crookes glow discharge tube

Hertz demonstrated that electromagnetic waves other than light can be created and transmitted over a distance without wires. These so-called "Hertzian Waves" were ten million times larger than light waves, which are from  $3.5$  to  $8 \times 10^{-7}$  metres long. At about the same time in history James Clark Maxwell was tying together gas physics with electromagnetics and showed that electricity and magnetism were two facets of the same force and that light and heat radiation are both forms of electromagnetic energy.

It was not until 1928 when Irving Langmuir in his basic studies of electrified gases in vacuum tubes coined the term "plasma", that the "fourth state of matter" was given a name of its own.

## 2.2 Glow Discharge Plasma

Glow discharge or low-temperature plasmas represent by definition plasmas that are essentially neutral, i.e. the number of negatively charged particles equals that of positively charged species. A local charge imbalance may exist, and its presence is established in the vicinity of the confining walls. While free electrons represent the bulk of the negatively charged species, many plasmas also contain negatively charged atoms and molecules. The plasma state may be described in terms of characteristic scale lengths [61]

$$r_c \ll n^{-1/3} \ll \lambda_D \ll \lambda_c \quad (2.1)$$

Where  $r_c = q^2/KT$  is the distance at which potential and kinetic energies are equal when two like charges approach each other,  $n^{-1/3}$  is the average interparticle separation,  $n$  is the number density of charges, and  $\lambda_D$  is the "Debye Length", i.e. the characteristic distance over which the potential of a charge is shielded by neighbouring charges.  $\lambda_c$  is the mean collision length, i.e.  $1/4\pi r_c^2 n$  [30] for simple Rutherford scattering.  $L_p$  is a dimension of the plasma. The main features in such a plasma are

- \* Freedom of movement of the charged particles
- \* Interaction by virtue of the long-range Coulomb force
- \* Collective interaction of the charged particles within a Debye length of a given charge, with  $\lambda_D \gg n^{-1/3}$

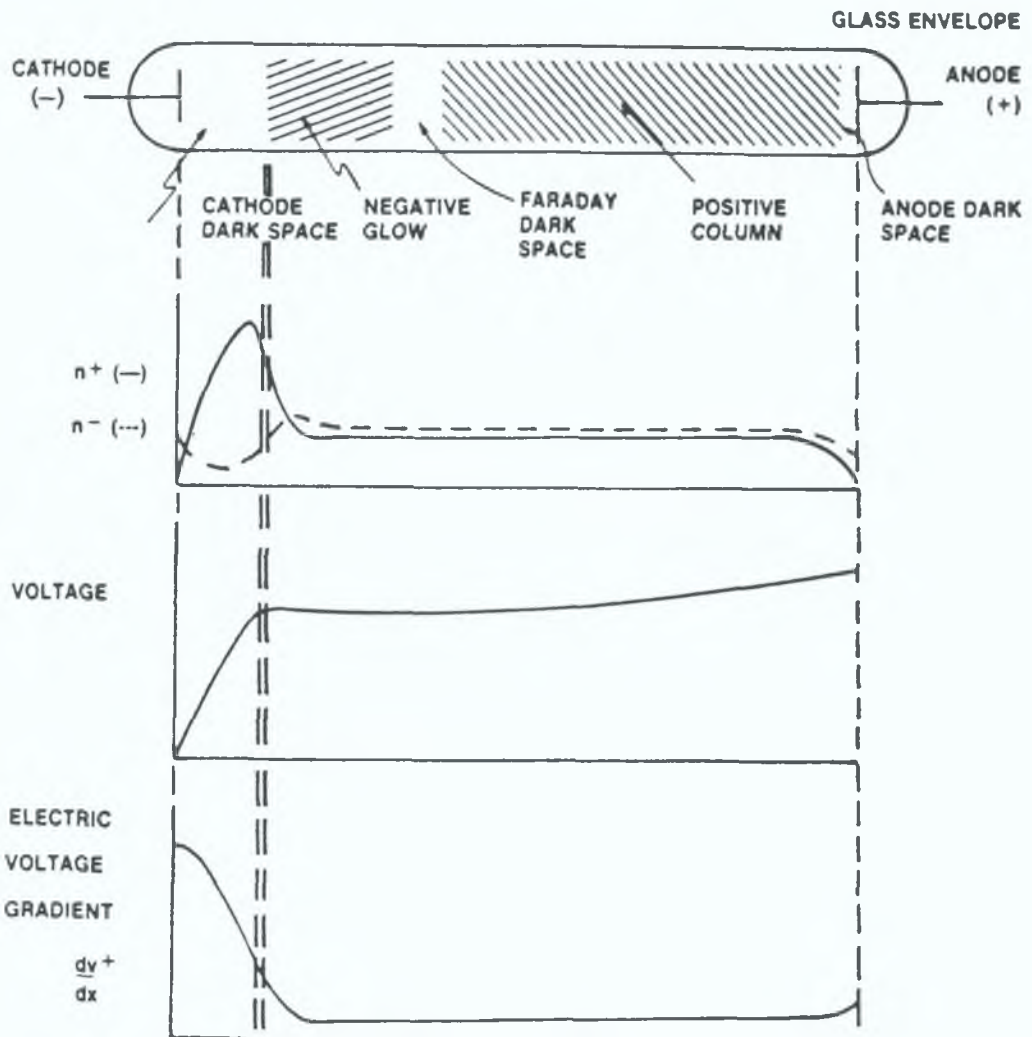


Figure 2.2 Discharge Tube

The first gas discharge to be used for purposes of sputter coating was the d.c. glow discharge which develops when a high d.c. voltage (1.5 KV) is applied to a gas at relatively low pressures. This type of gas discharge is known as a self-sustaining discharge because the charge carriers responsible for conduction are generated by collision processes which occur within the discharge. Argon gas is primarily used for such purposes and the predominant collision process responsible for charge carrier generation is that which occurs between a relatively fast electron and a neutral argon atom. This results in ionization of the argon atom via the reaction [62]:



This reaction requires that the ionization energy, 15.76 eV for argon, be supplied by the fast electron. This electron therefore suffers an energy loss upon collision, and is slowed. In addition, a second electron is generated by the collision. If both these electrons were to be accelerated by an electric field, then they could both gain enough energy to engage in further ionizing collisions. This process, therefore, results in an avalanche effect which very quickly results in an abundance of positive ions and electrons, which are able to migrate through the gas discharge and thereby carry current. The initial avalanche usually results quite spontaneously when a high voltage is applied to a low pressure gas, since natural radiation creates the initial electrons by ionization of a small fraction of the neutral gas atoms. The avalanche is known as a gas breakdown, and is marked by an abrupt drop in the voltage required to carry a given current. After breakdown, the glow discharge is established which typically appears as shown in figure 2.2

The glow discharge is seen to consist of brightly glowing regions which are due to the excitation of the gas, and therefore show spectral lines which are typical for the gas. The luminous regions are called the negative glow and the positive column. The glow does not extend to any surface of the tube. Near all surfaces, (including cathode and anode surfaces) dark regions form which are called sheaths or dark spaces.

The sheaths present in glow discharges are all due to a basic characteristic of the discharge, namely, the much greater mobility and kinetic energy of electrons compared with gaseous ions. The electrons have a much smaller mass, and are therefore accelerated more easily in the presence of any electric field. Furthermore, because electrons have such a small mass, elastic collision between electrons and gas atoms cause the electrons to simply "bounce off" the gas atoms without transference of any kinetic energy to the gas atoms. This property may be derived from the laws of conservation of momentum and kinetic energy which govern elastic collisions, and yields the basic expression for the kinetic energy of the electron after collision which is

$$E = E_0 \left[ \frac{m-M}{m+M} \right]^2 \quad (2.3)$$

Where  $E$  is the kinetic energy of the electron after collision

$E_0$  is the kinetic energy of the electron before collision

$m$  is the electron mass

$M$  is the atom mass

Since  $M \gg m$ , this shows that  $E \approx E_0$ , i.e. virtually no kinetic energy is lost by the electron, so long as the collision is an elastic collision

On the other hand, if the collision is inelastic, such that the gas atom is excited or ionized as the result of the collision, then kinetic energy can transfer from the electron to the gas atom, and thereby be converted to internal energy (ionization or excitation energy) of the struck gas atom, is given by

$$U_m = \left[ \frac{M}{m+M} \right] E_0 \quad (2.4)$$

Since  $M \gg m$ , it is seen from this that the electron has the capability of transferring almost all of the kinetic energy to the gas atom, provided that the proper conditions exist for the excitation or ionization of that atom. It is known that atoms can receive energy in only discrete amounts. Thus, if the value of  $U_m$  is less than the minimum energy that the atom can absorb, then the collision remains elastic and energy transfer from electron to gas atom is very inefficient.

The minimum amount of energy which an argon atom is capable of absorbing corresponds to the energy required to raise the outer electron from the ground state to the first excited state. This is called the first resonance potential, and in argon corresponds to an energy of approximately 11.5 eV. The resonance energies for some common elements are listed in table 2.1

ELEMENT	RESONANCE ENERGY	IONIZATION ENERGY
	eV	eV
H	10.2	13.6
He	20.91	24.58
N	6.3	14.54
O	9.11	13.61
Al	3.13	5.98

Table 2.1 Resonance and Ionization Energies

The gas may be visualised as consisting of an aggregate of relatively fast mobile electrons, and relatively slow, immobile ions and gas atoms. In the cathode dark space (also known as Crooke's dark space) it is noticed that this region consists of an abundance of positive ions, combined with a relative sparsity of electrons. In this region the negative voltage applied to the cathode has driven out the light mobile electrons, leaving behind the slow massive ions. As a consequence of this condition, most of the cathode voltage is screened off by the positive ion cloud. The tube

voltage falls off almost entirely across this dark space by virtue of this ion screening, with the result that only a small voltage drop exists across the remainder of the tube. It is apparent that the glow regions are excellent conductors. These glow regions are known as plasmas. They tend, on average, to be electrically neutral, containing an equal abundance of positive and negative charge. These plasma regions also tend to be almost free of any electric field. A typical d.c. gas discharge used for sputtering purposes will contain a concentration  $N_i$  of  $10^9$  to  $10^{10}$  ions per cubic centimetre and an equal concentration of electrons in the plasma regions. At a 60 millitorr pressure, the unexcited gas will contain  $n_0 \approx 2 \times 10^{15}$ , atoms, per cubic centimeter, thus the fractional degree of ionization is of the order of  $n_i/n_0 \approx 5 \times 10^{-6}$ . Hence, the plasmas are quite dilute.

The cathode dark space region is of vital importance to the sustenance of the discharge as well as the sputtering process. The large voltage drop which occurs across the dark space is responsible for the acceleration of ions which enter the dark space by diffusion from the negative glow region. These ions impact upon the cathode with considerable energy to give rise to the sputtering process. The ions are also neutralized by impacting the cathode. Important to the discharge is the fact that these ions also give rise to the liberation of electrons from the cathode. These latter electrons are accelerated away from the cathode by the dark space field and quickly gain enough energy to engage in ionizing collisions with neutral argon gas atoms. For the discharge to be self-sustaining each argon ion which is neutralised at the cathode must be replaced by another argon ion generated by an ionizing collision caused by a liberated electron. If this were not the case, then the cathode would simply drain ions from the negative glow region, neutralise these, and the discharge would quickly be extinguished. This latter condition can occur if the anode is brought very close to the cathode surface. Under such circumstances, the electron will reach the anode, before causing a sufficient number of ionizing collisions, and the discharge will extinguish. The anode spacing needed to accomplish such discharge extinction is the dark space distance. Thus, if one desires to prevent a discharge from forming near some portions of the cathode surface, the placement of an anode at a distance less than the dark space length, will accomplish this desire. This practice is common in plasma deposition systems, and the shielding is called dark space shielding, for obvious reasons.

The probability that a given type of collision will occur under given conditions is often expressed in terms of its collision cross section. A related parameter is the mean free path or average distance traversed by particles of given type between collisions of a specified type. The Mean Free Path  $\lambda$  for Electrons and producing a given type of reaction A of collision cross section  $\alpha_A$  is given by

$$\lambda_A = 1/N\alpha_A \quad (25)$$

where  $N$  = Particle density

$\alpha_A$  = Cross sectional area for reaction A

Thus the dark space shielding must be less than the mean free path

### 2.3 Events which occur at the cathode

The sputtering process [63] is the direct consequence of the ion bombardment which occurs at the cathode. The sputtering process occurs by virtue of momentum transfer between the impacting ion and the target lattice atom.

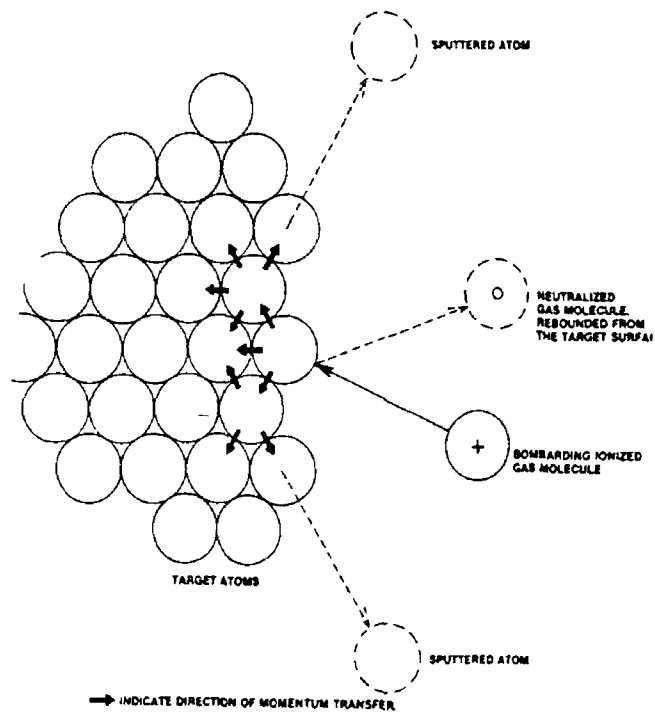


Figure 2.3 Collision Process of Atoms on Surface

The target face is a source of sputtered atoms as well as "fast" neutral gas atoms. Both of those particle types reach the anode which may also be the substrate.

A second process which occurs at the discharge cathode is the emission of electrons. These electrons are responsible for discharge sustenance via ionizing collisions with the gas atoms. Cathode electrons are emitted primarily by two processes: photoelectric effect and positive ion bombardment. The former process is the emission of electrons due to electromagnetic radiation from the nearby negative glow.

## 2.4 Events which occur in the dark space

It will be recalled that the dark space is characterised by an intense electric field. This field causes rapid acceleration of the emitted cathode electrons, with the obvious result that ionizing collisions with neutral gas atoms soon occur. Less obvious is a second consequence which results in high energy electron bombardment at the substrate.

The lack of obviousness of this second process results from the fact that up until now, electrons, ions and atoms have been considered to be hard spheres. This is not really the case. Consider, for example, the process whereby an electron moves through a space occupied by a population of atoms. Since electrons move much more rapidly than the atoms, it can be assumed that the space through which the electron moves is populated by stationary atoms. Consider a slab of unit cross sectional area and thickness  $\Delta x$ . If the gas atom density is  $n$  atoms per unit volume, and the effective collision cross-section of each atom is  $\alpha$ , then the probability that an electron will suffer a collision is given by  $n\alpha\Delta x$ , as it passes through  $\Delta x$  - the fraction of the cross-section area, occupied by atoms having a target of area  $\alpha$ .

A hard sphere model of the gas discharge would predict that  $\alpha$  is not a function of how fast the electron is moving. This is not the case, and it may be understood if one considers that the atom is not a hard sphere but instead consists of a positive nucleus and an orbiting cloud of electrons. An approaching electron will cause a displacement of this electron cloud, hence the positive nucleus will not totally be screened out. Thus the approaching electron is diverted from its path and strikes the atom, i.e. the atom appears "larger" than it actually is. The displacement of the electron cloud takes time however, and therefore a fast moving electron will not have been in the vicinity of the atom for a sufficiently long time to permit such a displacement. Thus, an atom will appear large to a slow moving electron, and small to a rapidly moving electron. This is quantitatively expressed by means of the curves shown in figure 2.4 [30]

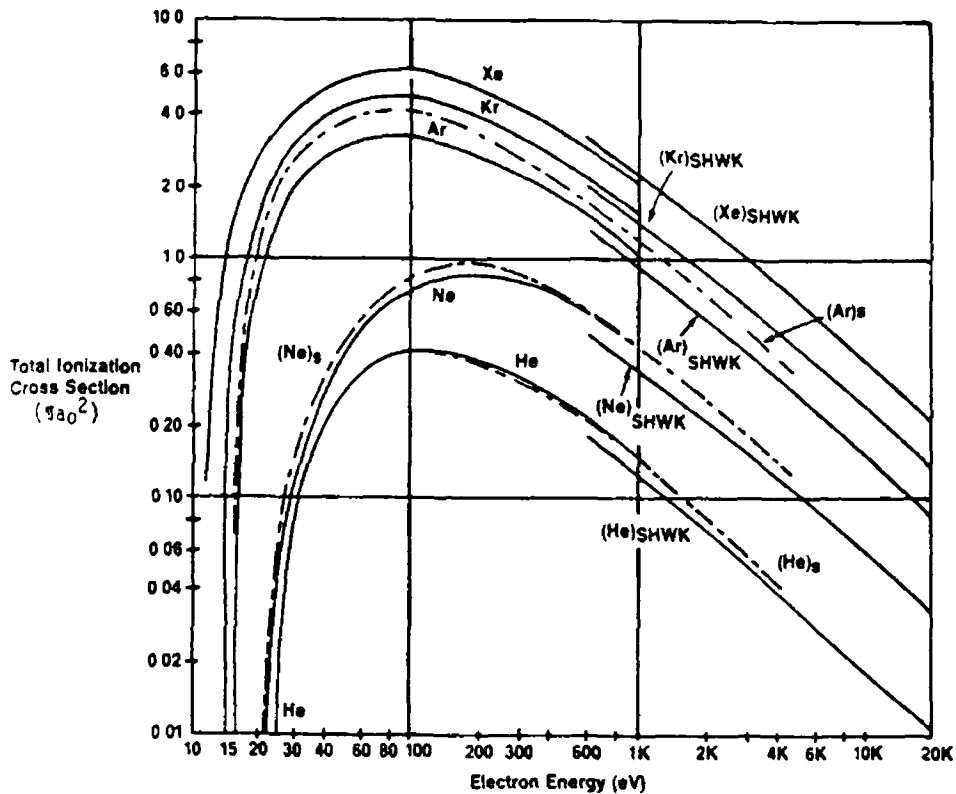


Figure 24 Ionization Cross Section

Here the cross section for ionization type collisions between an electron and various inert gases is expressed as a function of the electron velocity. The electron velocity is expressed in terms of electron kinetic energy, and the atom cross section is expressed in units of  $\pi\alpha_0^2$ , where  $\alpha_0$  is the radius of the first Bohr orbit of hydrogen.  $\pi\alpha_0^2$  has a value of  $8.82 \times 10^{-17} \text{ cm}^2$ . From these curves, it is seen that the higher the electron energy the smaller is the apparent size of the target atom. An appreciation for the magnitude of the effect can be obtained by means of equation 2.5, which expresses the mean free path  $\lambda_A$  (cm) of an electron as a function of the gas density  $n$  (atoms/cm<sup>3</sup>) and the cross sectional area  $\alpha$ .

The events in the dark space can now be visualised as follows: some electrons purely by chance suffer an ionizing collision with an argon atom very early in their travels through the dark space. These electrons are slowed, and create another slow electron. The mean free path remains short because these electrons are moving slowly. Other electrons travel a long distance through the dark space, and thereby gain a large amount of energy from the dark space field. These electrons now do not suffer any ionizing collisions because of their long mean free path, (i.e. atoms appear small to these electrons), and bombard the substrate with the full energy gained by traversing the space field. The events which occur in the dark space involving the slow electrons consist of ionization of the gas atoms accompanied by further generation of electrons, which are accelerated by the dark space field. Thus, an electron avalanche occurs, until at the leading edge of the negative glow, an abundance of electrons and ions exist. Here, the dark space field has fallen off to such a degree that excitation rather than ionization collisions occur. It is these latter excitation

collisions which give rise to the luminescence of the negative glow, ionizing collisions do not give rise to luminescence

The dark space length manifest by the gas discharge is a function of the pressure as well as the nature of the gas. As the pressure is reduced, the dark space lengthens, until at some point, the dark space length becomes equal to the anode-cathode spacing. At this point the discharge will extinguish.

Another effect which occurs in the dark space is a process of symmetric charge transfer. This is a process whereby an ion strikes a neutral atom, and charge is transferred, leaving the ion neutralized and the atom ionized. This process may be written as



where  $\text{Ar}^0$  designates the neutral argon atom

$\text{Ar}^+$  designates the argon ion.

The process is characterised by a collision cross-section which turns out to be quite large. As a consequence, an argon ion accelerating across the dark space travels only a short distance before it is neutralised, and is therefore no longer accelerated. A neutral atom is left behind which is moving towards the target and in addition a new ion is generated which is accelerated towards the target.

A final process which occurs in the cathode dark space region is the collision between sputtered atoms, and gas atoms. A consequence of this process is the scattering of sputtered atoms. These scattered sputtered atoms coat other parts of the sputtering system, and may indeed, even be scattered back to the cathode from which they originated.

## 2.5 The Negative Glow

The negative glow region of the discharge is the first region thus far encountered which can be characterised as a plasma. A plasma is defined as follows [38]

*"A plasma is a quasineutral gas of charged and neutral particles which exhibits collective behaviour"*

This definition implies that equal concentrations of electrons and ions exist in the negative glow, this concentration is typically  $10^{10}$  per  $\text{cm}^3$ . Collective behaviour results because of the fact that as these charged particles move, local concentrations of positive or negative charge can develop which give rise to relatively long range

electric fields. Similarly, charged particle motion gives rise to long range magnetic fields, which affect the motion of other charged particles far away.

The motion of the charged particles as well as the neutral atoms in the plasmas frequently have velocity distributions very similar to an ideal gas. The velocity distributions are therefore Maxwellian distributions which are characterized by a most probable velocity  $C_0$  which is given by

$$C_0 = [2\kappa T/m]^{1/2} \quad (2.7)$$

where

$m$  = Mass of the atom or molecule of which the gas is comprised

$T$  = Absolute temperature of the gas

$\kappa$  = Boltzmann's gas constant.

A plasma can be characterized by means of three Maxwellian distributions for respectively, the electrons, the ions and neutral atoms making up the plasma. An immediate implication of equation (2.7) is the fact that  $C_0$  is large when  $T$  is large, or a high velocity particle can be characterized as having a high "temperature". This is commonly done in describing its electron, ion, and neutral atom temperatures.

Quantitative descriptions of these temperatures, require the definition of two further velocities, which are commonly encountered when one discusses the Maxwellian velocity distribution. The velocities are the average velocity  $C_a$ , and the root mean square velocity  $C_r$ . The three velocities thus defined are interrelated in the following way [59]

$$C_a = (3/2)^{1/2} C_0 = 1.224 C_0 \quad (2.8)$$

$$C_r = (2C_0/\pi)^{1/2} = 1.128 C_0 \quad (2.9)$$

Practical forms of equations (2.8) and (2.9) are found by substituting in for Boltzmann's constant

$$C_0 = 1.656 \times 10^{-8} (T/m)^{1/2} \quad \text{cm/sec} \quad (2.10)$$

$$C_a = 2.027 \times 10^{-8} (T/m)^{1/2} \quad \text{cm/sec} \quad (2.11)$$

$$C_r = 1.868 \times 10^{-8} (T/m)^{1/2} \quad \text{cm/sec} \quad (2.12)$$

The energy content of a Maxwellian gas resides in the kinetic energy of the gas molecules. The "average" kinetic energy of the gas is related to the absolute temperature by the equation

$$mC^2 = 3 kT \quad (2.13)$$

The equation therefore serves for the quantitative characterisation of the plasma. For example, if the mean kinetic energy of the electrons in the plasma is 1 eV, then the electron temperature is that temperature at which  $kT$  is equal to 1 eV. A convenient term to remember in describing plasmas is the fact that 1 eV corresponds to an absolute temperature of 11,600 K.

In plasmas electrons tend to bounce off atoms until the electron energy is sufficient to excite or ionize the atom. Also, even during excitation or ionizing collisions transfer of kinetic energy to the atom is almost zero. Atom - atom, or ion - atom collisions result in efficient transfer of kinetic energy. Thus, electrons tend to move about with much higher velocities than the atoms or ions, and therefore have a higher temperature.

Another extremely useful equation which can be derived from the Maxwellian distribution is the rate at which particles strike a surface immersed in the plasma. This hit rate, expressed in terms of hits per  $\text{cm}^2$  per second is given by

$$\tau = \frac{1}{4} n C_a \quad \text{hits/cm}^2 \text{ sec} \quad (2.14)$$

where  $C_a$  = Average velocity

$n$  = Particle concentration (particles per cubic centimetre)

This equation can be used to calculate hit rates by ions, electrons, neutral atoms and residual impurity atoms, etc., provided that their velocity distributions follow the Maxwellian distributions.

The application of equations (2.14) to an object immersed in the negative glow immediately allows for the derivation of the "floating potential" of the negative glow. The floating potential is that potential that any dielectric or electrically isolated surface will achieve when immersed in the discharge. This potential arises because of the differing temperatures of the ions and electrons in the negative glow plasma. Thus, since  $N_i = N_e$  in the negative glow, the application of equation (2.14) predicts that the hit rate by electrons  $T_e$ , will be substantially higher than the hit rate by ions  $T_i$ .

This arises since  $C_e \gg C_i$ . Thus any floating surface immersed in the negative glow will rapidly acquire a negative voltage with respect to the plasma. This negative voltage will now cause some of the electrons to be repelled upon approaching the surface. The negative voltage will continue to grow until  $T_i = T_e$  at which point the charge building stops, since now the charge transfer by ions equals that due to the electrons. This equilibrium then characterises the floating potential.

When a surface acquires a floating potential, a sheath (or dark space) forms adjacent to this surface. The sheath has many of the same characteristics as the cathode dark space except that the voltage drop across the sheath is the difference between the plasma potential and the floating potential.

The magnitude of the sheath voltage drop (difference between floating and plasma potential) may be calculated by once again referring to the Maxwellian distribution function. This function predicts that the fraction  $N'_e/N_e$  of electrons which can penetrate the sheath is

$$N'_e/N_e = \text{Exp}(-eV/KT) \quad (2.15)$$

where  $V$  is the sheath voltage drop.

Now the equilibrium between ion and electron hit rates requires that

$$N'_e C_e = N_i C_i \quad (2.16)$$

Further application of the Maxwellian distribution shows that

$$C'_e = C_e = \left[ \frac{8KT_e}{\pi M_e} \right]^{1/2} \quad (2.17)$$

and that

$$C_i = \left[ \frac{8KT_i}{\pi M_i} \right]^{1/2} \quad (2.18)$$

By combining equations (2.15), (2.16), (2.17) and (2.18)

$$V = \frac{KT_e}{2e} \ln \frac{M_i T_e}{M_e T_i} \quad (2.19)$$

This equation now quantitatively relates the sheath voltage drop, or the difference between the plasma potential and the floating potential, to the electron and ion temperatures. This sheath voltage drop therefore is sufficient to repel enough electrons from reaching the substrate surface, such that the ion hits equal the electron hits. The ions which reach the surface now are accelerated by this same potential and therefore impact on the surface with considerably more energy than they possess in the plasma.

Another basic characteristic of the plasma is its ability to screen off any electric field which one attempts to apply to it. This screening occurs at the cathode sheath as well as the sheath which develops at any electrically floating surface. These surfaces both develop sheaths, over which a potential change occurs, leaving the plasma basically as a field free region. The plasma is field free for very much the same reason that the interior of an electrically conductive metal is field free.

The plasma differs however, in that the number and mobility of charge carriers is substantially less than in a metal. Thus, small fields applied to a plasma tend to fall off over a finite dimension known as the "Debye Length". This Debye length can be derived by applying the standard electrostatics equation (Poisson's equation) to the plasma, which then predicts that a voltage perturbation  $V_0$  applied to the plasma will fall off according to the law

$$V(e) = V_0 e^{-l/\lambda_D} \quad (2.20)$$

where

$V_0$  = Potential applied at a point

$V(e)$  = Potential at a distance  $l$  from the point

$\lambda_D$  = Debye length

The Debye length is therefore the length over which the applied voltage has fallen off to 0.37 of its initial value. Again, if one assumes Maxwellian velocity distributions, for ions and electrons, and an equal abundance of ions and electrons one can express the Debye length as

$$\lambda_D = [KT_e/4\pi N_e e^2]^{1/2} \quad (2.21)$$

By substitution

$$\lambda_D = 6.9 \times (T_e/N_e)^{1/2} \quad (2.22)$$

Where  $T_e$  = Electron temperature K

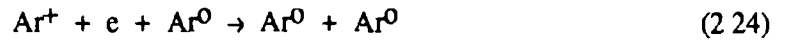
$N_e$  = Electron concentration  $\text{cm}^{-3}$

Hence a plasma is an equipotential region, except for small voltage fluctuations which fall off over a dimension  $\lambda_D$

An alternative way of studying the negative glow plasma, is to realise that the plasma is like a gas, having neutral atoms, ions and electrons. It is known that the velocity distributions can be described by three distinct Maxwellian distributions having characteristic temperatures  $T_0$ ,  $T_i$  and  $T_e$ , and that a high temperature signifies a high particle energy or velocity. Also,  $T_e$  is high and  $T_i$  and  $T_0$  are close to room temperature. Suppose now that a plasma ball suspended in space is created and one can examine what happens to the ball. Firstly, one might expect that the electrons, having a high velocity, would simply race out of the ball and leave the slow ions behind. However, this would generate a large electric field which would restrain the electrons. In fact, the electrons do not have enough energy ( $T_e$ ) to get away from the ions by more than approximately one Debye length. Thus the electrons are held into the ball by the slow moving ions. The ions on the other hand, feel that tug of the electrons and are slowly dragged out of the plasma ball. Thus, the ball will dissipate by this tug and drag action, known as "ambipolar diffusion". In a deposition system in which there is a cathode and anode, a plasma region exists between these and then there is a large space surrounding these until one arrives at the system chamber walls, one can conceptually appreciate the similarity between this situation and the previously imagined plasma ball suspended in space. Thus, it is easy to visualise that electrons and ions drift out of the plasma, toward the chamber walls, at a rate controlled by the aforementioned ambipolar diffusion process. This causes a concentration gradient of ions and electrons to develop in the plasma. This has consequences in film sputtering rates across the cathode, and gives rise to lower sputtering rates from those portions of the cathode near the edge of the glow.

Considering the plasma ball in space, one might ask "Why don't the ions and electrons simply combine to yield neutral atoms?" The plasma would then simply disappear by recombination of the electrons and ions. This process does indeed occur, but it occurs slowly. The reason for the slow recombination rate lies in the energetics of the recombination process. The recombination is the collision process which requires the simultaneous satisfaction of both the law of conservation of momentum and kinetic energy. Thus, the ionization energy liberated by the recombination process would have to be absorbed by the increased kinetic energy of the newly neutralised atom. This however would not allow for the conservation of the momentum for the entire collision process. Thus, recombination requires a three body collision such as





For the simultaneous satisfaction of both the laws of conservation of momentum and energy. Three body collisions are relatively rare in the plasma, and as a consequence, electron-ion recombination rates are very slow. Thus, however, is not the case near a chamber wall. Here the electrons and ions can recombine and dissipate their energy as heat to the chamber wall. The chamber wall is thereby heated, and the ions and electrons are neutralised. For this reason, the chamber acts as a recombination sink for the plasma. The plasma particles diffuse to the chamber walls by the ambipolar diffusion process at which location they coalesce to form a neutral atom. Chamber walls, by acting in this capacity, thereby have a very decided influence over the plasma density gradients which develop, and thereby ultimately have a decided influence on deposited film uniformity.

The negative glow plasma is a region which is rich in collision events between electrons and the gas atoms. Analysis has been restricted to noble gases such as argon, where the predominant events are excitation and ionization. If one now considers a more complex molecular gas, then a wide variety of other events occur. These events form the basis of plasma etching and plasma deposition processes.

## 2.6 Radio Frequency Gas Discharge

The utility of rf methods [59,64] lies in the capability of sputtering dielectric materials, greater ease in sputtering reactive metals, and the lower pressure operation afforded by this method. Rf discharges are very similar to dc discharges, in that sheath regions and plasma regions develop.

Recalling figure 2.2, imagine now that a pair of diametrically opposed electrodes are attached to the outside of the glass tube. The placement of these electrodes is adjacent to the negative glow region of the discharge. The electrodes are further connected to a battery through a switching arrangement which permits the periodic reversal of the electrode polarity. The arrangement shown has electrode 2 connected to the negative terminal of the battery, and electrode 1 connected to the positive terminal. The switch is closed at time  $t_0$ , and current flow occurs because the plasma and tube walls, here assumed to be glass, it behaves as a large capacitor, with a time dependent polarization. The dc current flows because the capacitor is charging, as shown in figure 2.6.

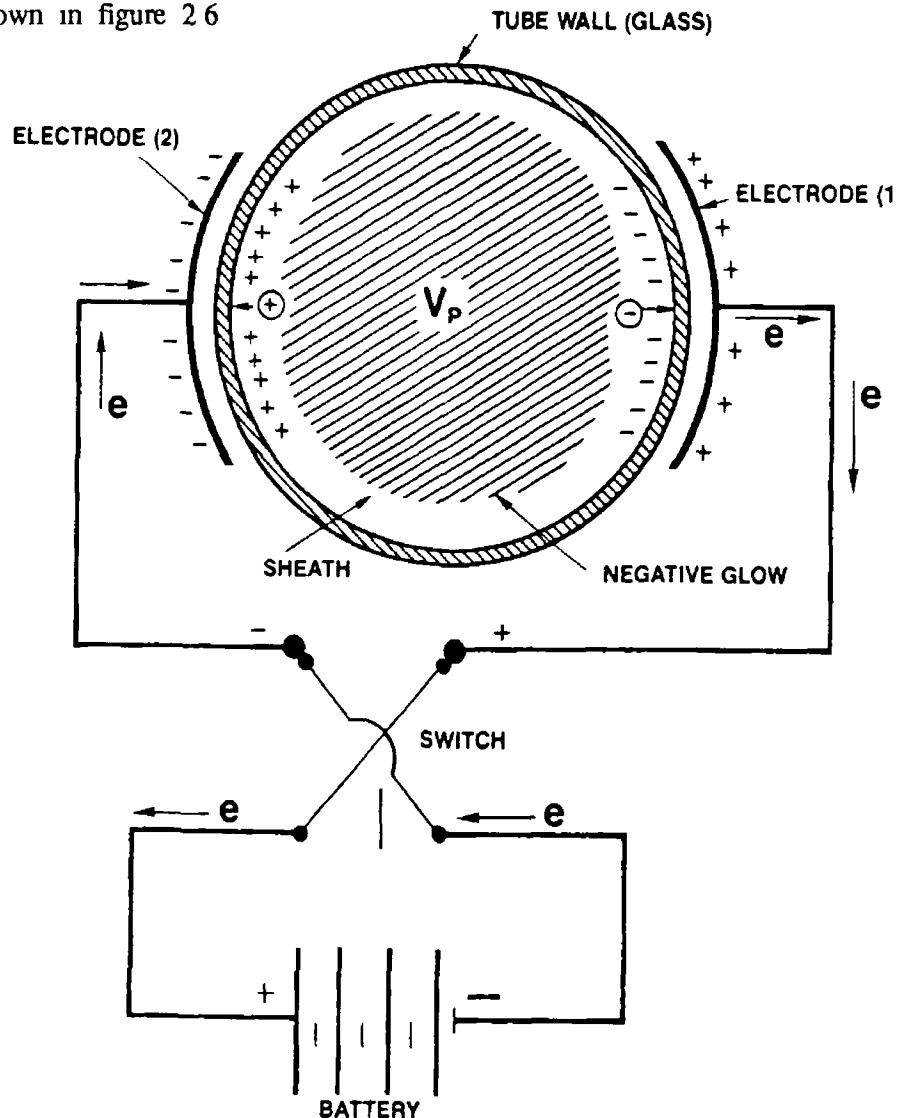


Figure 2.5 Glow Discharge Tube with Externally Attached Electrodes [59]

Firstly, examining what happens at electrode 2, the negative electrode. The plasma inside the tube feels the electric field from electrode 2, and accordingly responds. Positive ions are attracted to the tube wall, and travel across the plasma sheath. Upon striking the tube wall the positive ions strip an electron from the glass tube wall, and are converted to neutral gas atoms, leaving behind a positive charge on the wall surface. This positive charge attracts electrons in the external electrode 2, and an electron current  $i$  to flow into electrode 2. This current is illustrated in figure 2.6, as the current commencing at  $t_0$  and ending at  $t_2$ . At  $t_2$  the accumulated positive charge on the inside of the tube wall, completely screens off the field from electrode 2, and no further ions are attracted to the tube.

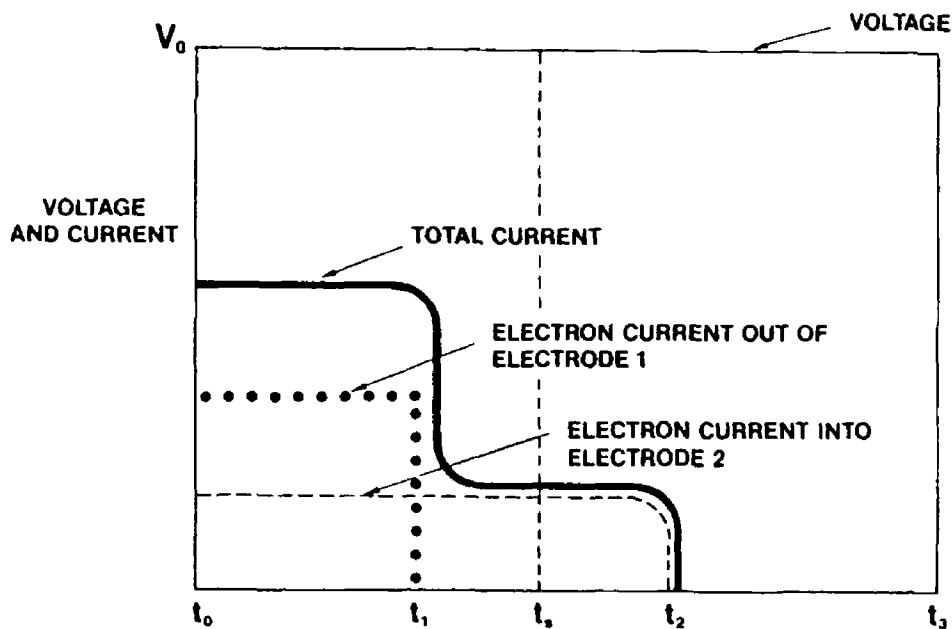


Figure 2.6 Current Flow in the Figure 2.5 Circuit

At the site of electrode 1, the positive electrode, electrons are attracted across the sheath causing a negative charge accumulation on the tube wall, which causes electrons in the external electrode to flow out of the electrode as shown in figure 2.5. This flow continues until the accumulation of negative charge on the tube wall completely screens off the field from electrode 1, at which point current flow ceases. This is shown in figure 2.6, as the current flow which extends over the time interval  $t_0$  to  $t_1$ . This yields a total current flow in the external circuit shown by the solid step-shaped curve. Notice that the current flow to electrode 1 occurs over a shorter time interval  $t_0$  to  $t_1$ , compared with electrode 2, where the current flows for an interval  $t_0$  to  $t_2$ . This phenomenon is fundamental to the properties of the plasma and is the basic reason why r f deposition is feasible.

The sheath current opposite electrode 1 is an electrode current. The sheath current opposite electrode 2 is an ion current. Since electrons are more mobile than ions, the current flow interval is shorter opposite electrode 1, because electrons travel

across the sheath with greater speed. Notice further that the total charge transfer (area under the current-time curves) is the same for each electrode. If this were not the case, the plasma would end up with a net excess of positive or negative charge which would result in very large electric fields. Notice further that the time period of voltage application  $t_0$  to  $t_3$  is sufficient for all current flow to cease, and equilibrium conditions to be established.

If the voltage is now reversed, and maintained over the same time period, the sheath currents as well as the electron current in the external circuit will reverse. At electrode 2 a sheath electron current flows, and at electrode 1 a sheath positive ion current flows. At electrode 1, the positive ion current first neutralizes the accumulated negative charge on the tube wall, and then continues, with an imagery electron flow into the external electrode. Similar events occur at electrode 2, resulting in an equilibrium state which is just the reverse of the condition shown in figure 2.5. Having an a.c. voltage source instead of the switch and battery will permit an a.c. current to flow.

If the frequency of polarity reversal on the external electrodes is increased, at some point one reaches a frequency ( $\approx 1\text{MHz}$ ), where ions are not given sufficient time to travel across the plasma sheath to neutralize the previously accumulated negative charge on the glass wall opposite each electrode. Thus, each polarity reversal results in a net residue of negative charge on the inside of the glass tube opposite each electrode, thereby causing the glass tube to acquire a negative d.c. bias with respect to the plasma. On the next polarity reversal sequence, the previously accumulated negative charge causes a greater acceleration of the ions, and a retardation of the electrons during their respective flows across the plasma sheath, with the result that the net residue of negative charge on the glass has been increased to a lesser extent after the second cycle compared with the first. The negative bias grows, but to a lesser extent. Continuing this reasoning, one can understand that the d.c. bias grows until the respective ion and electron currents reaching the glass surface become equal, at which point no further charge accumulation will occur, and a time invariant d.c. bias offset exists. This situation is depicted in figure 2.7, which shows the voltage wave form on the external electrodes (generation) versus the voltage wave form on the glass tube wall opposite the electrodes (target). In both cases, the voltage zero is taken to be the plasma potential. It is noticed that during the bulk of the sinusoidal cycle, the target surface is negative with respect to the plasma. Ions are extracted from the plasma, travel across the sheath and impact into the target, thereby causing sputtering. During each sinusoidal cycle the target surface goes positive relative to the plasma for a very short time period, during which time the electron current balances the previous ion current, such that, over the complete cycle,

no net current flows to or from the target Figure 27 further shows that the d c voltage offset which occurs is almost equal to the rf peak voltage The target surface, in the case of figure 27, runs through a voltage range in which it varies from slightly positive relative to the plasma, all the way to a -2KV negative This voltage falls off across the plasma sheath, leaving the plasma as an isopotential region through the entire cycle (This is true except for a small a c field of the order of  $\approx$  2-5 volts per cm which penetrates into the plasma)

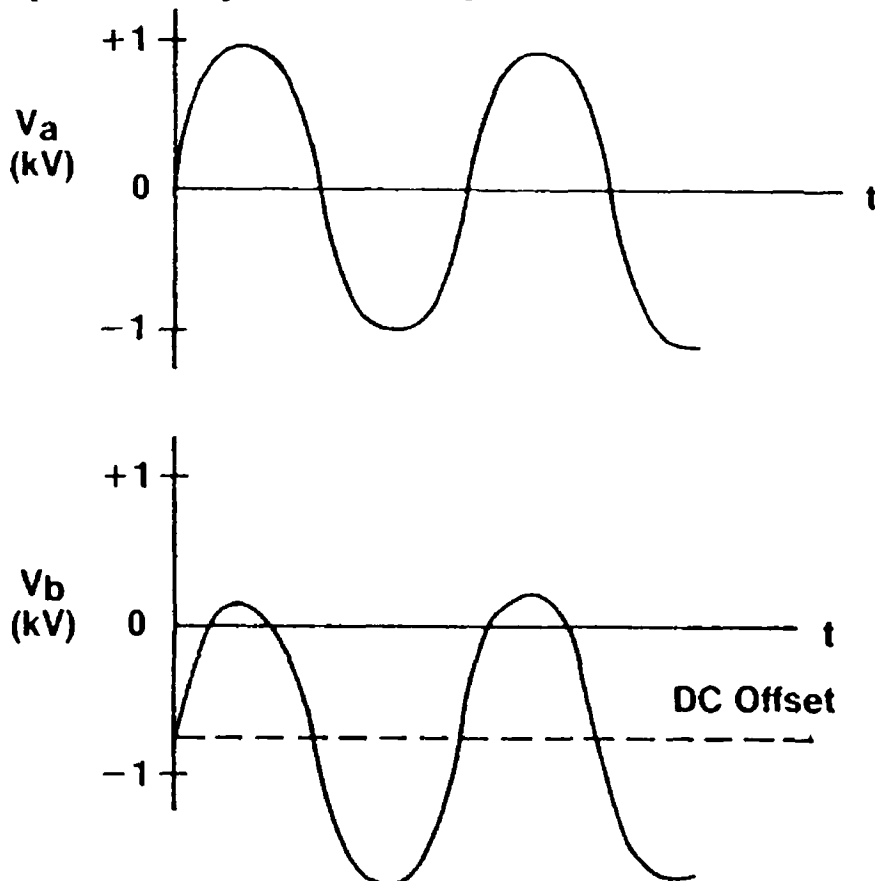
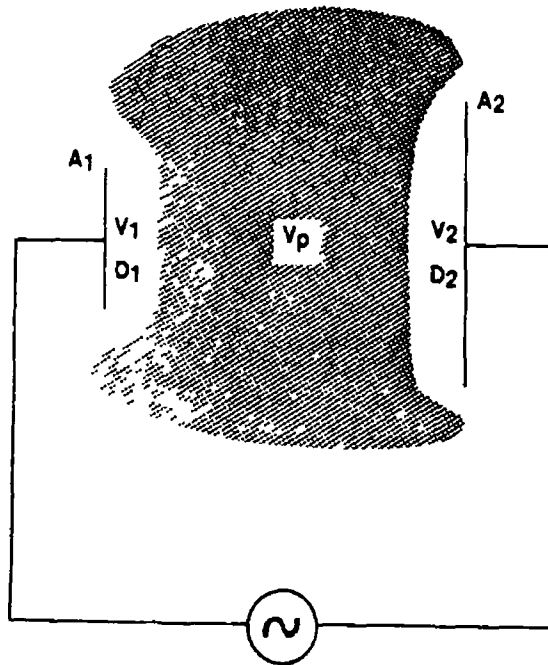


Figure 27 Voltage waveforms at generator ( $V_a$ ) and target ( $V_b$ ) in a conventional sinusoidally excited rf discharge

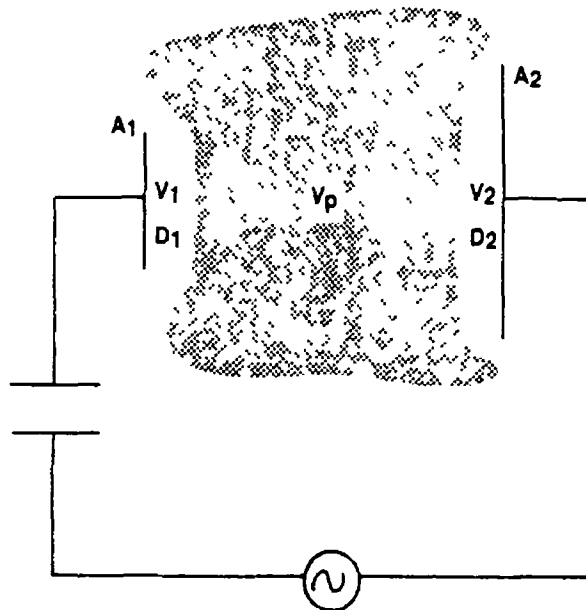
With rf voltages of the magnitude described here, the need for an independent d c cathode and anode such as were present in this discussion, become superfluous. The fields necessary to generate the initial gas breakdown are entirely provided by the two rf electrodes. Similarly, a pair of metal electrodes, or one metal electrode and one metal electrode faced with a dielectric, will also accomplish the objective of establishing the gas discharge and the symmetrical sheath configuration which was previously described. Thus, one can sputter from a configuration such as depicted in figure 28. Here one has a plasma (shaded region) which is at potential  $V_p$ , sheaths of length  $D_1$  and  $D_2$  opposite each of the electrodes, across which d c voltage drops  $V_1$  and  $V_2$  occur. In this configuration, equal sheath voltage drops occur and one sputters from each of the electrodes. As in the previous discussion, the plasma region is an equipotential region and is very similar to the d c negative glow previously discussed.



$$V_1 = V_2$$

Figure 2 8 Voltage Distribution - without blocking capacitor

This type of configuration is inconvenient, in that both electrodes sputter. However, by the simple placement of a series capacitor into the r f circuit, one can substantially alter the distributions of sheath voltages, such that sputtering occurs from only one electrode, and deposition on the other. A simple two electrode sputtering system thereby occurs whereby one electrode does not sputter, and thereby serves as a convenient surface for placement of the substrates.



$$\left( \frac{V_1}{V_2} \right) = \left( \frac{A_2}{A_1} \right)^4$$

Figure 2 9 Voltage Distribution - with blocking capacitor

The understanding of how the sheath voltage redistribution occurs may be achieved by consideration of the law which relates the ion flux through the sheath, to the voltage across the sheath. If one assumes a space charge limited current then this ion current flux  $J_1$  is given by the Child-Langmuir equation

$$J_1 = C \frac{V^{3/2}}{m^{1/2}D^2} \quad (2.25)$$

where  $V$  is the voltage drop across the sheath

$D$  is the sheath length

$m$  is the ion mass

$C$  is a constant.

If one requires that the current density of positive ions is equal at both electrodes, then this equation predicts

$$\frac{V_1^{3/2}}{D_1^2} = \frac{V_2^{3/2}}{D_2^2} \quad (2.26)$$

where  $D_1$ ,  $D_2$  and  $V_1$  and  $V_2$  refer to the respective voltage drops, and sheath lengths associated with two electrodes having electrode areas  $A_1$  and  $A_2$

As we recall, the sheath region is associated with a large voltage drop. This implies a very limited conductivity across the sheath. The electrode sheath-plasma configuration may therefore be regarded as a capacitor, having a capacitance given by

$$C = k \frac{A}{D} \quad (2.27)$$

where  $k$  is the dielectric constant associated with the sheath. Now it is known that an r.f. voltage will divide between the two capacitances present here, according to

$$\frac{V_1}{V_2} = \frac{C_2}{C_1} \quad (2.28)$$

Using equation (2.27) and (2.28)

$$\frac{V_1}{V_2} = \frac{A_2}{A_1} \frac{D_1}{D_2} \quad (2.29)$$

and substituting this into equation (2.26) gives

$$\frac{V_1^{3/2}}{V_2^{3/2}} = \frac{D_1^2}{D_2^2} = \left[ \frac{A_1 V_1}{A_2 V_2} \right]^2 \quad (2.30)$$

$$\frac{V_1}{V_2} = \left[ \frac{A_2}{A_1} \right]^4 \quad (2.31)$$

Thus a larger sheath voltage will develop across the electrode having the smaller area. Now since the plasma is an isopotential region, these differing sheath voltages imply that a d.c. voltage difference will exist between the two electrodes. The power supply cannot support these d.c. voltage differences, and for this reason a blocking capacitor is placed in series between the supply and the electrode as shown in figure 2.9. In practical systems for deposition the substrates are placed on the powered electrode and the top plate and chamber walls act as the second electrode.

In addition to serving as a source of high energy electrons, the target in sputtering systems and sheath regions also serve as a source of electro-magnetic radiation, fast neutral atoms, and negative ions, the generation of which was discussed in the previous section on d.c. gas discharges. Similarly, the r.f. plasma is very similar to the d.c. plasma, and gives rise to random ion and electron bombardment of the substrate.

A difference between the r.f. and d.c. discharges is the observation that an equivalently dense plasma can be achieved at lower operating pressures. Thus, r.f. sputtering is usually accomplished at a pressure of 10 millitorr as opposed to the 40 - 60 millitorr pressures utilised with d.c. sputtering. The greater ionization efficiency of the r.f. discharge is not well understood. It is believed that the most important ionization source is due to electrons oscillating in response to the very weak r.f. field which succeeds in penetrating the plasma. This oscillation coupled with properly timed elastic collisions between electrons and atoms, permits the electrons to gain sufficient energy despite the weak field, to cause ionization events.

## CHAPTER 3

### THEORY OF FILM DEPOSITION

#### 3 1 Introduction to film deposition

##### 3 1 1 Vacuum Technology

In man's quest for economy and perfection, thin films have been deposited on substrates for the enhancement of the mechanical, electrical, chemical, optical or decorative properties. The deposition of thin films with controlled properties requires an operating environment which interferes as little as possible with the process of film formation. High vacuums are attained to minimise the interaction between residual gases and the surfaces of growing films.

A vacuum [65] is defined as a region of space where pressure is below that of the surrounding atmosphere. Absolute vacuum is practically impossible in any system, the nearest being that of Space, which is often described as an absolute vacuum. The terminology used for the varying degrees of vacuum, which are distinguished according to pressure ranges are

Low Vacuum	760 - 25	Torr
Medium Vacuum	25 - $10^{-3}$	Torr
High Vacuum	$10^{-3}$ - $10^{-6}$	Torr
Very High Vacuum	$10^{-6}$ - $10^{-9}$	Torr
Ultrahigh Vacuum	Below $10^{-9}$	Torr

##### 3 1 2 Physical Vapour Deposition (PVD)

PVD technology [30] consists of the techniques of evaporation, ion plating and sputtering. It is used to deposit films and coatings on self-supported shapes such as sheet, foil, tubing, etc. Their use has been increasing at a very rapid rate, since modern technology demands multiple and often conflicting sets of properties from engineering materials, e.g. combination of two or more of the following - high

temperature strength, impact strength, specific optical, electrical or magnetic properties, wear resistance, fabricability into complex shapes, cost, etc. A single or monolithic material cannot meet such demands in high technological applications. The resultant solution is therefore a composite material, i.e. a core material and a coating each having the requisite properties to fulfill the specifications.

In general deposition processes may principally be divided into two types: 1) those involving droplet transfer such as plasma spraying, arc spraying, wire explosion spraying, detonation gun coating and 2) those involving an atom by atom transfer mode such as physical vapour deposition processes of evaporation, ion plating, and sputtering, chemical vapour deposition and electrodeposition. The chief disadvantage of the droplet transfer process is the porosity in the final deposit which affects the properties.

There are three steps in the formation of any deposit:

- 1) Synthesis of the material to be deposited
  - a) Transition from a condensed phase (liquid or solid) to the vapour phase
  - b) For deposition of compounds, a reaction between the components of the compounds some of which may be introduced into the chamber as a gas or vapour
- 2) Transport of the vapours between the source and substrate
- 3) Condensation of vapours (and gases) followed by film nucleation and growth.

There are significant differences between the various atom transfer processes. In chemical vapour deposition and electrodeposition processes, all of the three steps mentioned above take place simultaneously at the substrate and cannot be independently controlled. Thus, if a choice is made for a process parameter such as substrate temperature, the resultant film microstructure and properties are predetermined. On the other hand in PVD processes, these steps (particularly steps 1 and 3) can be independently controlled and one can therefore have a much greater degree of flexibility in controlling the structure and properties and deposition rate.

### 3 1 3 PVD Processes

There are three physical vapour deposition processes [59], namely, evaporation, ion plating and sputtering. In the evaporation process, vapours are produced from a material located in a source which is heated by direct resistance, radiation, eddy currents, electron beam, laser beam or an arc discharge. The process is usually carried out in vacuum (typically  $10^{-5}$  to  $10^{-6}$  torr), so that the evaporated atoms undergo an essentially collisionless line-of-sight transport prior to condensation on the substrate. The substrate is usually at ground potential (i.e. not biased).

It is noticed that the deposit thickness is greatest directly above the centre-line of the source and decreases away from it. This problem is overcome by imparting a complex motion to substrates (e.g. in a planetary or rotating substrate holder), so as to even out the vapour flux on all parts of the substrate or by introducing a gas at a pressure of 0.5 to 1.0 mbar into the chamber so that the vapour species undergo multiple collisions during transport from the source to substrate, thus producing a reasonably uniform thickness of coating on the substrate. This technique is called gas-scattering evaporation or pressure plating.

In the ion-plating process the material is vapourised in a manner similar to that in the evaporation process through a gaseous glow discharge on its way to the substrate, thus ionising some of the vapourised atoms. The glow discharge is produced by biasing the substrate to a high negative potential (-2 to -5 KV) and admitting a gas, usually argon.

In this simple mode, which is known as diode ion-plating the substrate is bombarded by high energy gas ions which sputter off the material present on the surface. This results in a constant cleaning of the substrate (i.e. removal of surface impurities by sputtering), which is desirable for producing better adhesion and lower impurity content. This ion bombardment also causes a modification in the microstructure and residual stresses in the deposit. On the other hand, it produces the undesirable effect of decreasing the deposition rates since some of the deposit is sputtered off, as well as causing a considerable heating of the substrate by the intense gas ion bombardment. The latter problem can be alleviated by using the supported discharge ion-plating process where the substrate is no longer at the high negative potential, the electrons necessary for supporting the discharge coming from an auxiliary heating tungsten filament. The high gas pressure during deposition causes a reasonably uniform deposition of all surfaces due to gas-scattering as discussed above.

In the sputtering process, positive gas ions (usually argon ions) produced in a glow discharge bombard the target material (also called the cathode) dislodging groups of atoms which then pass into the vapour phase and deposit onto the substrate. Sputtering is an inefficient way to induce a solid-to-vapour transition. Typical yields (atoms sputtered per incident ion) for a 50 eV argon ion incident on a metal surface are unity. Thus the phase change energy cost is from 3 to 10 times larger than evaporation. Sputtering is a mechanical action, where the coating flux is not dependent on the melting point of the sputtered material. The deposition is usually very uniform.

There are several advantages of PVD [31] processes over competitive processes such as electrodeposition, CVD, plasma spraying. They are

- 1 - Extreme versatility in composition of deposit.
- 2 - The ability to produce unusual microstructures and new crystallographic modifications e.g. amorphous deposits
- 3 - The substrate temperature can be varied within very wide limits from sub-zero to high temperatures
- 4 - Ability to produce coatings of self-supported shapes at high deposition rates
- 5 - Deposits can have very high purity
- 6 - Excellent bonding to the substrate
- 7 - Excellent surface finish which can be equal to that of the substrate
- 8 - Eliminations of pollutants and effluents from the process which is a very important ecological factor

The present limitations of PVD processes are

- 1 - Inability to deposit polymeric materials with certain exceptions
- 2 - Higher degree of sophistication of the processing equipment and hence a higher initial cost.
- 3 - Relatively new vacuum technology, hence expensive

### 3.1.4 Chemical Vapour Deposition [38]

CVD is the process by which chemicals are mixed in a vapour phase in a chamber and heated to very high temperatures, to cause chemical reactions

The compounds thus formed diffuse onto the substrates. CVD is a reaction in which two types of gas, C(g) and D(g), react about one atmosphere and high temperature to form a solid phase A(s) and a gas phase B(g)



## 3.2 Plasma Enhanced Chemical Vapour Deposition

### 3.2.1 Introduction

The rapidly rising application of plasma - CVD technology has led to there being a need for the understanding of the basic reaction mechanisms

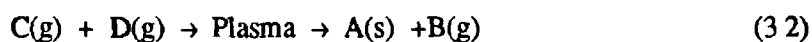
Ion-molecule and radical-molecule mechanisms are responsible for the dissociation of organic and organic-inorganic molecules and for the formation of polymerised species in the plasma state. There is still a lot of uncertainty about reactions and depositions. Most of the advances are through experimentation rather than modelling. The complexity of the field is enormous and each advance in the art in one direction must be considered in the context of all impacting parameters.

All types of electrical discharges have three elements in common: 1) They are sustained by a source of electric power; 2) The electric power is delivered by means of a coupling mechanism; 3) It is delivered to a plasma environment associated with a particular design.

Plasma deposition has for a long time been used in the electronic industry, plasma-deposited nitride and oxide are utilised as inter layer dielectric films between metallisation levels. In recent years, glow discharge-produced amorphous silicon has attained considerable importance as a new electronic material for fabricating thin film devices such as solar cells, transistors, sensors and photoreceptors. Further developments of PECVD techniques to prepare metal thin films or novel organic materials are expected in the near future, based upon better understanding of the chemistry in the glow discharge.

As all CVD processes require high temperatures, this limits their application for coating temperature sensitive materials. Using a plasma source the thermal heat is reduced so that chemical reactions take place at equivalently high temperatures due to high ion and electron temperatures.

Plasma CVD is a gas-phase reaction in a low temperature plasma that forms a thin solid film on a substrate,



For example, ordinary and plasma CVD of silicon nitride films are expressed as



With the use of plasmas, substrate temperature can be lowered and thermal damage of the film reduced. A comparison of different reactions for CVD and plasma CVD is given in table 3.1

**Precipitation Temperature in atm. CVD and Plasma CVD**

Compounds	Reacting Material	Atm CVD °C	PCVD °C
$\text{Si}_3\text{N}_4$	$\text{SiH}_4$ $\text{NH}_3(\text{N}_2)$	700-900	300-500
$\text{SiO}_2$	$\text{SiH}_4$ $\text{N}_2\text{O}$	900-1200	200-300
$\text{Al}_2\text{O}_3$	$\text{AlCl}_3$ $\text{O}_2$	700-1000	100-500

**Table 3 1**

In a low-temperature plasma, the energy of the electron is larger than that of the ions or neutral particles and are thermally in a non-equilibrium state. Although the energy of the ions or neutral particles is relatively low, these particles become excited by colliding with electrons. This excited state is equivalent to a high temperature state, and the effective reaction can thus proceed at a low temperature. Various states of the species in the plasma depend on the generating plasma pressure, and other parameters. When the plasma is generated by a high potential and low current no dissociation of molecules is detected. At a relatively low potential and high current, however, some dissociation can be detected. When the reaction is thermodynamically possible in the CVD method but has a very slow rate, the excited states can be induced by the catalytic action of the plasma, and the reaction is accelerated. When atoms are formed by dissociation of the molecules in the plasma and participate in the reaction, reactions that were previously thermodynamically impossible can occur.

### Energy Flow Diagram in Plasma

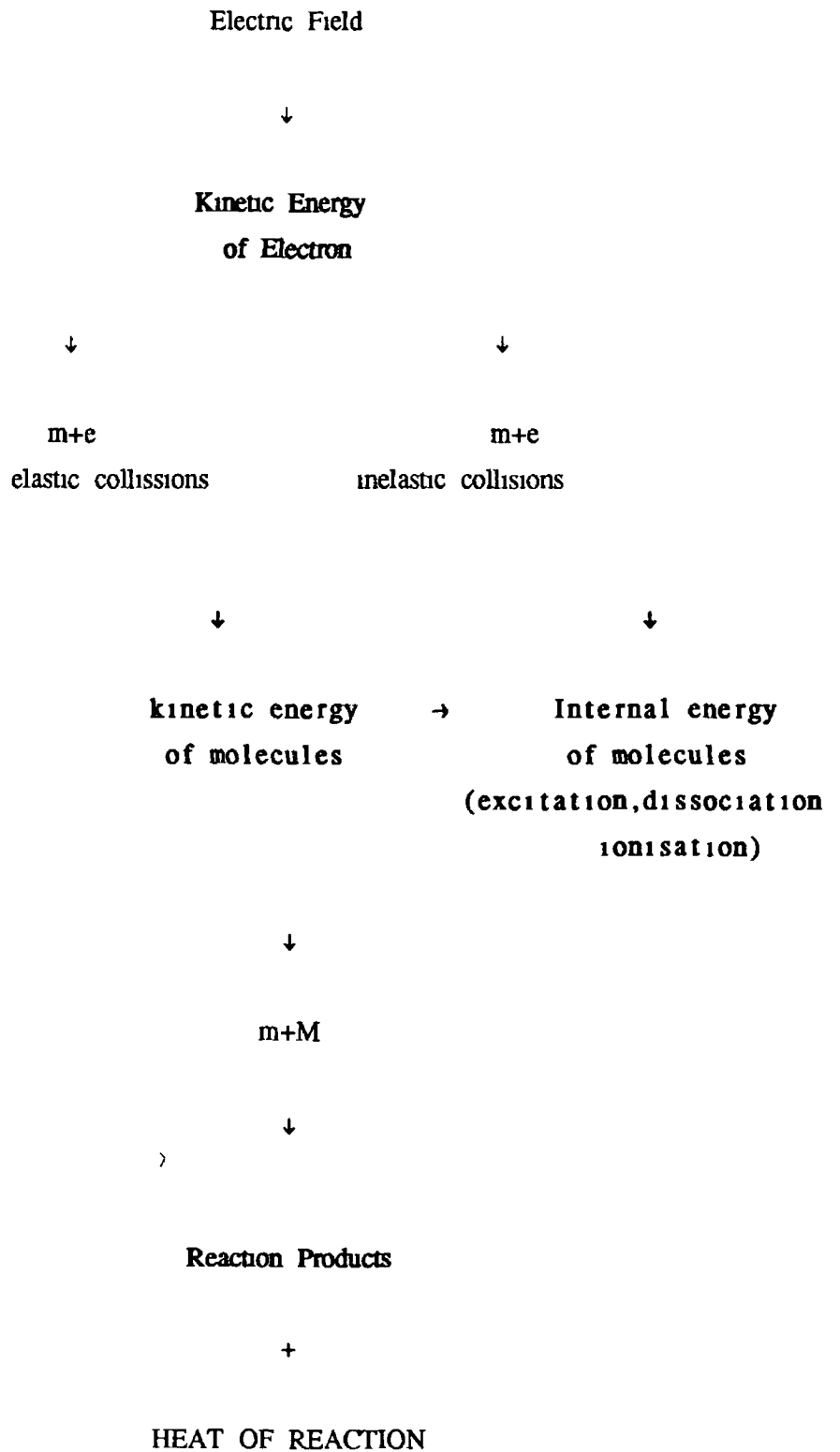


Figure 3 1

### 3.2.2 General Features of Plasma Deposition.

Electron-impact dissociation of precursor gases in the glow discharge is the primary step for chemical reactions in a plasma CVD system

Figure 3.2 [66] gives a schematic representation for the kinetic processes in a methane plasma. We consider here a model based on a set of rate equations for  $\text{CH}_4$ , and various species produced, in the plasma. Fifteen kinds of neutral species and twenty kinds of ionic species are considered in the model as shown.

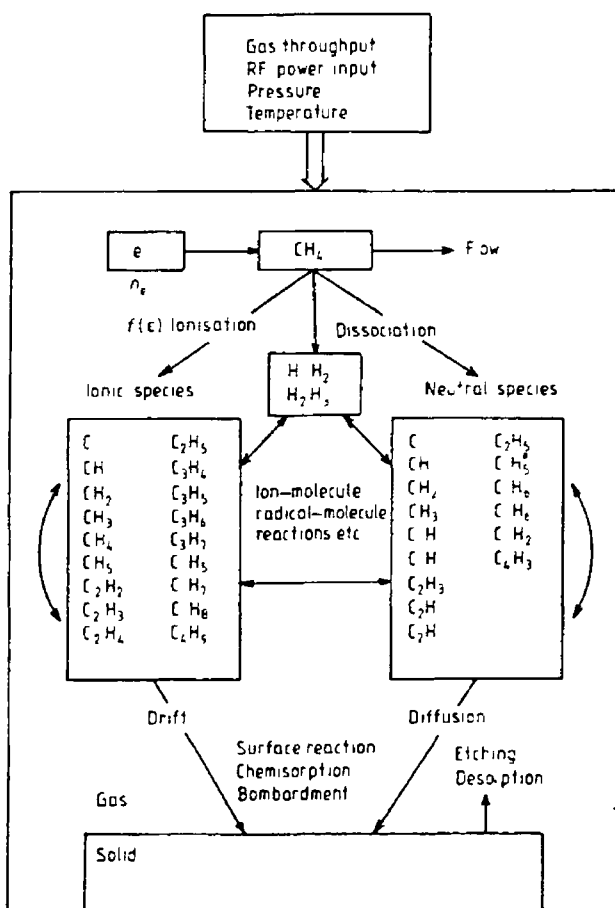


Figure 3.2 Schematic of the Kinetic Processes in a Methane Plasma

The neutral fragments (radicals), produced in the gas phase, diffuse toward the substrate and chamber wall, and ionic species move toward the electrodes under the influence of the applied field. Some of the neutral species are electronically or vibrationally excited by electron impact and emit light whose wavelength ranges from UV to IR. Secondary processes such as ion-molecule and neutral-molecule reactions take place through collisions in the gas phase. Finally, heterogeneous chemical reactions among reactive atoms, molecules and ions impinging onto surface may proceed to form a deposit.

### 3.2.3 Deposition Variables

Many variables must be controlled in plasma deposition, such as power, total pressure, reactant partial pressure, gas flow rates, pumping speed, sample temperature, electrode spacing, discharge frequency, electrode materials and reactor geometry [31,67]. These variables mutually interact [58] in determining material properties as well as deposition rates. These variables are shown schematically in figure 3.3.

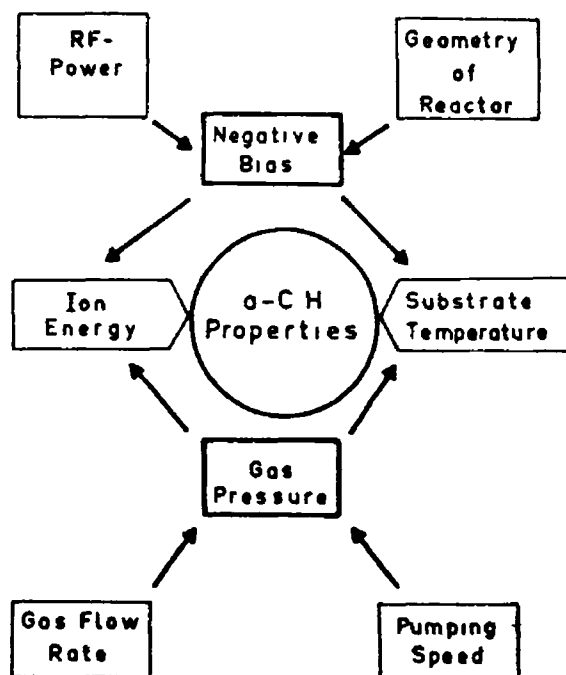


Figure 3.3 Parameters of the rf plasma deposition process

It should be noted that higher power or current results in higher electron densities in the plasma, while lowering of pressure leads to an increase of electron temperature. The decomposition reaction rate  $R_1$  is given by Bell [68]

$$R_1 = n_e k_1 [P] \quad (3.5)$$

where  $n_e$  = electron density,  $k_1$  is the rate constant for the dissociation reaction, and  $[P]$  is the concentration of the reactant. The rate constant  $k_1$  is given by

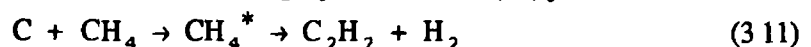
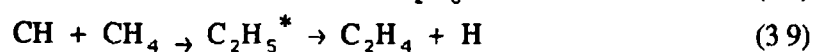
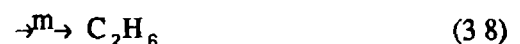
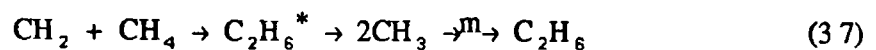
$$k_1 = (2/M_e)^{1/2} \int E^{1/2} f(E) \sigma_1(E) dE \quad (3.6)$$

where  $M_e$  is the electron mass,  $E$  is the Electron energy,  $f(E)$  is the normalised electron distribution function and  $\sigma_1(E)$  is the cross section for the reaction. Therefore, a change in the pressure or electron temperature primarily affects the rate constant of the reaction  $k_1$  in equation 1, and hence the chemical reaction pathway is often influenced by pressure, while applied electric power is basically related to the electron concentration  $n_e$ . The partial pressure of the reactant gas determines the magnitude of  $[P]$  in equation (3.5). It is evident that the deposition rate, or  $R_1$ , can be increased by increasing the power or partial pressure of the gas without changing the major pathway of decomposition reactions when the total pressure is kept unchanged. The gas-flow rate and pumping speed determine the residence time of the reactive gas in the active region of plasma. This strongly influences reaction of the gas in the active region of plasma, which in turn strongly influences the deposition kinetics. Attainment of equilibrium depends on whether or not the residence time is shorter than the characteristic time of the reaction or the overall reaction-time constant [69].

### 3.2.4 Plasma Volume Reactions

#### 3.2.4.1 Dissociation Reactions of Reactants

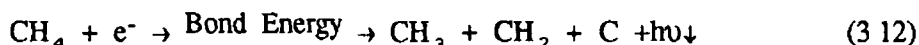
The photolytic decomposition of the gas can provide useful insights in the most probable primary processes in the glow discharge. The major reactive species [70] in the plasma of methane are  $CH_3$ ,  $CH_2$ ,  $CH$  and  $C$ .



Methyl radicals, which are mainly formed by the reaction of  $CH_2$  with  $CH_4$  are the precursors for the formation of  $C_2H_6$  (reaction 3.7). At 77k the contribution of

reaction (3.8) becomes also significant. Ethylene is formed by the reaction of CH with CH<sub>4</sub> (reaction 3.9). At 77k, a greater part of C<sub>2</sub>H<sub>5</sub> species are stabilised by the third body and n-C<sub>4</sub>H<sub>10</sub> are formed by the recombination reactions of stabilised C<sub>2</sub>H<sub>5</sub> radicals. The lifetime of C<sub>2</sub>H<sub>4</sub><sup>\*</sup> which is formed by the reaction of C with CH<sub>4</sub>, is too short to be stabilised, and it decomposes unimolecularly to acetylene and hydrogen even at 77k.

The basic reaction on the surface is given by



Existence of C must be greater than the lifetime  $\tau$  to deposit. The carbon atom must be free from reaction and in the area of the substrate long enough for C=C bands to form.

### 3.2.4.2 Electron Interaction with Atoms and Molecules

As seen it is the electrons which are mainly responsible for the ionization. The resultant products are active species, and radicals having much different chemical activities than those of the parent gas. Electron ionization processes are obviously important in the sustaining of plasma discharges. The excitation and dissociation processes are important in plasma chemistry and form the basis for PECVD and plasma polymerisation. An electron with a kinetic energy which exceeds the ionization energy of an atom, can either cause excitation or ionization as it passes in close proximity to it.

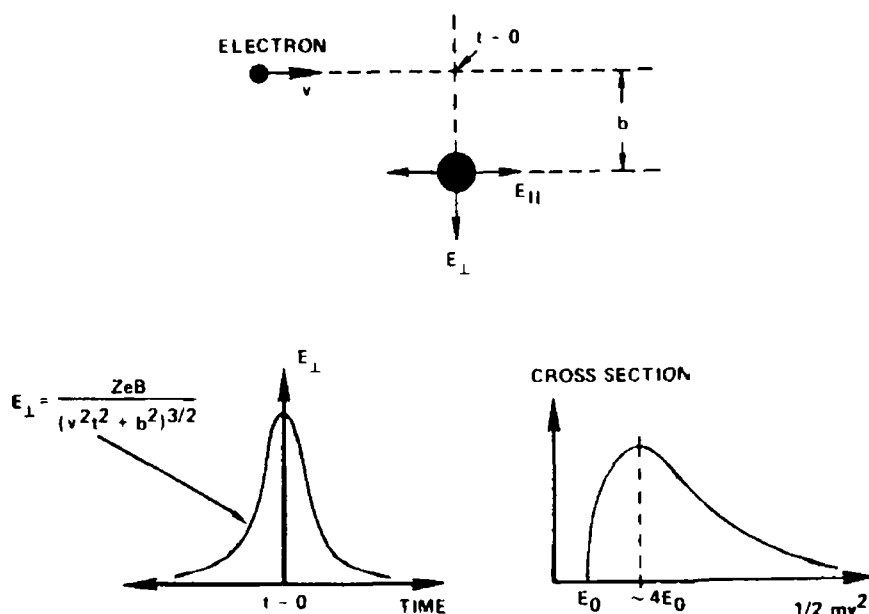


Figure 3.4 Electron-atom collision from the point of view of the virtual photon model.

The Coulomb force from the electron produces an electric field at the atom. The component of this field which is perpendicular to the direction of electron motion ( $E_{\perp}$ ) produces a time-varying "impulsive" electric field which can act on the components of the atom. This electric field pulse is equivalent to a beam of photons having frequencies corresponding to the Fourier components of the pulse. The point is that an electron passing closely by an atom does not simply knock an electron out of the atom, but produces a perturbation at the atom which is approximated by a beam of white light that induces electronic excitation and ionization in proportion to the optical oscillator strengths.

The important factor [59] is the Average energy  $W$  spent by an electron in creating an electron-ion pair. It is seen in the table 3.2 that  $W/X = 2.1$  e almost equal probability of ionization or excitation in atmosphere, but slightly more excitation in molecules, where  $X$  is the ionization potential.

Atom/Molecule	W	X	W/X
He	46	24.58	1.87
Ne	37	21.56	1.71
Ar	26	15.56	1.65
Kr	24	14.00	1.71
Xe	22	12.13	1.81
H <sub>2</sub>	36	15.43	2.33
N <sub>2</sub>	36	15.59	2.31
NO	29	9.25	3.13
CO	35	14.04	2.49
O <sub>2</sub>	32	12.15	2.63
CO <sub>2</sub>	34	13.81	2.46
C <sub>2</sub> H <sub>2</sub>	28	11.4	2.45
CH <sub>4</sub>	29	12.99	2.23
C <sub>2</sub> H <sub>4</sub>	28	10.54	2.65
C <sub>2</sub> H <sub>6</sub>	27	11.65	2.31
C <sub>3</sub> H <sub>6</sub>	27	9.73	2.77
C <sub>3</sub> H <sub>8</sub>	26	11.15	2.33
C <sub>6</sub> H <sub>6</sub>	27	9.23	2.92

Table 3.2 Probability of ionization

Electron interaction with molecules produce excitation and ionization via mechanisms essentially identical to those for atoms as described above. The difference between the atoms and molecules is what ultimately happens to the excitation energy. In the atomic case, the excitation energy is lost by radiation unless the transitions are quantum-mechanically forbidden. In the molecular case, it may result in dissociation of the molecules.

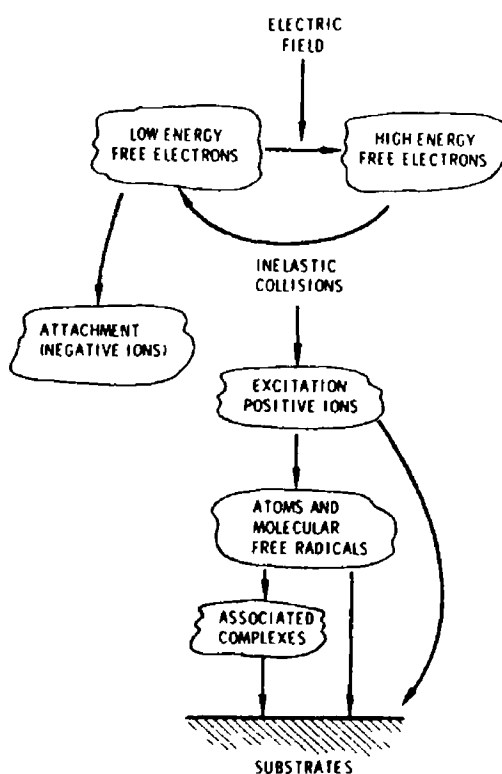


Figure 3.5 Production of Active Species

## CHAPTER 4

### NATURE OF THIN FILMS

#### 4.1 The Free Surface

A newly exposed surface's atoms relax [65] into an equilibrium configuration which differs from their bulk configuration, the surface plane often relaxes outwards, with the atomic arrangement parallel to the surface remaining unchanged. Such effects may result in the occurrence of a surface electric dipole moment. Surface electronic properties invariably differ from those of the bulk simply because the three dimensional periodic potential variation in the bulk has been disrupted. Electrons may occupy energy levels in the surface which do not exist in the bulk and this may have profound implications for the electron affinity and chemical reactivity of the surface. Also, chemical bonds may be kept "dangling" from a free surface.

Perfect surfaces are very difficult to preserve. Sputter etching, while samples are situated in deposition chamber, can be used to clean up contaminated surfaces but this will cause surface damage.

The atoms in a surface vibrate about their mean lattice positions, they are far from motionless. In fact, surface atoms tend to vibrate with amplitudes larger than those of bulk atoms because they have neighbours on one side only. If an atom requires an amount of energy  $W$  in order to move to a different position in the surface, then the probability that it will make this move is given by

$$A \exp (-W/KT) \quad (4.1)$$

As expected, surface diffusion occurs much more readily as the temperature is increased. As will be discussed later, adatom mobility is influenced by pressure and temperature, for a good film coverage high temperature and low pressure are needed.

## 4.2 Film Growth

### 4.2.1 Adsorption and Nucleation Processes

Adsorption of atoms onto a substrate surface may occur either with or without the transfer of electrons, processes which are called chemisorption and physisorption, respectively

Physisorption is the most basic phenomenon, binding energies are typically 0.25 eV and attachment is by virtue of relatively weak Van der Waals forces, which are both undirected and nonspecific

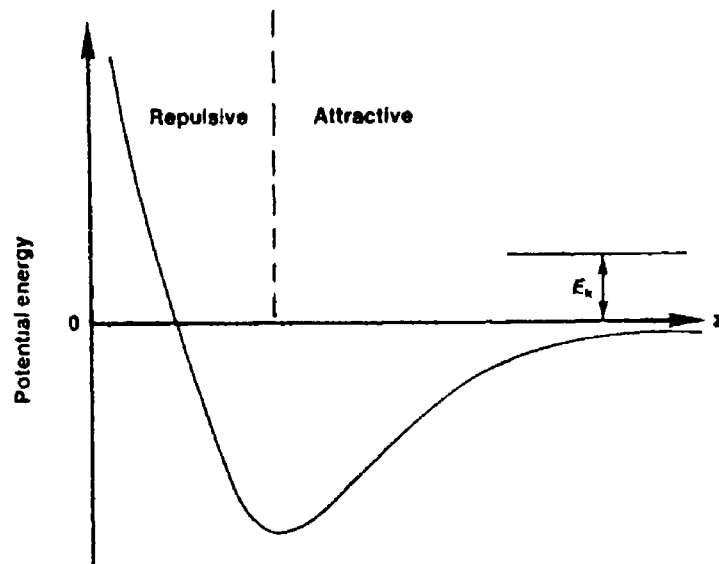


Figure 4.1 Change of Potential Energy of Physisorbing Atom.

The above diagram of figure 4.1, shows the decrease in potential energy of an atom undergoing physisorption, the atom will not remain on the substrate unless at least its kinetic energy is transferred to the surface. Such behaviour, which is reversible, is typical of inert gases adsorbing onto metals. Physisorbed species tend to desorb readily, unless very low substrate temperatures are employed.

Figure 4.2 below depicts potential energy variations during chemisorption. It can be seen that physisorption occurs as a preliminary step and that an activation energy ( $E_p + E_c$ ) determines whether this will be followed by chemisorption. In such a process which is basically the formation of a surface compound, the bonding electrons are generally thought of as occupying orbitals between the film and substrate.

Although in extreme cases pure ionic bonding may occur Binding energies are much larger than in physisorption, e.g. 8.4 eV for oxygen on tungsten, and the process is seldom reversible. The condensation of metal atoms on metallic substrates also requires electron transfer, and leads to the phenomenon of metallic bonding through the sharing of free electrons.

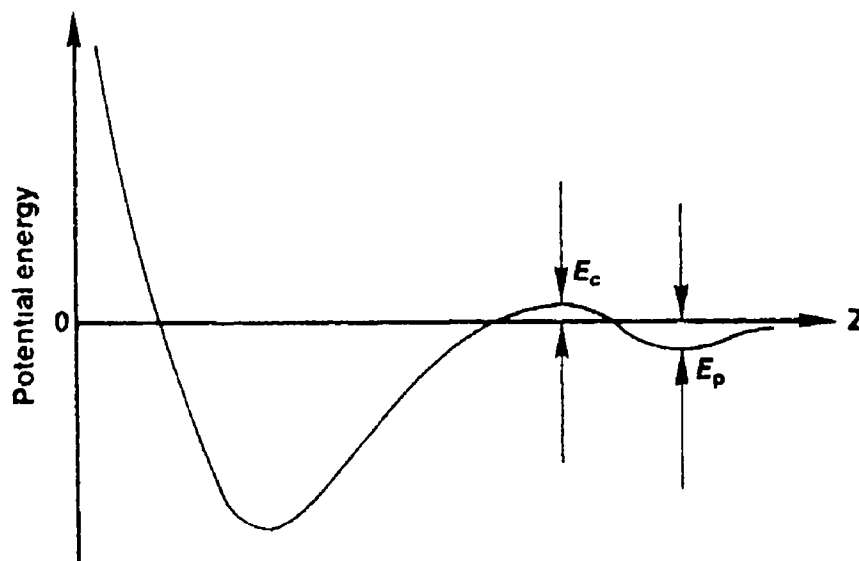


Figure 4.2 Change in Potential Energy of a Chemisorbing Atom.

The probability of an atom sticking to a surface depends usually upon the proportion of the surface already covered by adsorbates. The situation exists in which as the surface sites become filled, the probability of an impinging atom finding its own site gets smaller, and multi-layer formation does not take place. This is demonstrated in figure 4.3.

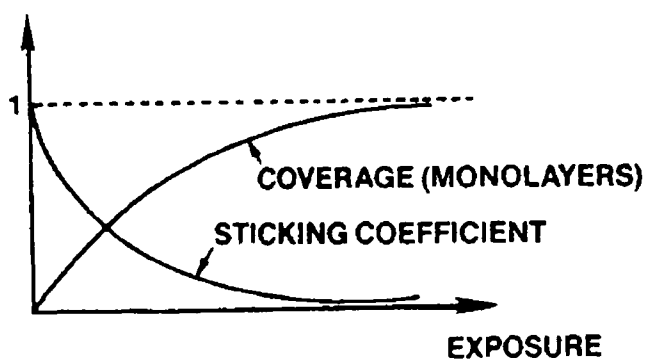


Figure 4.3 Sticking Coefficient Variation with Coverage (e.g. gas on metal)

Alternatively, figure 4.4 shows a different type of behaviour, here the sticking coefficient [67] remains constant until a monolayer has formed, when it changes to a different value as adsorption continues upon this monolayer

The basic theory of homogeneous nucleation was developed by Gibbs [72] for the case of liquid droplet condensation from a vapour. The theory shows that for molecular clusters greater than a critical size, the total free energy decreases with increasing size, so that continued growth is energetically favourable. This approach is applicable to the case of condensation on a surface provided that desorption and surface diffusion are taken into account and that only nuclei with more than 100 atoms are considered.

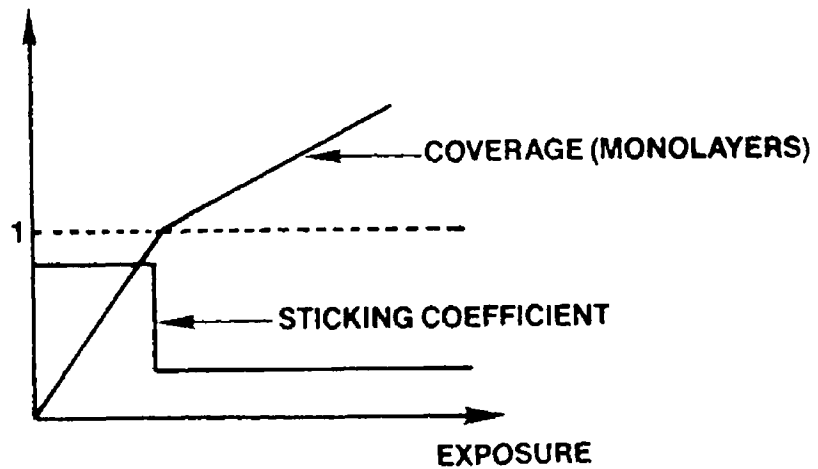


Figure 4.4 Sticking Coefficient Variation with Coverage (e.g. metal on metal)

Systems containing small numbers of molecules can be described only in terms of dynamic, as opposed to thermodynamic, variables. Since some critical nuclei apparently consist of two or three atoms, a more elaborate theory of heterogeneous nucleation must be resorted to. The atomistic model of Walton and Rhodin [72,73] predicts that the rate of formation of critical clusters depends mainly on this factor:

$$\text{Exp} \left[ \frac{(n_c+1)E_a + E_c - E_d}{KT} \right] \quad (4.2)$$

where  $n_c$  = number of atoms in a critical nucleus

$E_a$  = activation energy for desorption

$E_c$  = dissociation energy of a critical cluster

$E_d$  = activation energy for diffusion

From plots of the log of nucleation rate versus  $T^{-1}$  discrete changes in  $n_c$  have indeed been manifested at certain temperatures. The model also predicts an experimentally verified dependence of nucleation rate upon deposition rate.

## 4.2.2 The Four Stages of Film Growth

The general picture of the sequence of the nucleation and growth steps [65] to form a continuous film which emerges from nucleation theory and electron-microscopic observations is as follows

- 1 - Formation of adsorbed monomers
- 2 - Formation of subcritical embryos of various size
- 3 - Formation of critically sized nuclei (nucleation step)
- 4 - Growth of these nuclei to supercritical dimensions with the resulting depletion of monomers in the capture zone around them
- 5 - Concurrent with step 4, there will be nucleation of critical clusters in areas not depleted of monomers
- 6 - Clusters touch and coalesce to form a new island occupying an area smaller than the sum of the original two, thus exposing fresh substrate surface
- 7 - Monomer adsorbs on these freshly exposed areas, and "secondary" nucleation occurs
- 8 - Large islands grow together, leaving channels or holes of exposed substrate
- 9 - The channels or holes fill via secondary nucleation to give a continuous film

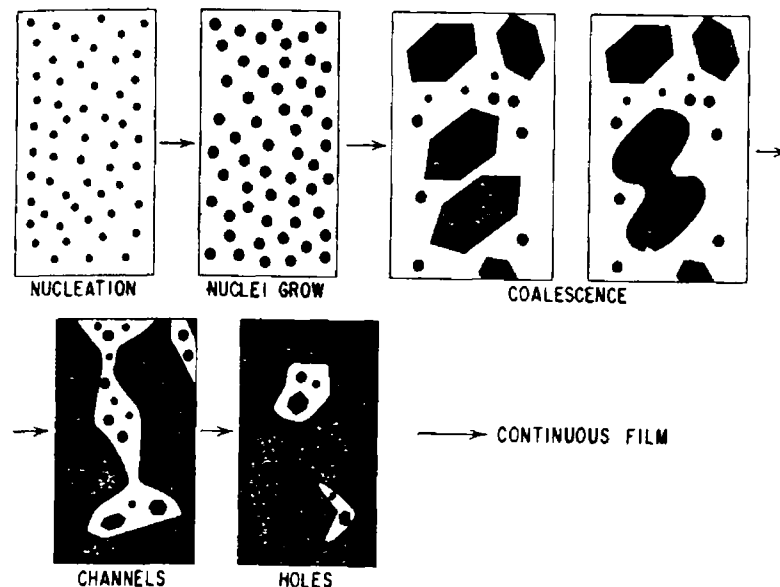


Figure 4.5 Schematic of the stages of film growth.

Four distinct stages [73] of the growth process can be clearly identified

**a) The Island Stage**

First stage observable of film growth is the sudden appearance of nuclei of similar size. This is probably because growth occurs largely by the surface diffusion of monomers on the substrate, rather than by direct impingement from the vapour phase.

**b) The Coalescence Stage**

The figure 4.6 illustrates the manner of coalescence of two rounded nuclei. The coalescence occurs in less than 0.1 sec for the small nuclei and is characterised by a decrease in total projected area of the nuclei on the substrate (and an increase in their height).

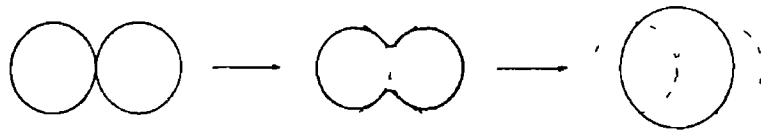


**Figure 4.6 Schematic of the shape changes during coalescence**

In addition nuclei having well-defined crystallographic shapes before coalescence become rounded during the event. After coalescence the islands assume a more hexagonal profile and are often faulted.

The liquid-like character of the coalescence leads to enlargements of the uncovered areas of the substrate, with the result that secondary nuclei form between the islands. This effect becomes noticeable when the primary islands have grown to about 1  $\mu\text{m}$ , and continues until the final hole-free film is formed. A secondary nucleus grows until it touches a neighbour, and if this happens to be a much larger island, the secondary nucleus coalesces very rapidly and becomes completely incorporated in the large island. The coalescence behaviour is best explained by surface diffusion.

**c) The Channel Stage**

As the islands grow, there is a decreasing tendency for them to become completely rounded after coalescence. Large shape changes still occur, but these are

confined mainly to the regions in the vicinity of the junction of the islands. Consequently, the islands become elongated and join to form a continuous network structure in which the deposited material is separated by long irregular and narrow channels of width 0.05 to 0.2  $\mu\text{m}$ . As the islands coalesce, bare regions are exposed. The liquid-like behaviour of the deposit persists until a complete film is obtained. In the channel and hole stages, secondary nuclei (islands) are pulled into the more massive regions of the film.

It is clear that both the liquid-like behaviour of coalescing nuclei and the rapid elimination of channels are manifestations of the same physical effects, namely the minimization of total surface energy of the overgrowth by the elimination of regions of high surface curvature.

#### **d) The Continuous Film**

During the coalescing stage, orientations are set and islands align to each other. The continuous film stage signifies the end of the nucleation stage. The film continues to grow at a rate determined by the sticking coefficient of the deposited material.

### **4.3 Surface Reactions**

Surfaces in contact with plasmas are bombarded by electrons, ions and photons. The electron and ion bombardment is particularly important. The relative number of ions and electrons which are incident on a surface depends on whether it is biased as a cathode or anode or is electrically isolated.

#### **4.3.1 Ion Bombardment**

The momentum exchange associated with ion bombardment can cause rearrangement and ejection (sputter) of surface atoms. The rearrangement can have dramatic effects on the structure and properties of a growing film, and is of importance in the processes of ion plating and bias sputtering. The ejection is important in the processes of sputter cleaning and deposition.

Ion bombardment can greatly influence the processes involved in the adsorption of molecules into surfaces and their subsequent reactions. These processes are of obvious importance in plasma-enhanced CVD and etching and in plasma polymerisation. The process of molecular adsorption and surface compound formation are directly influenced by ion bombardment.

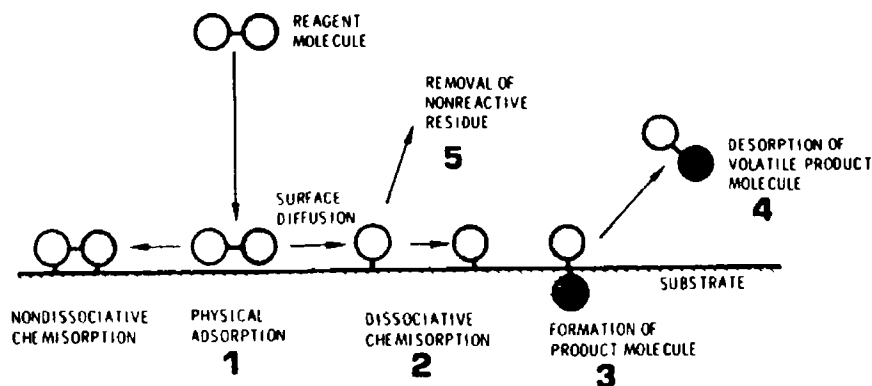


**Figure 47 Schematic representation of surface chemisorption and volatile compound formation in gas phase etching.**

The CVD case with the formation of a non-volatile product is obviously very similar. Physical adsorption is due to polarization (Van der Waals) bonding. It is a non-activated process and occurs with all gas surface combinations under appropriate conditions of temperature and pressure. Adsorption energies are typically less than 0.5 eV. Chemisorption involves a rearrangement of the valence electrons of the adsorbed and surface atoms to form a chemical bond. It involves an activation energy and has a high degree of specificity between gas surface combinations. Adsorption energies are typically 1 to 10 eV. Molecules may be chemisorbed in their molecular state or may dissociate into atoms. The latter case is known as dissociative chemisorption. Dissociative chemisorption is generally a precursor to compound formation, which is also an activated process. Various types of chemisorption bond sites can exist on a solid surface. Thus both molecular and dissociative chemisorption can occur simultaneously on the same surface. Ion bombardment can influence these processes in the following ways

- 1- Ion bombardment can cause adsorbed molecules to dissociate, thereby overcoming the activation energy for this process. Ion bombardment dissociation is expected to be a sputter-type momentum transfer.
- 2- Ion bombardment can create surface defect sites, which have reduced activation

energies for the occurrence of dissociative chemisorption or for the formation of a solid compound

3- Ion bombardment can remove (by sputtering) foreign species from a surface. Such species may interfere with the dissociative chemisorption of a preferred species

#### **4.3.2 Electron Bombardment**

Electron bombardment of atoms and molecules adsorbed on surfaces is believed to produce excitation and ionization in processes which are similar to those which occur in the gas phase. Thus atoms are ionized and also excited into states from which there is a probability of dissociation or bond rearrangement. Electron bombardment can dissociate molecules and cause them to pass into a form that has a high probability of desorption (electron-stimulated desorption). Finally, electron-induced bond rearrangement can cause polymerisation of adsorbed surface species

#### **4.3.3 Preferential Sputtering and Initial Etching in an R.F. Plasma**

##### **I Initial Substrate etching**

As long ago as the 1950's Holland and Ojha [89,74] among others reported on the possibility of growing diamond like carbon films by cracking a hydrocarbon gas in an R.F. discharge and by extracting the ionised hydrocarbon fragments on to a negatively biased substrate. Yet still, no model of the reaction between the incoming hydrocarbon and substrate can be fully developed as the process is extremely complex. In the process of normal sputtering, the sticking coefficient for the impinging carbon fragments is greater than the sputtering yield for the same fragment. This means that the cracking products of the butane plasma have a larger possibility to condense carbon on the substrate surface than to sputter off carbon from the substrate surface

In order to verify this description, Andersson and Berg [75,76] studied experimentally the interaction between the butane plasma and different substrate materials. It was found that the ionized cracking products of the butane plasma, in fact, initially sputter etched the substrate surfaces. The etch rates correspond closely to what could be expected from the sputtering yield values of the substrates. The sputtering yield from carbon, however, is low, and thus the substrates after some time will be totally covered by a carbon film that prevents further etching of the underlying substrate. The results of such a process are drawn schematically in figure 4.8

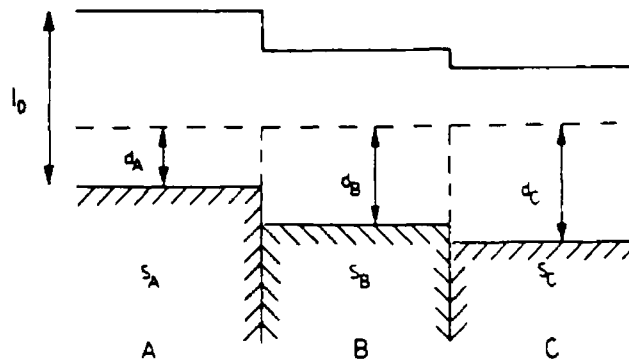


Figure 48 Subsequent etching of substrate materials and the deposition of a carbon film.

The substrate contains three regions of different materials A, B and C, with sputtering yields  $S_A$ ,  $S_B$  and  $S_C$ , respectively. After some time the surface will be covered with a carbon film of thickness  $l_0$ , evenly distributed all over the surface. However, during the initial growth of  $l_0$  sputter etching of the surface took place, thereby etching  $d_A$ ,  $d_B$  and  $d_C$  away from regions A, B, and C. The thickness  $d_A$ ,  $d_B$ , and  $d_C$  of the material removed depends on the sputtering yield  $S_A$ ,  $S_B$  and  $S_C$  of the substrate material A, B, and C.

H. Norstrom and R. Olafson [77] found similar results. They related the partial pressures and gas type to the initial etching. The ratio oxygen/hydrocarbon gas and argon/hydrocarbon gas that resulted in zero deposition/etching was determined. The ratios obtained clearly indicate that chemical reaction is the dominating mechanism in the case of oxygen-mixture but pure physical sputtering is dominant in an argon mixture.

## II Preferential Sputtering

The preferential sputter hypothesis was first advanced by Spencer et al [78]. Tetrahedrally bonded ( $Sp^3$ ) structures are assumed to be more resistant to sputtering than trigonally bonded graphitic precursors. The ion flux to the growing surface serves both as a source of new material and as an agent for re-sputtering non- $Sp^3$  structures e.g. graphitic, olefinic and cumulene nuclei. This hypothesis is supported by the relative energies of the various processes.

The energies of importance to carbon film growth [32] are listed in table 4.1. It is noticeable that the typical impact energies, from 50 to 500 eV, are just above the sputtering threshold for carbon, at the reported displacement energies, and very significantly below the energy where the sputter yield is greater than unity. These considerations indicate that both sputtering and deposition take place simultaneously during film growth.

### ENERGIES OF VARIOUS PROCESSES

ITEM	ENERGY (eV)
Ion energy for C when self sputter yield = 1	2000
Ion energy for C, sputter yield = 0.15 with $Ar^+$	600
Displacement energy of carbon atoms in Diamond	80
Approximate Energies of incident ions	50-500
Displacement energy of Carbon atoms in graphite	25
Threshold energy for graphite sputtering	15
Intraplanar bond energy in graphite	7.43
Bond energy of diamond	7.41
C-H bond energy	3.5
Interplanar bond energy in graphite	0.86

Table 4.1

Furthermore, the bonding energy of graphite precursors to the surface would be closer to the interplanar bond energy (0.86 eV) than to the intraplanar bond energy (7.43 eV), making the probability of sputtering of these nuclei more likely. Typical

sticking coefficients of approximately 0.13 => 0.5 found by experimentors [44,49] are consistent with a mechanism involving simultaneous sputtering and deposition

Also of interest is the C-H bond energy, which is significantly less than the C-C bond energies. Furthermore, low mass atoms are sputtered more efficiently than high mass atoms. Hydrogen should therefore be preferentially sputtered from a carbon surface. Mori and Namba [79] found that when ion beams derived from methane were used at impact energies greater than 200 eV, the hydrogen content could be reduced to low values. Carbon has an anomalously low sputter yield compared to other materials. This unusual behaviour permits a wide range of conditions under which preferential sputtering of hydrogen and hydrocarbon structures can be expected to occur.

#### 4.3.4 Role of Hydrogen

The trend throughout the literature seems to be toward the addition of hydrogen gas to the hydrocarbon gas. It has been suggested [80,81] that at least 95% of the gas mixture needs to be hydrogen for two main reasons: 1) Reduction of hydrogen-carbon groups with a lower concentration of  $\text{CH}_2$ , 2) Chemical erosion of graphite by hydrogen impact.

Classically the hydrogen atoms can attain high speeds within the plasma. The collision of these H atoms into the hydrocarbon molecules can cause C-H bonds to be broken. There is evidence that hydrogen incorporation lowers the density of carbon films [87]. This is not primarily a mass effect, but reflects the reduction of cross linking due to hydrogen incorporation.

The main scientific instrument to determine C-H groups on films grown on silicon wafers is Infra-red Spectroscopy [52,54,74] which has revealed that dense a-C:H films [82] (amorphous Carbon-Hydrogen) contain mainly CH groups with a lower concentration of  $\text{CH}_2$ . In less dense films additional  $\text{CH}_3$  groups have been observed. Angus and Jansen [83] defined "Diamond-Like Films" as films with hydrogen atom fractions from 0.5 to 0.6 which select a structure with an average coordination number close to the theoretical value at which stabilisation by bonding and destabilization by strain energy are balanced. This coordination number is achieved by the incorporation of the hydrogen and by the presence of trigonally ( $\text{Sp}^2$ ) bonded carbon in the carbon skeletal network. The question of optimum cross linking in a covalent random network has been treated by Phillips [84,85]. He considered the mismatch between bonding constraints and the degrees of freedom in three dimensions, showing that an

average coordination number of

$$m = 6^{1/2} = 2.45 \quad (4.3)$$

represents the best compromise between mechanical stability (due to cross linking) and stress minimisation (due to minimal bond length and bond angle disorder)

A significant quality of hydrogen is its ability to chemically erode graphite [86]. Although graphite is more thermodynamically stable in a PECVD system, diamond growth is made possible because hydrogen erodes graphite and is less likely to erode diamond. The displacement energy of carbon atoms is substantially higher than the carbon atoms in graphite (80 eV), compared to 25 eV respectively. The process of hydrogen etching the graphite is complex and not fully explained. In most diamond growth environments, hydrogen gas must be kept above a certain concentration (95%) to deposit films with nearly no graphitic component.

## 4.4 Structures of Carbon Forms

### 4.4.1 Introduction

The term "structure" [88] encompasses a variety of concepts which describe on various scales, the arrangement of the building blocks of a material. On an atomic scale, one deals with the crystal structure, which is defined by the crystallographic data of the unit cell. These data contain the shape and dimensions of the unit cell and the atomic positions within it. They are obtained by x-ray diffraction experiments.

On a coarser scale, one deals with microscopic observations of the microstructure which characterises the sizes, shapes and mutual arrangements of individual crystal grains. It also includes the morphology of the surface of the material.

An intermediate range is occupied by the defect structure, which is concerned with deviations of the regular arrangement of unit cells within one crystal grain, examples are point defects, dislocations and stacking faults. In studying the defect structure, one makes use of both direct microscopic (mainly electron microscope) observation and diffraction evidence. In addition, one can utilise measurements of structure sensitive properties which are related to defects in crystals, e.g. resistance due to point defects and impurities.

### 4.4.2 The Carbon Atom and the Nature of the Carbon - Carbon Bond

To determine the structure of carbon [89], one needs to look at the ways in which carbon atoms can be connected together to form a solid material. There are three possible configurations of the outer electrons when a carbon atom is bonded to others.

1) Tetrahedral or  $Sp_3$  state. In this state all four electrons are bonded into four evenly spaced hybrid orbitals. The most probable positions for the surrounding four atoms would then be at points which form a tetrahedron with the carbon nucleus at the centre. The  $\sigma$  bonds formed with four neighbours will then be at  $109^\circ 28'$  to each other. There are no electrons available to form subsidiary  $\pi$  bonds.

An example of tetrahedral carbon atoms bonded together would be in the gas ethane ( $H_3C-CH_3$ ) which is at the start of a homologous series culminating in the long chain polymer polyethylene, consisting of a chain of methylene ( $-CH_2-$ ) groups. Such carbon atoms can be bonded in three dimensions to form the cubic diamond.

lattice, thus producing a hard crystalline solid.

2) Trigonal or  $Sp_2$  state In this state three electrons are bonded in a symmetrical hybridised orbital system. The most probable positions for the orbital axes are coplanar and mutually at  $120^\circ$ . The extra electron is in the free p state and is available for forming a subsidiary  $\pi$  bond.

An example of carbon atoms bonded together in the trigonal state would be the gas ethylene  $CH_2=CH_2$ .

All graphitic materials consist of extensive parallel sheets of such carbon atoms arranged in such a pattern. Polymeric carbons are also made up of  $Sp_2$  atoms but arranged to form networks of long, narrow, entwined graphitic ribbons.

3) Diagonal or  $Sp$  state This is the state with symmetrical hybridised orbitals whose electrons are capable of being bonded in a molecular orbital bonding system. The only possible arrangement for neighbouring carbon atoms is on either side of the nucleus, the  $\sigma$  bonds being colinear and the co-ordination number being two. The remaining two electrons are in the free p state and are available for forming subsidiary  $\pi$  bonds.

Examples of molecules containing carbon atoms in this state are the gas acetylene ( $HC\equiv CH$ ) and "carbyne" ( $C\equiv C$ )<sub>n</sub> which consists of chains of  $Sp$  carbon atoms.

The bond energy between carbon atoms and their separation depend on the number of electrons contributing. The bond energy between two carbon atoms in the  $Sp_3$  state is  $83 \text{ kcal mole}^{-1}$ , and the distance between is 1.54 Angstroms. This is so in such widely differing molecules as ethane, polyethylene and diamond.

With carbon atoms in the  $Sp_2$  state the extra p electrons increase the bond energy and decrease the atomic spacing. These changes are attributed to an increase in "percentage double bond character". Thus the C-C distance in ethylene is 1.353 Angstroms. There exists a range of possible interatomic distances from 1.54 to 1.35 Angstroms depending on the degree of participation by the extra electrons. The bond energy is increased to  $147 \text{ kcal mole}^{-1}$  for the case of ethylene. With atoms in the  $Sp$  state, there is a further increase in bond energy and reduction in interatomic distance.

There exists a variability in bond distance within a molecule containing carbon atoms in the  $Sp_2$  and  $Sp$  states. This is important in that carbon-carbon bond

distances are not necessarily characteristics of the presence of carbon in any one of the possible states

An important factor is the ability of carbon atoms to rotate about a C-C bond. If the partners are in the  $Sp_3$  state and the bond is purely  $\sigma$  in character, rotation is easy and a high degree of flexibility in molecular orientation is possible. If the bond has any  $\pi$  component, however, rotation is severely hampered and a much more rigid inflexible structure is inevitable.

The bonds between the molecular units (the intermolecular cohesion) can only be weak Van der Waals forces since no electrons are left over to form strong primary bonds. The small molecules or units will therefore be gases and liquids at room temperature. Polyethylene chains can be sheared past each other and oriented easily by cold work at room temperature. Perfect graphite sheets slide over each other easily at room temperature and will do so even down to 10 K. Diamond incorporates just one extended unit and so is extremely hard. Polycrystalline graphites and carbon must also have covalent cross-links between graphite sheets in neighbouring crystals in order to exist as covalent materials of significant strength.

#### 4.4.3 Structure of Carbons

There are only two crystalline forms of carbon - graphite and diamond. Graphite consists of sheets of carbon atoms in the  $Sp_2$  state, each sheet being stacked in a hexagonal ABA sequence above each other as in figure 4.9.

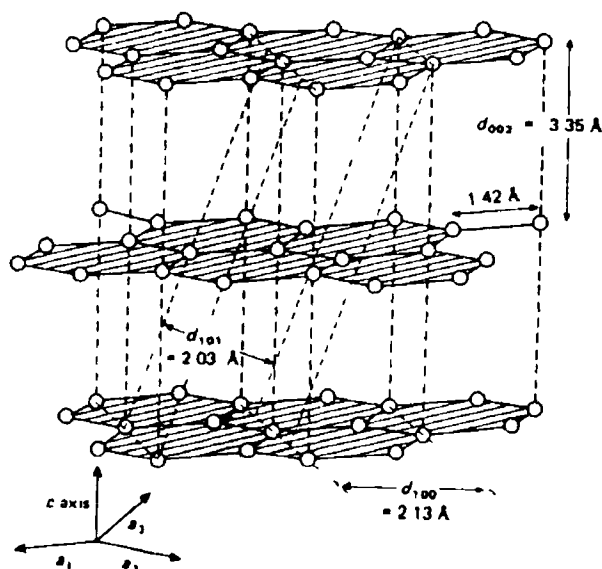


Figure 4.9 Atomic structure of a perfect graphitic crystal [88]

The bonds in the basal plane are extremely stiff and strong and so the modulus in a-directions is very high, the material can withstand temperatures of 33000 °C before breaking up by thermal degradation alone. The bonds between the planes are of weak Van der Waals type and so the crystal can be sheared and cleaned easily in the plane perpendicular to the c-axis even at very low temperatures. The distance between carbon atoms in the sheets is 1.42 Angstroms while between perfect sheets the interlayer Spacing is 3.354 Angstroms. Graphite can be distorted permanently with ease by simply bending or shearing the sheets.

When carbons are formed at low temperatures they contain many grown-in defects because thermal energy is not then sufficient to break carbon-carbon bonds once formed. The presence of such defects increases interlamellar cohesion considerably and so such carbons are generally hard. The overall morphology of the graphite sheets is also laid down during carbonisation. Simple annealing at high temperature does not destroy this morphology.

Diamond consists of carbon atoms in the tetrahedral state bonded to accommodate all electrons without distortion, the carbon atoms fitting into the classic diamond type cubic lattice, consisting of two interpenetrating cubic (F) lattices based on 000 and  $\frac{1}{4}\frac{1}{4}\frac{1}{4}$ . Since all the bonds are equally strong and stiff, distortion is very difficult. It is possible to introduce dislocations and plastic flow at high temperatures but the structure will not tolerate the high degree of distortion possible in the graphite structure. Hence, diamond is only found in the crystalline state and the lattice constants never vary. This contrasts with graphite in which the interlayer spacing can be varied easily and with the quasicrystalline states of some carbons which are quite stable.

Because of the strong covalent bonding which prevents easy glide on all possible planes, diamond is hard and brittle. It reverts to graphite merely by heating above 1800 °C in an inert atmosphere. It is concluded that at such temperature the  $Sp_2$  state is much more stable than the  $Sp_3$  state. Small distorted volumes of carbon in the  $Sp_3$  state will clearly revert at much lower temperatures than large perfect crystals.

#### 4.4.4 Structure of Polymers

Polymers [90] consist of long chains held together by intermolecular forces of different amounts and intensities depending on the nature of the groupings attached to the chains and their ability to lie parallel to each other to form crystalline regions.

Some polymers, such as atactic polystyrene lack symmetry so that it becomes

impossible for the chains to pack closely they can only exist as polymeric glasses with no crystallinity whatsoever. The chains are arranged completely randomly in space and can, in fact, be described quite adequately by three-dimensional random walk theory [88]. Above the glass point, such materials are rubber-like - a condition in which chain segments are free to move by thermal activation to allow the free chains to assume a limitless number of configurations between fixed points, which are generally physical entanglements in thermoplastic materials and chemical cross-links in thermo-setting materials. Others, such as polythene, with a symmetrical arrangement of hydrogen atoms, crystallise easily. Crystalline regions consist of straight chain segments of polymer lying parallel to each other and separated by a constant distance. They are thus highly anisotropic, the strong and stiff covalent bonds only affecting the strain response in one direction (along the chain length). The strength and stiffness in all other directions are governed only by weak intermolecular cohesion. In high tensile polymer fibres all the crystalline regions lie approximately parallel to each other with the chains lying parallel to the fibre axis, and thus show a high degree of preferred orientation. In isotropic polymers the orientation of these essentially anisotropic crystallites is completely random and there is continuity of C-C bonding from one crystallite to another, usually via an "amorphous" zone.

In recent years it has been demonstrated that in many crystalline polymers, the polymer chains cluster together to form "fibrils" or "microfibrils". The crystalline regions detected by X-rays are merely parts where fibrils happen to be taut. The full extent of a fibril is therefore not revealed by X-rays but only by the new technique of high resolution electron imaging.

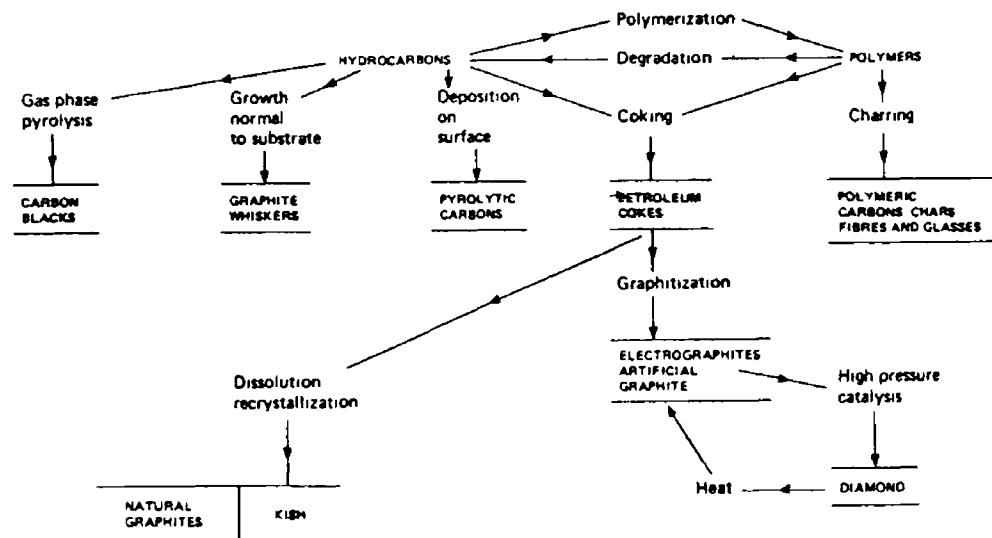


Figure 4.10 The Various forms of Carbon [88]

## 4.5 Structure of Thin Films

The microstructure of thin films [65] depends on many factors. Some of the most important are

- \* Rate of Deposition of condensing atoms
- \* Pressure of working gas
- \* Temperature of substrate
- \* Substrate surface roughness
- \* Bombardment of substrate with ions or electrons

### 4.5.1 Deposition Rate

It may be experimentally very difficult to isolate the influence of deposition rate per second from the influences of other deposition variables. For example, increasing the RF power to the chamber will raise the energy of atoms on the surface. Hence they will be more mobile on the substrate surface, which is equivalent to raising the substrate temperature. It has been found that the occurrence of voided structures is less likely at low deposition rates, because the adatom surface mobility is adequate to prevent holes from forming [91].

Under normal conditions, pure metallic films invariably have a crystalline structure. This may not be true of alloys and compounds, however, since the impinging atoms and molecules have considerably reduced surface mobilities. The influence of deposition rate on crystallinity [92] is difficult to predict. The texture of metallic films is known to be related to the kinetic energy of the incident particles.

### 4.5.2 Pressure, Temperature and Surface Roughness

The influence of pressure, temperature and substrate surface roughness on film structure was considered in a famous article by Thornton [93]. Basically, higher inert gas pressures are thought to limit the mobility of adatoms upon the substrate surface, inert gas atoms are themselves adsorbed and hence limit the surface diffusion of arriving species. Increased substrate temperature, on the other hand, enhances surface mobility and also conventional bulk diffusion. Thornton's model is depicted schematically in figure 4.11. In zone 1, protuberances on the adsorbing surface preferentially collect incident atoms which, because of low substrate temperature, do not have sufficient thermal energy to diffuse away and form a continuous structure.

Film growth in Zone 1 tends to yield open, i.e. porous, grain boundaries. In Zone T, the temperature is still too low to permit diffusion at significant rates, but the surface here is considered smooth because enough diffusion has occurred to overcome the main surface irregularities, the dense fibrous structure is the same as that within the open grains of Zone 1. At low deposition temperatures an increase in inert gas pressure promotes the growth of a more porous structure through the detrimental effect on surface mobility described above. Inert gas adsorption and its consequences are lower temperature phenomena. Zone 2 is dominated by surface diffusion processes, in this region the film generally consists of columnar grains with fully dense boundaries. The high temperatures defining Zone 3 produce substantial bulk diffusion, re-crystallisation and grain growth may, therefore, take place in this regime.

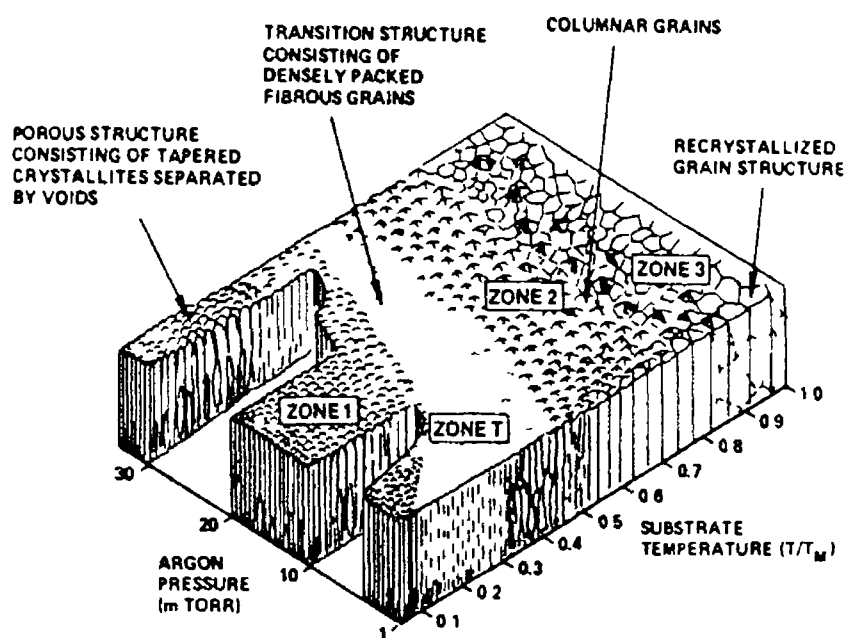


Figure 4.11 Influence of substrate temperature and argon pressure on the microstructure of thin films. [93]

Changes in substrate temperature during the deposition process may cause the formation of "hillocks". These features occur as a result of differences in thermal expansivity between the film and substrate materials. They consist of small projections normal to the film surface, or in the case of 'negative' hillocks, of holes. For example, if deposition commences on a cold substrate of relatively low expansivity and heating takes place as deposition continues, the initial deposit will 'want to' expand more than the small expansion of the substrate permits, the outcome is a relief of the compressive stress in the film by the "pushing up" of hillocks. Figure 4.12 illustrates precisely this situation for the case of aluminium or silicon. Addition of copper to Al growth can reduce hillocks. Also, periodically introducing oxygen

during film growth produces alternate layers under tensile (pure aluminium) and compressive (aluminium oxide) stress, and hence leads to an overall reduction in film stress

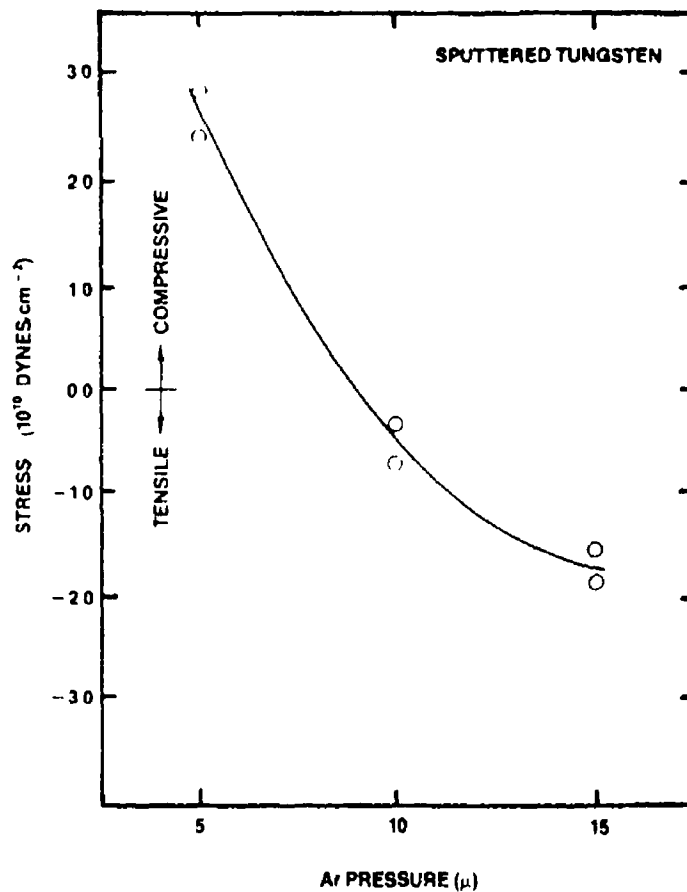


Figure 4.12 Influence of argon pressure on stress in sputtered tungsten.

#### 4.5.3 Influence of Substrate Bias

If thin film deposition is accompanied by high energy electron bombardment, an increase in the density of nuclei on the substrate surface is found to occur. This phenomenon is apparently due to the creation of defects which act as nucleation centers, since electron bombardment has no effect on substrates for which the energy required to create surface defects is very high.

Thin films are often subjected to ion bombardment during growth, primarily for redistribution of deposited materials to areas that would otherwise be difficult to coat. Of course, increasing the energy of bombarding ions will eventually produce a net sputter erosion of the film, but sputtering yields are generally so low with ion energies below 100 eV that the deposited mass will remain virtually constant. Bias of the substrate may also affect the crystal orientation [65] and preferential sputtering of certain planes.

For a particular film morphology it has been recognised that substrate temperature and bias voltage play inverse roles [94]. "High temperature" deposits may be obtained at low temperatures provided that substrate bias is employed. Also, at high bias conditions large levels of inert gas entrapment may occur.

## 46 Stresses in Thin Films

Stresses in thin films result from two basic causes

- 1 Distortion of the crystal lattice leading to so called "intrinsic stress"
- 2 A difference in thermal expansivity between the film and substrate materials, leading to the development of stress upon cool-down from the deposition temperatures

The origin of thermal stresses is easy to comprehend. Intrinsic stresses, on the other hand, are more complex in nature and may be due to a variety of causes

- a) Lattice mismatch between the substrate and film inevitably leading to interfacial distortion
- b) Incorporation of impurities in the growing deposit which precludes the growth of a perfectly ordered, strain-free lattice
- c) Rapid film growth, which does not allow sufficient time for the formation of a defect-free lattice
- d) In the sputtering-off of already deposited atoms by impinging atoms and ions

Highly stressed films are generally more susceptible to corrosion and are more likely to exhibit poor adhesion. Film stress may be compressive (i.e. the film would like to expand, parallel to the surface), so that in extreme cases it may buckle up on the substrate. Alternatively the film may be in tensile stress (i.e. the film would like to contract), and in certain cases the forces may be high enough to exceed the elastic limit of the film so that it breaks up. A tensile stress will bend it so that the film surface is concave, and a compressive stress so that it is convex. Ways of measuring this stress depend mostly on this fact and include disk techniques, bending-beam, etc. Many factors influence the stress developed and the most important of these are [95]

### I Deposition Rate

Relevant data is rather ambiguous, but defects caused by rapid deposition are the definite causes of stress

## II Pressure

It has been postulated that one of the main contributions to the tensile stress in an evaporated film is the annealing and shrinkage of disordered material which has been buried during further deposition. The mechanism proposed to explain the increasing compressive stress with reducing pressure is based upon the higher mean free path of sputtered atoms and energetic neutral inert gas atoms at lower pressures. It is proposed that such energetic particles arrive at the substrate and pack the deposited material more closely by a type of compressing "atomic peening" interaction.

Figure 4.13 [96] shows the kind of behaviour which is invariably observed, i.e. a transition from compressive to tensile stress as the pressure is increased through a critical point.

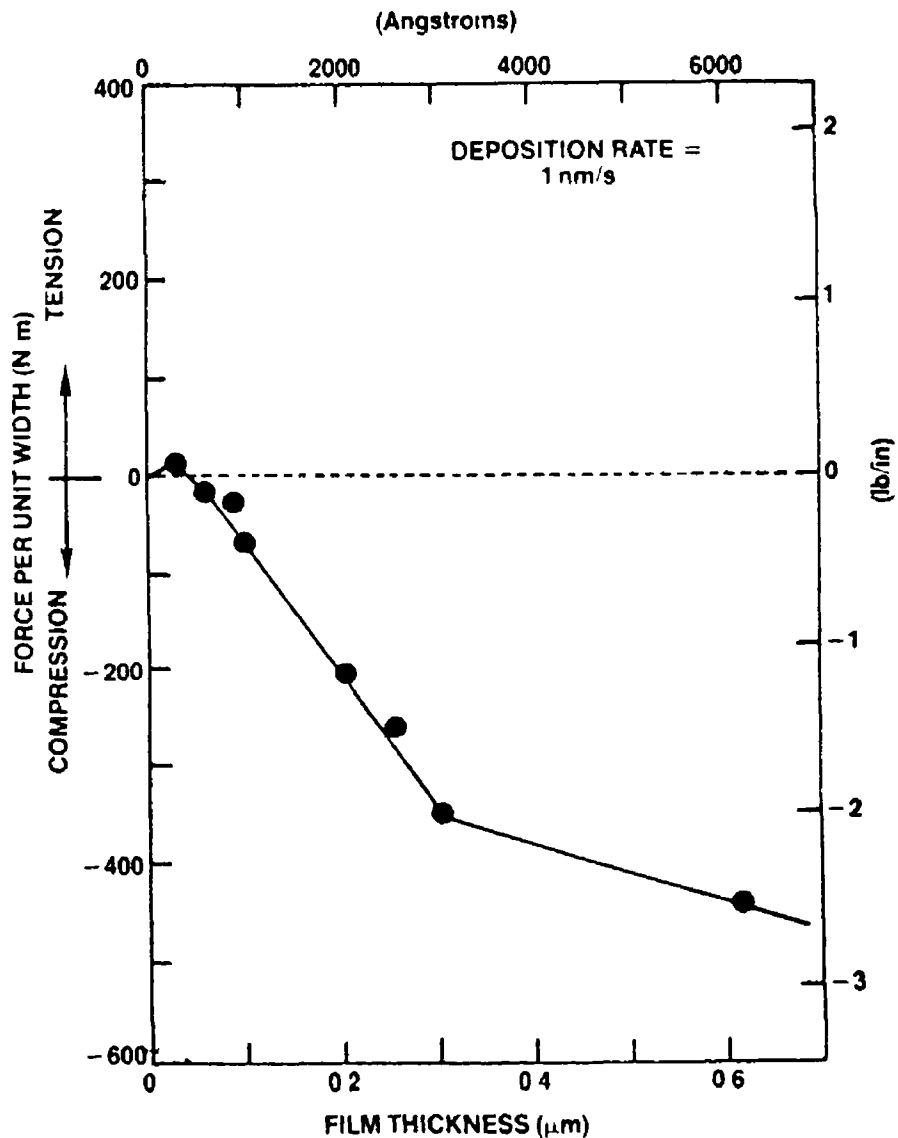


Figure 4.13 Force per unit width vs Film thickness for sputtered chromium

### III Thickness

It is well known that the stress in a thin film varies with depth, a phenomenon well evidenced by the fact that films frequently curl upon removal from their substrates. Such behaviour may reflect a change in the film structure with depth. The film may begin to grow with the lattice constant, of the substrate and with gradually accumulating strain energy, until eventually a thickness is reached at which dislocations are introduced and the film relaxes to assume the lattice constant of the bulk.

### IV Substrate Bias

Negative substrate bias would seem to have the same general effect as reducing the working gas pressure, namely of introducing more and more compressive stress as the voltage is made more negative. The application of negative bias usually influences the amount of gas incorporated in the growing deposit.

Gas species film composition and incorporation of argon and hydrogen have all been investigated and effects on internal stress studied. In an article by D Nir [95] the compressive stresses in the films were attributed mainly to the bombarding energy of the ion beam. An additional contribution to the compressive stresses probably came from the complex species in the discharge. The contribution of the hydrogen to the stresses in the films did not seem to be obvious.

### V Other Influences

Other factors which may influence the stress in a thin film in a complicated way are, contamination of the film during growth and variations in substrate temperature. Interstitial impurities may migrate to regions of high strain energy (vacancies, dislocations and grain boundaries) and relieve the stress in those regions. Indeed, it has been shown that oxygen co-deposited with evaporated aluminium migrates over long periods at ambient temperatures to the film substrate interface [97]. The incorporated oxygen conferred compressive stress on the aluminium.

Higher substrate temperatures may cause diffusion. If one material diffuses into another such that vacancies flow in the reverse direction, then one side of the interface will gain mass while the other will gain porosity. The former will consequently develop compressive stress and the latter tensile stress. This situation may result in plastic deformation within the interface, and to recrystallisation and grain

growth

Higher substrate temperatures may also result in a larger grain size and a lower level of intrinsic stress. The reduction in stress when higher temperatures are employed is believed to be related to the higher rate of annealing of disordered material, for minimal stress, this obviously must be greater than the rate of deposition.

#### 4.7 Adhesion of Thin Films

Adhesion [65] may be defined as the sum of all the inter-molecular interactions between two different materials placed side by side. These interactions [89] may be metallic, ionic, covalent, Van der Waals, etc., and are a function of the separation of the adhering surfaces [98].

If the work functions of the opposing surfaces are different, charge transfer from one to the other will occur upon contact. This will result in an electrostatic attraction, which actually varies much more slowly with distance than the attraction due to Van der Waals forces. It has been demonstrated experimentally that in some cases charge transfer has a substantial effect on adhesion and it is felt that the long range nature of the electrostatic force may be particularly significant.

Substrate surface roughness may also be important. Increased roughness may promote adhesion because of the larger surface area involved as well as through the type of interlocking illustrated in figure 4.14. Excessive roughness on the other hand can result in coating defects which may promote adhesion failure.

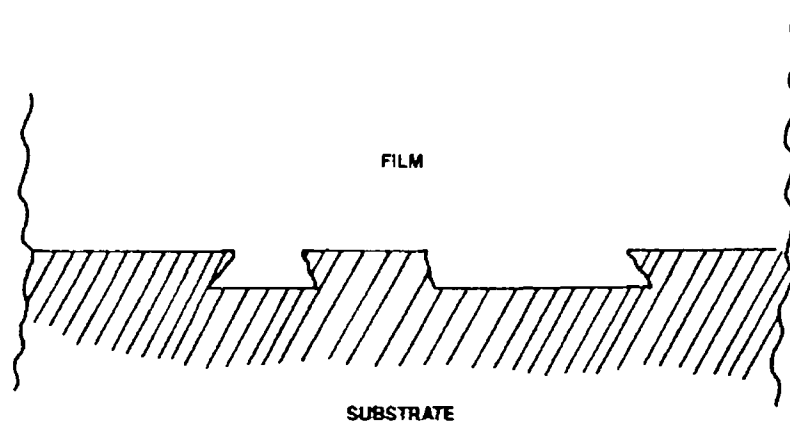


Figure 4.14 Mechanical interlocking of film and substrate

In many film coatings, intermediate layer adhesion is used. This may chemically match film and substrate. This may be in the form of an oxide coating or, for example, with titanium nitride (TiN) films a thin layer of titanium is first applied to the substrate. An intermediate layer of mid-way thermal expansivity coefficient material is often used to index match film to the substrate.

#### 4.7.1 Control of Adhesion

Factors which are known to strongly influence thin film adhesion [65] are the intrinsic stress in the film and the cleanliness of the substrate surface prior to deposition.

As far as substrate cleaning is concerned, weakly bound species such as oils and grease may impair adhesion, as materials which act as a barrier to diffusion when diffusion is necessary, for example, an oxide coating.

Contaminants may be removed by conventional chemical means and by sputter etching techniques. It was found that best surfaces for adhesion were: 1) Polished mechanically to a surface finish of at least  $6\ \mu\text{m}$ , 2) Ultrasonically cleaned for half an hour; 3) Argon plasma sputter etched in the chamber for at least forty-five minutes.

There may be a connection between the stress to which a thin film is subjected and its adhesion to the substrate. Generally, however, the intrinsic stress in a thin film is not adequate to cause delamination unless the film is very thick. Failure will occur at the weakest point, which may alternatively be a breakdown of the substrate or film cohesion.

## CHAPTER 5

### DESIGN AND IMPLEMENTATION OF PLASMA DEPOSITION SYSTEM

#### 5.1 Types of Deposition Reactor

A typical PECVD system [31] consists of a plasma generating section, a gas introduction section, a vacuum system, a power source, and a control system with adequate metering to establish the various parameter values. Rf plasma CVD equipment can be classified into inductive and capacitive coupling types, based on the method of exciting the reactive gas.

The inductive coupling method consists of a tube of quartz glass wrapped in a coil, to which the rf signal is applied, thus generating a plasma within the tube. This structure has the following properties:

- 1) The structure is small and simple.
- 2) Contamination from coil to plasma is minimised.
- 3) Power is concentrated and a high density plasma is formed, although it is difficult to maintain this density across the complete substrate.

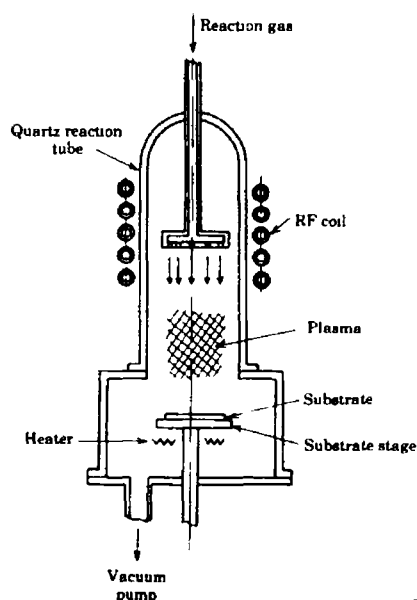


Figure 5.1 Inductively Coupled Reactor

The capacitive coupling method was shown in figure 1.1. The advantages are that of both coating distribution and high productivity. The parallel plate reactor is most commonly used for material processing. The design is basically the same as first constructed by Remberg [67]. In his system a circular electrode is placed parallel to an rf electrode. The gas flows from the top electrode down over the substrate and off the sides. It is the intention to compensate for the electric field gradient from the centre of the electrode toward the edge by the gas concentration distribution and thus obtain a uniform film.

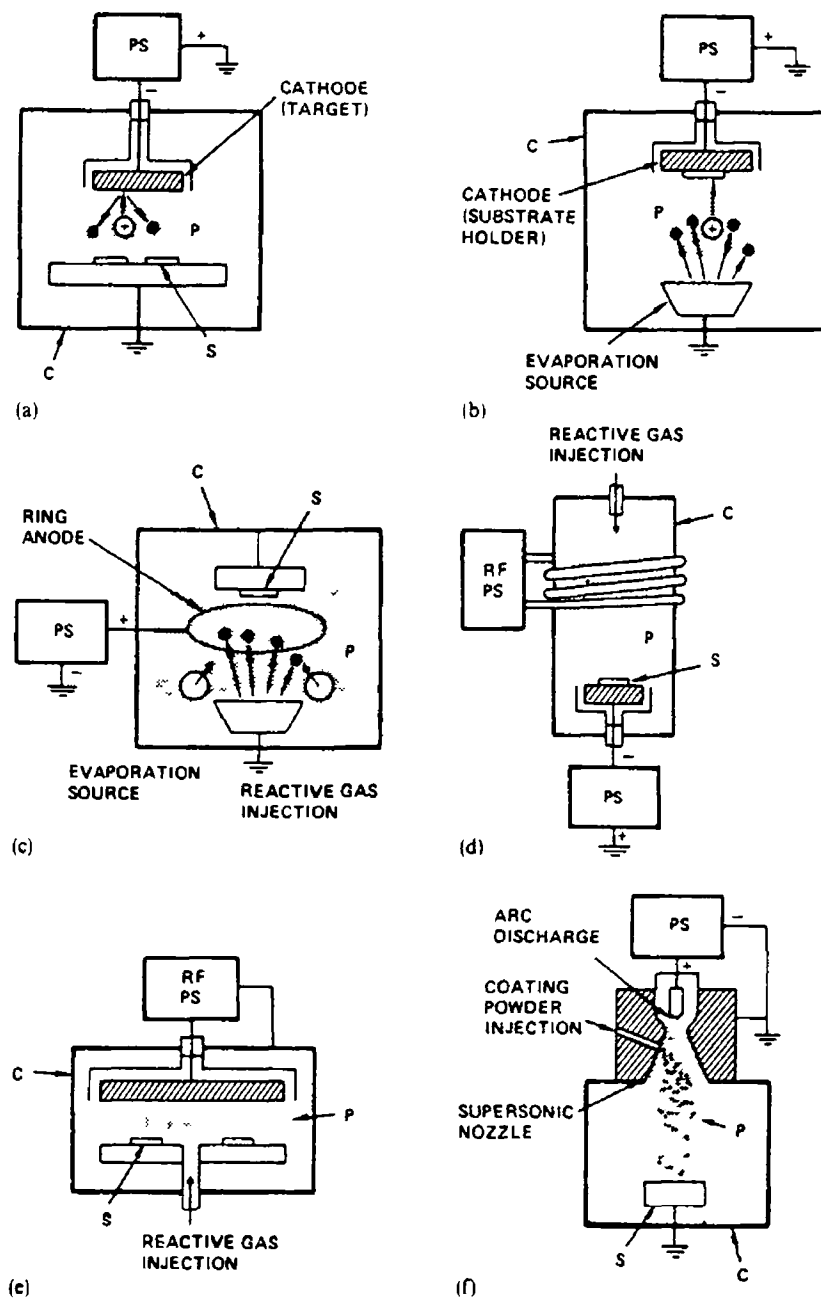


Figure 5.2 Configurations used in PECVD [99]

## 5.2 Components of PECVD System

There are many deposition variables which need to be controlled or monitored. Very many of these parameters have direct film characteristic relationships. A general rule of thumb used in the design was to monitor as much as possible and as accurately as possible. Close attention was paid to the practical considerations for rf plasma deposition systems and to possible future applications in the research laboratory. The reliability of the unit must be high for maintenance of quality. This means that the capacity of each component element should be stable and the reliability should be high.

### (i) Pumping System

The pumping system must be able to evacuate the chamber down to  $10^{-6}$  mbar to eliminate any impurities, especially water moisture. Reactive and decomposed gases can be either corrosive, flammable, or toxic. Since a large quantity of diluted gas or carrier gas is used, exhaust gas after the reaction contains a large amount of unreacted gas. Hydrogen gas for instance can lodge in pipes and pumps and forms an explosive mixture with air. Exhaust pipes should be of non-permeable type and rising from the chamber, with no drops or bends.

a) Type of Pump The type of pump used varies with the pressure range and gas load. A rotary oil pump backing a diffusion pump is the usual arrangement.

b) Protection of Pumping System

- 1) Foreline Trap, In order to prevent damage to the pump by granular materials or condensable materials, a filter, a trap, or a baffle is used between the pump and the system.
- 2) Oil Replenishment, When an oil rotary pump is operated for a prolonged period, microparticles or nonreacted materials enter the oil, gradually increasing its viscosity and rendering it useless. Regular checks and periodic changes of the oil can prevent this.
- 3) Back-streaming of oil and contamination of chamber; If the oil rotary pump or diffusion pump are operated for extended periods below 0.1 mbar, the pump oil can back-stream toward the high vacuum region. Measures must be taken to prevent this, such as not operating on rotary pump alone below 0.1 mbar and using a liquid nitrogen trap at the top of the diffusion pump.
- 4) Removal of Pollutants, If toxic gases are involved they should be suitably scrubbed before release to atmosphere. If highly inflammable or explosive gases are used the gases should be diluted with an inert gas such as nitrogen, before release to the atmosphere.

### **(ii) Electrodes and Substrate Holders**

The electrode is used to form the plasma, and the substrate support is used to hold the substrate in place and maintain it at a given temperature. The shape and structure of the substrate support determine the operability of the unit and its production capacity. The substrate support should have the following properties and functions [31]

- 1) Support samples beneath top electrode
- 2) Supply rf power to the cavity
- 3) Concentrate plasma by the use of Debye Shields
- 4) Externally heat the substrate
- 5) Be adjustable in height and position.
- 6) Made of a material that does not absorb too much heat or interfere with the plasma
- 7) Made of a noncorroding material
- 8) Dimensional integrity should be maintained during thermal cycling
- 9) Sputtering yield should be small
- 10) Made of a cheap and machinable material

In most carbon deposition systems the self biasing technique of the substrate electrode is used. This means the electrode must be electrically isolated. All deposition techniques require external heat to be applied to the substrates, this can be done by hot filament, infra-red or radiant heat sources.

As was mentioned in section 2.2, the electrodes must also incorporate dark space shielding, to confine the plasma and to prevent loss of power.

### **(iii) R.F Power Source**

This is probably the most difficult part of the apparatus to design and install. The rf source consists of three main parts [100] (1) Oscillator (2) Power Amplifier and (3) Impedance matching network.

The film characteristics will be directly effected by its plasma density. Important aspects of the rf design are A) Power of rf source B) Transmission of rf to electrodes C) Cable and Chamber attenuation and D) Effective tuning to the impedance of the cavity. The generator must be able to supply sufficient power to dissociate the gas. The frequency chosen is 13.56 MHz. The signal must be clear and reproducible, with minimal reflected power. The stability of the power source is critical, since between runs of varying parameters, only one variable must change and absolute control over all other variables must be maintained.

A fully equipped power source will have the following controls/functions

- \* AC on/off
- \* Variac for variable power control
- \* Manual switches for tuning, one for each phase and load
- \* Forward/reflected power indicators
- \* Appropriate protection circuitry
- \* Power meters

#### **(iv) Gas Introduction System**

The supply of the reactive gas and its control are important. The parameters to be controlled [101] are 1) gas composition 2) flow rate 3) pressure and 4) temperature. The number of reactive species in the gas plasma is related to the gas density of the system. Gas density is a function of volume, pressure, and temperature. In order to hold the quality of the film constant, it is necessary not only to maintain constant pressure, but to prevent changes in the flow rate. The system must be accurate and reliable for all depositions. Reproducibility of the exact gas flow conditions are critical.

#### **(v) Control and Monitoring Systems**

The control can be divided into two separate areas. One part monitors the various parameters necessary for deposition i.e. pressure, flow rate, substrate temperature etc. The other part may monitor each process of deposition and sequencing. It would be the former type that will concern this design. Due to the rf interference with electronic monitors it was found that analogue controls offered isolation, independence and immunity to stray rf. It is necessary to know exactly the stages of system dynamics related to film growth.

#### **(vi) Pressure Measurement**

The PCVD reaction is usually in the range 0.1 mbar to several mbars. Single gases or a mixture of gases may be used at any one time. The sensitivity of vacuum gauges utilising thermal conduction or ionisation changes may vary with the type of gas. Also the gauge can corrode due to a corrosive gas atmosphere. Reliability of the pressure gauge is very poor [102] as often the pressure is just below atmospheric level where gauges are inaccurate. Ideally a diaphragm gauge would be used which is independent of gas used and gives an absolute pressure reading.

### 5.3 Design Criteria for Deposition System

Before the design [103] can be drawn up the limitations of the project along with the goals must be specified

**Frequency** The licensed international standard for rf plasma deposition is 13.56 MHz. Any operation outside of this frequency is in breach of the broadcast and licensing authorities act.

**Rf Shielding** Along with the need to protect the system's own electronic circuitry there is a legal obligation not to pollute the airwaves or electric mains with rf noise.

**Flexibility** Any research apparatus must be capable of adapting to a change in project direction. This is particularly important when the technology is unknown and several minor projects may also use the primary apparatus in fulfilling the overall project objectives, for example spectral monitoring of the plasma reactions requires that special optical ports be provided to the chamber.

**Simplicity of Design** Ideally the design should use standard components and fittings. This allows the easy addition of equipment and reduction in cost. Generally complex designs of components and fittings to the system should be avoided.

**Load size** The system should be able to take a range of substrates so that several different film tests may be carried out e.g. glass, steel, silicon etc. Also the area of the top electrode should be much larger than the substrate holder, so that plasma and hence the uniformity is maintained. This limits the size of the substrate holder.

**Process Cycle Time** Cycle time for a plasma system is limited by the temperature stabilisation which is the time required for a large thermal mass (the electrode assembly) to reach deposition temperature. Plasma deposition systems must incorporate specially designed heating systems that can rapidly heat the electrodes to the process temperature, or use electrodes that are never thermally cycled.

**Deposition Rate** Deposition rate increases with applied power. The deposition rate is limited by the gas phase reactions with acceptable rates being about 500 Angstroms per Hour. For a given spacing, electrode geometry and frequency, there is a unique power at which the plasma intensity across a parallel plate will provide uniform deposition. Deposition times should be at most six to seven hours for practical use.

**Within-substrate Uniformity** In plasma enhanced CVD systems this is controlled by plasma uniformity across the surface of the substrate. With electrodes much larger than the size of the substrate, within-substrate uniformity is easily achieved. With electrodes of a size comparable to the substrate, the field is higher at the edges of an electrode when high frequency rf power is used. This increases deposition rates at the edges and leads to nonuniformity in film coverage.

**Reproducibility of Depositions** In order that conclusive results can be drawn from operating parameters, the parameters must be stable and reproducible from deposit to deposit.

**Cost** As with all high technological areas, components and equipment are very expensive. This increases the need to make the system as flexible and durable as possible. The costs may also limit the designer's choice in materials and labour available.

The raw materials for carbon films are very cheap i.e. methane and hydrogen, which makes the process very attractive in the long term for large-scale commercial production.

#### **5.4 Initial Trial Reactor**

In facing a new technological field of science, the best knowledge is gained by trial and error, so it was decided to build an initial deposition system. This proved most beneficial for the following reasons:

- \* Rf generator could be developed on a capacitive load
- \* Substrate holder could be developed
- \* Inlet gas nozzle and top electrode plate was perfected
- \* Rf shielding techniques and filtering proved necessary
- \* Range of parameters and degree of control needed was gained
- \* Effect of different gases on film properties
- \* Confirmation that the rf generator was capable of dissociating the hydrocarbon gas
- \* Idea for the range of parameter settings for hard films

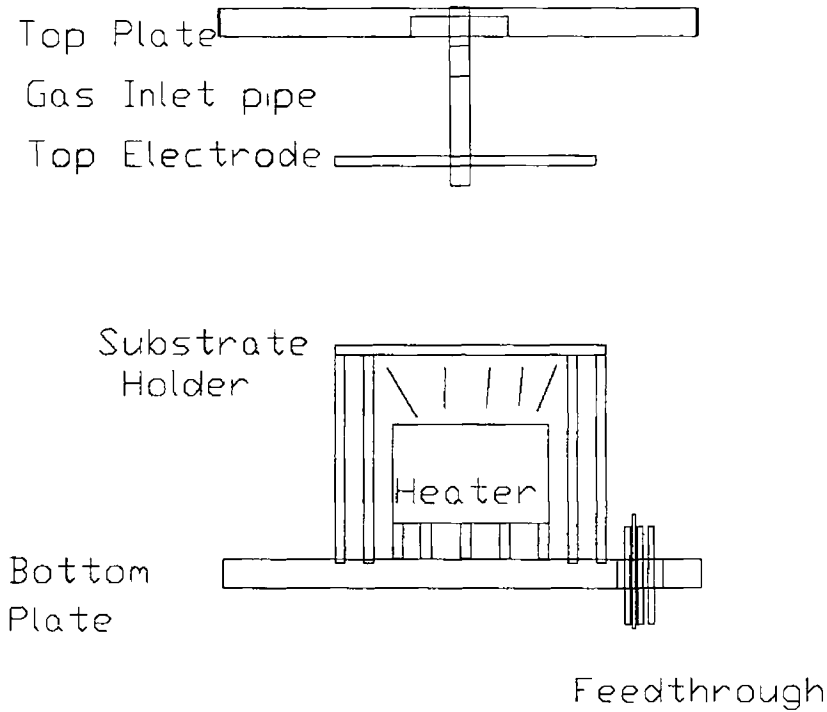


**Figure 53 Trial Reactor**

#### **5 4 1 Deposition Apparatus**

The chamber consisted of a 8" diameter glass tube, 6" in height, with polished steel plates on either end as shown in figure 5 3 The pumping system consisted of a four stage rotary pump directly coupled beneath the chamber The gases were controlled by in line needle valves and meters and piped directly into the top of the chamber, through a 1/4 " stainless steel tube The top electrode, was a circular aluminium of 50 mm in diameter The substrate holder was an aluminium plate with insulating supports and a high intensity light bulb cradled beneath to provide substrate heating Additionally an electrical and thermocouple feed-through enabled substrate temperature to be applied and controlled, respectively

## 5.5 R.f Power Generator

### 5.5.1 Specifications

The function of the generator is to supply rf power to the chamber in order to excite the gas into a plasma state. The generator, at a rf frequency of 13.56 MHz, has an electrical power input of 100 watts to the power amplifiers. This low power, is compensated for by the fact that the substrate area is small ( $1.96 \times 10^{-3} \text{ m}^2$ ), hence the power density is quite high.

The rf generator consists of the following parts 1) Power supply 2) Oscillator 3) Driver Circuit 4) Power Amplifier and 5) Impedance matching network.

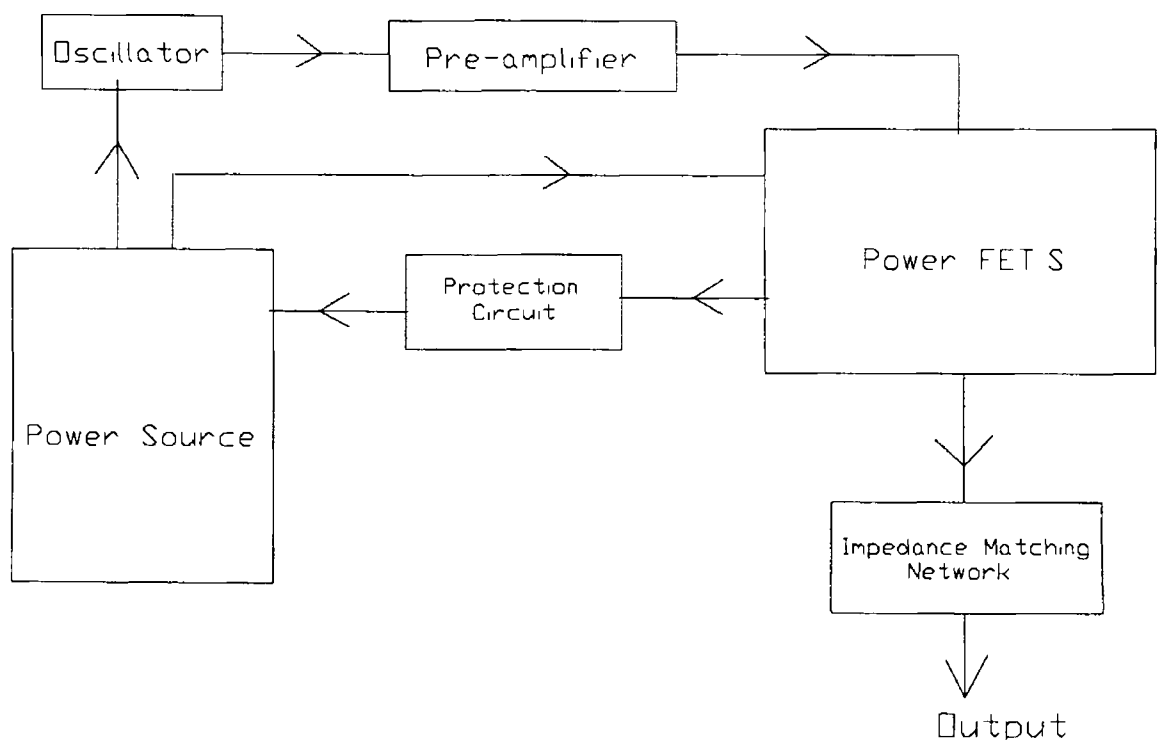


Figure 5.4 R.F Generator Components

### 5.5.2 Impedance Matching

Electrical theory [104] reveals that maximum power in d c circuits will be transferred from a source to its load if the load resistance equals the source resistance. In dealing with a c or time-varying waveforms the maximum transfer of power, from its source to its load, occurs when the load impedance ( $Z_L$ ) is equal to the complex conjugate of the source impedance. When the source is said to drive its complex conjugate, it is simply the condition in which any source reactance is resonated with an equal and opposite load reactance.

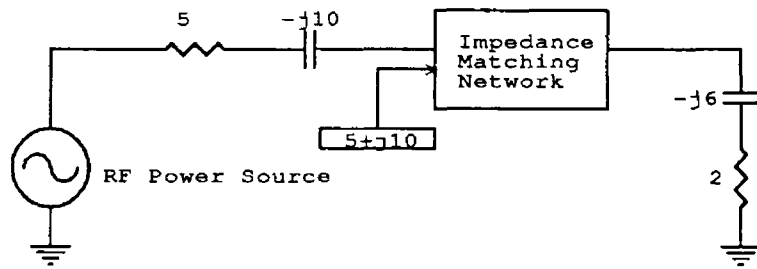


Figure 5 5 Impedance Transformation

There are many possible networks which could perform this task. The best known is probably the L network. This network receives its name because of its component orientation which resembles the shape of an L.

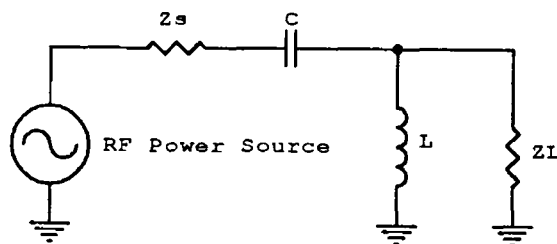


Figure 5 6 The L Network

The fixed inductor, L, is connected in series with two variable capacitors. This allows the varying of L by adding or subtracting an opposite reactance.

### 5.5.3 Complex Loads

In designing the matching network [105] of an rf generator to a load, one assumes ideal resistive loads for example 50 ohms. In practice the load may not be a real impedance. The plasma cavity's impedance is a function of the pressure, area, power, gas type, etc and can change dramatically depending on the process parameters. Transistor input and output impedances are almost always complex, that is they contain both resistive and reactive components ( $R \pm jX$ ). Transmission lines, sources and loads are no different in this respect.

There are two basic approaches in handling complex loads

- 1) Absorption To absorb any stray reactances into the impedance matching network itself. This can be done through prudent placement of each matching element such that element capacitors are placed in parallel with stray capacitances, and element inductors are placed in series with any stray inductances.
- 2) Resonance To resonate any stray reactance with an equal and opposite reactance at the frequency of interest.

The impedance matching network utilises both approaches. In its implementation a lot of the refinement is through a process of trial and error. The L network was used to match parts of the internal circuitry of the generator. The matching arrangement that was chosen between the generator and the chamber [106] is shown in figure 5.7

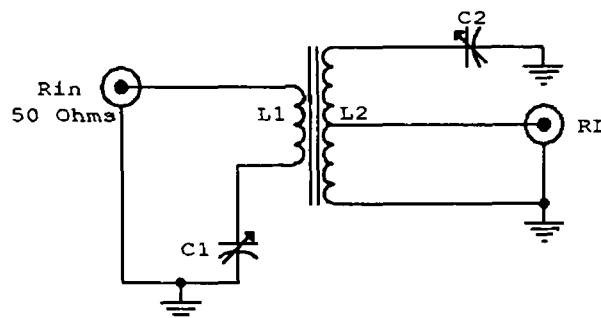


Figure 5.7 Unbalanced Bandpass Network

This network utilises the advantages of harmonic suppression characteristics and is described as a tunable transformer arrangement. The tunable transformer network was used to match the output to the chamber, which has external switches on the generator cabinet for manually tuning to the plasma impedance. This circuit was chosen because it gave a wide band of tunable impedances and offers the facility of grounding the output, if so desired.

#### 5.5.4 Matching to Coaxial Feedlines

At the transmitter end of the coaxial feedline, the impedance that the output transistor actually sees is not only a function of the chamber's resistance, but also is a function of the length of the coaxial feedline. It is extremely difficult to estimate the actual input impedance of any transmission line unless the line is terminated in its characteristic impedance i.e. 50 ohms. This is hardly ever the case when driving practical plasma discharge cavities, so the matching network must be tunable over a wide range of impedance values.

The attenuation of the signal through a coaxial will increase when the line terminates into a load other than 50 ohms. The increased attenuation is given by [92]

$$A_a = A(\rho^2 + 1/2\rho) \quad (4.1)$$

A = Initial Attenuation

$A_a$  = Final corrected value of attenuation

$\rho$  = Voltage standing wave ratio VSWR

The power losses can be dramatic and have unpredictable changes in system power calibration. It is most important to use the appropriate cable of low attenuation to rf signals.

## 5.6 Design of Components in Carbon Film Deposition System

### 5.6.1 R.f Shielding

In order to prevent loss in plasma power [107] and interference with electrical equipment great care must be taken to properly screen the rf signals [108]. The following are the steps taken to achieve this:

- 1) Rf generator was enclosed in a suitable metal box, with no gaps greater than 3 mm.
- 2) All coaxial cables to the chamber were grounded, and the length of these cables was as short as possible.
- 3) Rf filtering was necessary on the electrical mains to prevent mains contamination. If possible an independent mains source should be used for the rf power generator.
- 4) A true ground source was used.
- 5) All ground lines were arranged in a star network with the common earth at the centre. This was done to prevent an electrical spike going to ground via a piece of equipment.

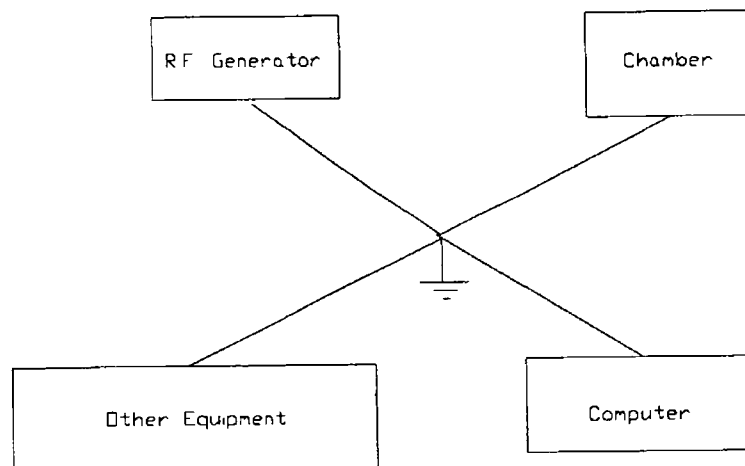


Figure 5.8 Ground Line Network

- 6) All exposed rf connectors were screened with earthed aluminium tape.
- 7) All dc signal and power lines were passed through rf chokes before entering equipment. These lines were also screened.

8) A Faraday cage enclosing the complete system proved necessary, because of stray airborn rf from the chamber This consisted of a tight steel mesh walled room, 8' x 8' x 4' with a door at one end

### 5 6 2 Pumping System

The pumping system must be able to pump to  $10^{-6}$  mbar for initial purging of the system and sustain the chamber pressure of  $10^{-2}$  mbar when the deposition through put of the system is about 50 sccm

The system chosen was the base of the Edwards 306A vacuum evaporation system The pumping mechanism consisted of a two stage ( 8 cubic litres per minute) rotary pump backing a 6 " diffusion pump with a liquid nitrogen cooled stack

### 5 6 3 Inlet Gas Control and Mixing

Three gases in all were needed to be controlled and mixed together before entry into the chamber They consisted of a reactive gas e.g  $\text{CH}_4$ , a catalyst gas to help the deposition e.g hydrogen and a carrier or pre-etch gas e.g argon

The three gases were controlled by needle valves with a glass bearing meter It was realised that fine control over the reactive gas flow rate would be needed so a mass flow controller was installed inline A schematic representation of the gas input system is shown in figure 5 9

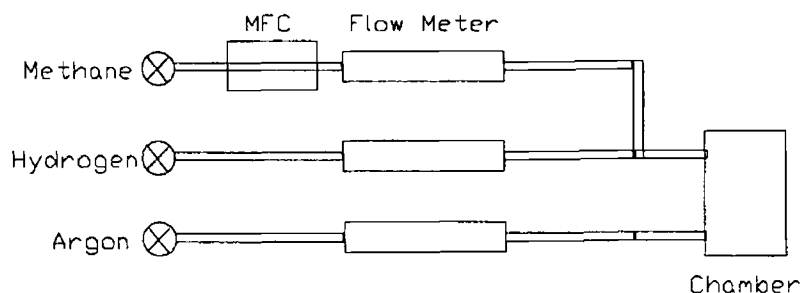


Figure 5 9 Gas Input System

The reactive and catalyst gases were mixed immediately after the control valves The carrier gas was not mixed until the inlet to the chamber This was done to allow flexibility of gas mixes

## 5 6 4 Chamber Geometry

The chamber was an Edwards pyrex glass cylinder, 12" diameter and 14" in height, with L-shaped gaskets. The top plate was a polished disk of aluminium, 14" in diameter and 3/4 " thick. This plate's preparation and design are important for the present deposition and for future applications of the apparatus.

The top plate had five ports machined into it. The central port was 25 mm in diameter for the insulating PTFE feedthrough for the gas inlet pipe. Symmetrically about the centre were four other holes, three of which are 26 mm in diameter with outer "O" ring grooves. These ports are for future optical emission spectroscopy experiments of the plasma [109] and can be blocked off with commercially available blanking plugs when not in use. There are also available a wide selection of feedthroughs that will fit into these ports. The other port was a large 40 mm diameter hole with the associated screw holes for a blanking cap. This port was intended for use as a plasma probe [110] access point, presently being developed within the college.

The bottom plate of the chamber was the base of the Edwards deposition system as shown schematically in the diagram 5 10. It had fourteen possible access ports. Installed were a thermocouple, rf, electrical and an internal movable arm feedthroughs. The remaining ten ports are available for further development using standard feedthroughs.

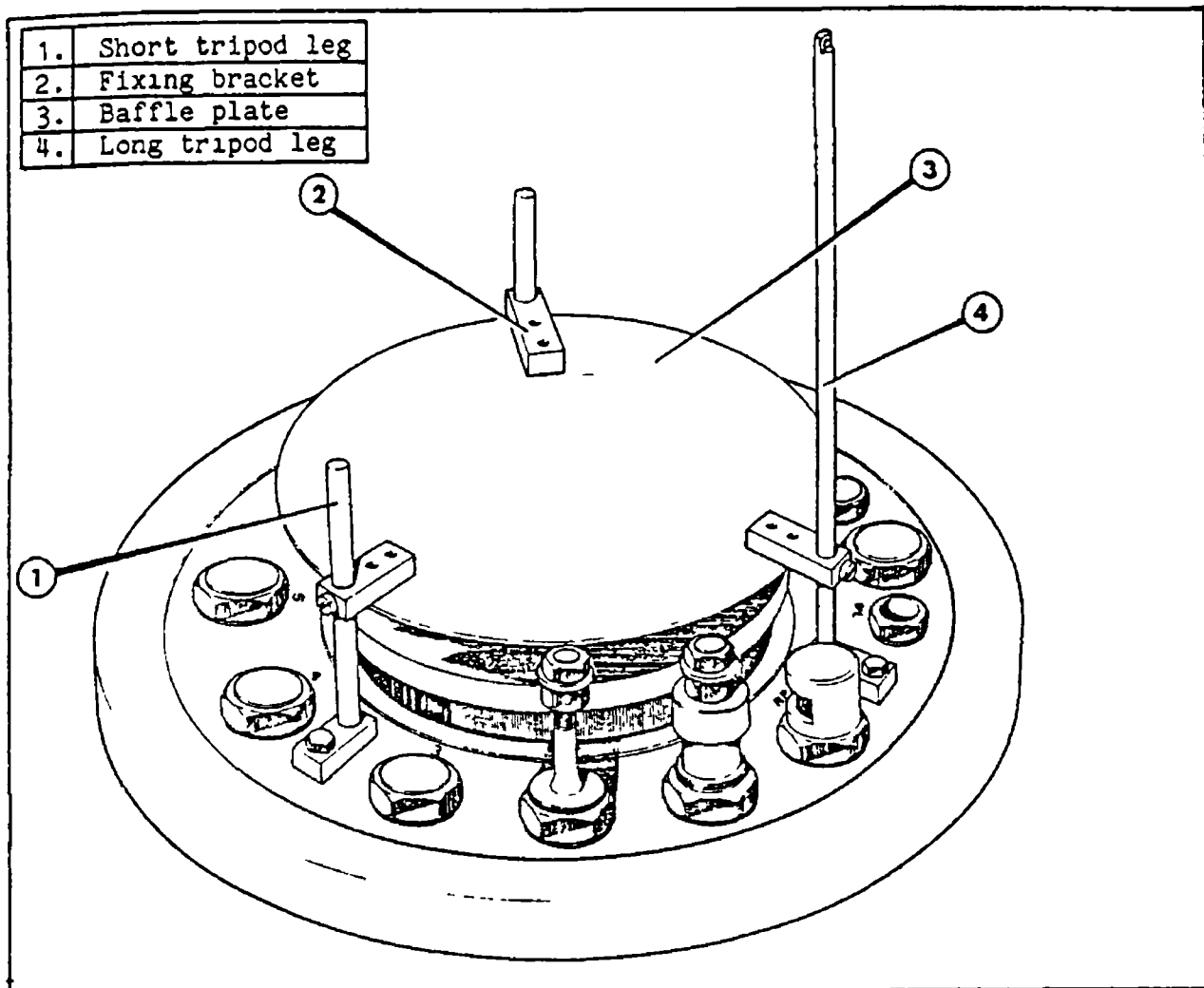


Figure 5 10 Vacuum Chamber's Base Plate [102]

### 5.6.5 Substrate Holder and Heater

The substrate holder is shown figure 5 11 It was made of sheet aluminium, with a crew connector for the rf supply The holder rested on ceramic tubes beneath which at a distance of 5 mm was a perforated sheet of aluminium to act as the Debye shield Perforated aluminium was chosen to reduce entrapment of gas and improve even gas flow over the substrate holder It also was of a lower mass hence absorption of conducted heat was reduced [111]

A stainless steel tube carried the rf power line within to the bottom electrode and also supported the whole assembly This support was adjustable vertically and horizontally

The heat was supplied by tungsten wire filaments The wire was fed through high temperature ceramic tubing in parallel lines beneath the substrate plate which rested upon these tubes

## 5 6 6 Gas Inlet Nozzle

It was found from experiment on the initial deposition system that that the input flow pattern of the gas over the substrates was crucial for good film coverage. In the initial system no film was formed directly under the inlet pipe and ridges of varying thicknesses of film radiated out from the centre.

In order to solve this problem and achieve an even flow of gas over the substrates a "shower-head" type nozzle was designed. This was made of aluminium in a cone shape which allowed a back pressure of gas to form behind a sintered glass filter which dispersed the gas evenly over the substrate.

The nozzle was made in two parts to facilitate filter replacement and cleaning. The area of the top electrode could be easily changed by the addition of various sizes of circular disks around the top of the nozzle. The gas inlet nozzle is shown in figure 5 11.

## 5 6 7 Parameter Control and Monitoring

The main parameters to monitor are the gas flow, pressure, substrate bias, peak to peak voltage of r f waveform, substrate temperature and r f power. It is important to monitor as accurately as possible the above parameters. Most can be simply monitored using various meters. The substrate temperature is very important for the film qualities, but presents a difficulty in its measurement because of r f interference with the thermocouple. The thermocouple cannot measure the temperature or be in contact with the electrode, when the r f is on. In order to overcome this problem a thermocouple was fitted onto a movable arm, as shown in figure 5 11, which could be moved over onto any part of the substrate surface momentarily when the r f source is turned off.

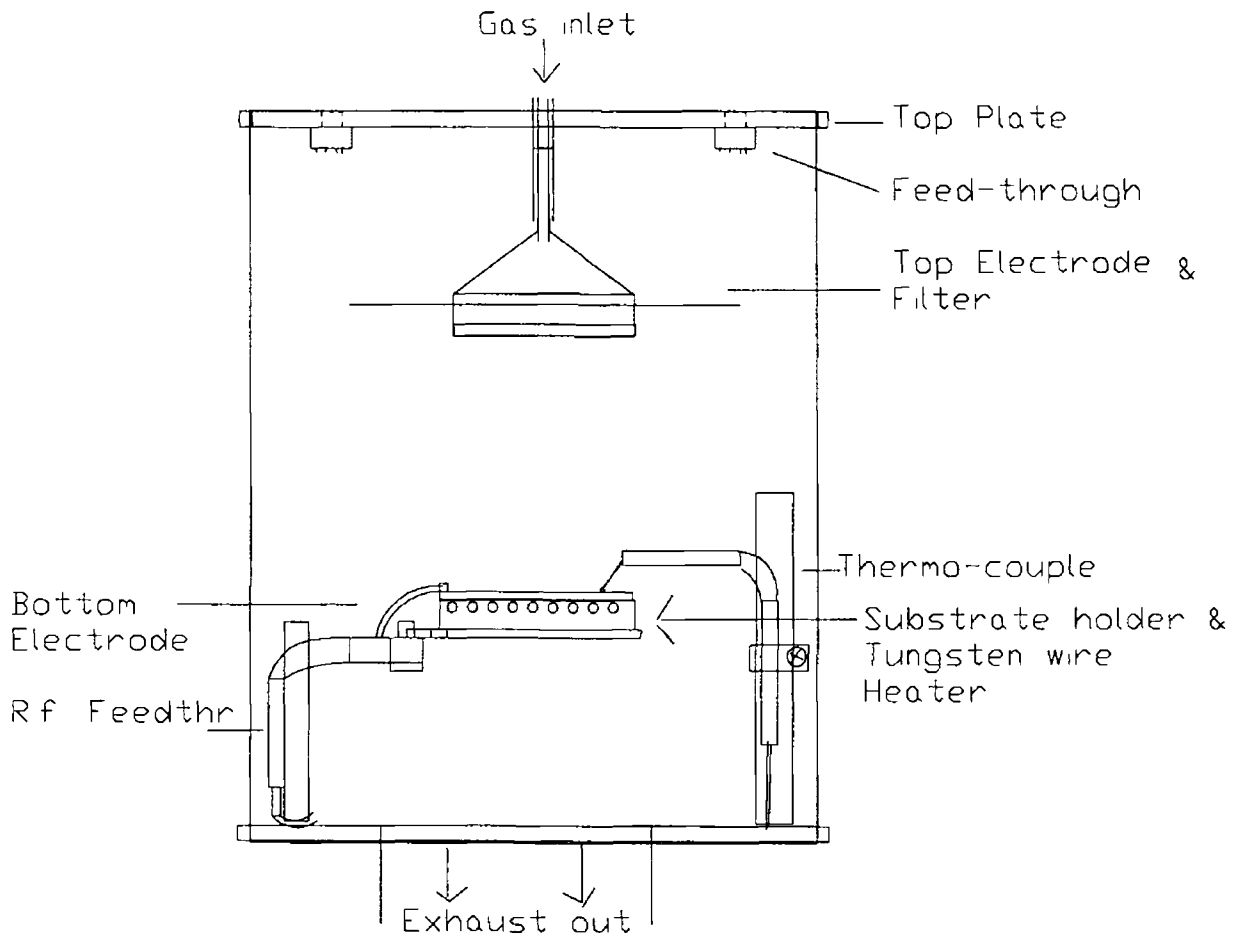


**Figure 5 11 Plasma Deposition System**

## 5 7 Substrate Preparation

### 5 7 1 Introduction

Although the substrate [65] is a mandatory part of any deposition system, without which the concept of films is lost, the substrate is often forgotten about or obliquely referred to. Specific application and film tests require different substrate materials which offer an acceptable compromise for the purpose on hand. Ideally, the substrate should provide only mechanical support, but not interact with the film except for sufficient adhesion. Main factors to be considered when choosing substrates would be their usefulness in a range of mechanical, optical, chemical and electrical tests on the films.

### 5 7.2 Thermal and Mechanical Considerations

When films are being deposited the substrate is placed under thermal and mechanical strain. Heating of materials is always followed by expansion. Upon removal of heat the substrate and film will cool at different rates depending on their thermal conductivity.

The basic properties which must be considered in this category are coefficient of expansion and the thermal conductivity. There are two types of situations in which a substrate encounters temperature changes. One occurs during processing when the entire substrate is heated - for example, to deposit a film - and subsequently cooled. The other time is when the film heats due to mechanical or electrical effects producing local regions of heating. This can be a greater stress as some regions will expand while others retain their dimensions. This is a problem with 1-carbon films, in that their coefficient of thermal expansivity is very different from that of the steel substrates.

### 5 7 3 Choice of Substrates

High Speed Steel (HSS) Steel substrates were chosen because it was ultimately hoped to be able to coat drill bits. The samples were 1" square by 1/8" thick. These could be easily polished to a finish of 3  $\mu\text{m}$ . This polish is necessary for adhesion of film to substrate. Also polished samples are necessary for hardness tests using a diamond indenter and wear abrasion tests using a rubber wheel abrasion tester.

Silicon was selected because it is transparent to infra-red light down to

approximately  $600 \text{ nm}^{-1}$ . This allows the determination of CH bonding structure and whether bonding is  $\text{SP}_2$  or  $\text{SP}_3$  type, through infra-red absorption spectroscopy

Glass availability of smooth clean surfaces and also the fact that it was easier to deposit on glass than on steel. Useful thickness tests, colour, transparency and optical absorption can be conducted on glass samples

Glass cover slip very thin glass disks of 19 mm in diameter were used as a means of determining the stress in films. Depending on the radius of curvature of these disks the induced film stress force can be determined

#### 5.7.4 Substrate Cleaning

The adhesion of a film to a substrate is effected greatly by the cleanliness [65,112] of the surface. Oil, dust, etc., can act as a boundary layer between film and substrate [113]. The surfaces must also be flat and smooth to facilitate even film coverage. The following procedure was adapted in the cleaning and preparation of samples

1 - Solvent cleaning suitable reagents for substrate cleaning include aqueous solutions of acids and alkalis as well as organic solvents such as alcohols, ketones, and chlorinated hydrocarbons. The cleaning effect of acids is due to the conversion of some oxides and greases into water-soluble compounds

2 - Substrate Polishing applicable to steel only, since glass and silicon wafers are both pre-polished. The process is a tedious one of step polishing down the surface to a  $3 \mu\text{m}$  finish on rotating desk polishing disks

3 - Ultrasonic Activation all samples except the silicon can be placed in a bath of alcohol and placed in an ultrasonic activator for up to two hours. Particularly important for the polished steel samples as it removes oil and swarf

4 - Substrate heating a convenient in situ procedure of heating the samples using the substrate holder heater assembly. This should be done when the system is being pumped down to its lowest limit. Particularly good at expelling water vapour and residual gases

5 - Glow-discharge cleaning again, a convenient in situ cleaning using an argon plasma. The heavy argon atoms crash onto the surface heating it, expelling loosely bound atoms and etching the surface, removing any oxides or grease

The pre-etch has been well documented for enhanced nucleation during subsequent film deposition. This etch is particularly important for film adhesion. In fact, without an argon pre-etch film adhesion is found to be extremely poor [114]

## CHAPTER 6

### RESULTS

#### 6.1 Growth Rate of Films

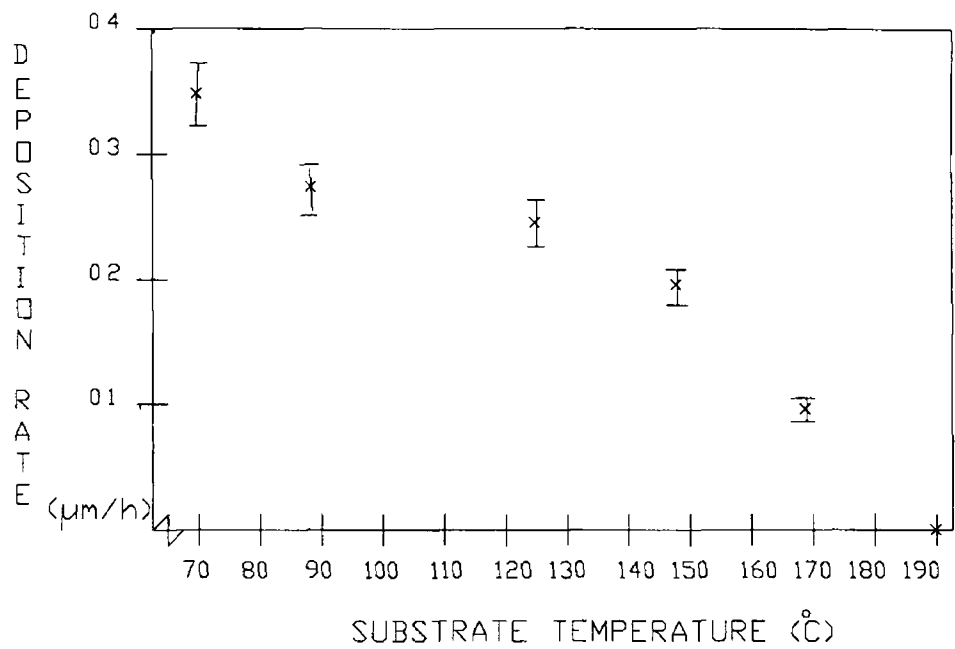
The growth rate of films is an important process parameter. It may also affect the structural and compositional properties of the film due to the variations in the ion flux arriving at the substrate surface.

Figure 6.1 shows the effect of substrate temperature on deposition rate. A monotonic decrease with increasing temperature was observed. Above 190 °C no film growth whatsoever occurred. This suggests that a surface reaction is taking place whereby volatile species from the gas phase condense on the substrate surface and are then incorporated into the growing film with desorption of by-products. Increase in substrate temperature decreases the residence time of these species on the surface and thus reduces the likelihood of their incorporation into the film.

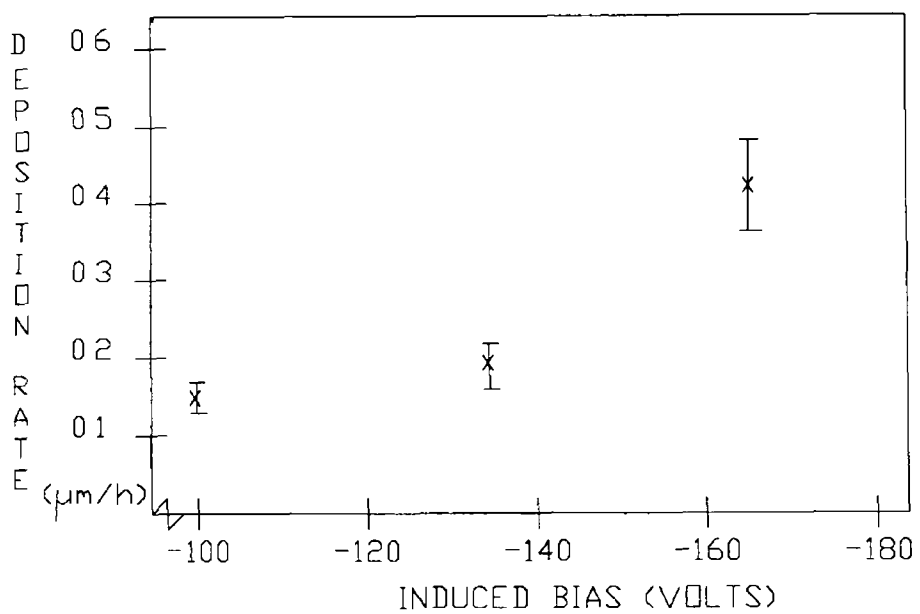
Figure 6.2 shows the effect of substrate bias voltage on the deposition rate. Bias voltage is related to the rf power supplied to the plasma - increasing rf power increases the substrate bias voltage. Increasing power will increase ionisation and therefore increase the active species in the discharge. Increase in bias will also increase the energy of ions arriving at the substrate and thus will probably increase the reaction rate of adsorbed species.

Figure 6.3 shows that the deposition rate increases with gas pressure. A higher gas pressure will provide a higher concentration of reactant materials.

Figure 6.4 shows the effect of top electrode diameter upon deposition rate. At point (A) on the graph the deposition rate is low because of high power density which leads to a large sputtering effect, therefore the net deposition is low. At point (C) there is a low power density hence the gas is not being dissociated effectively in the plasma. This leads to a low deposition rate. At point (B) conditions are optimal and a good net deposition rate is achievable.



**Figure 61 Deposition Rate vs Substrate Temperature**



**Figure 62 Deposition Rate vs Induced Bias**

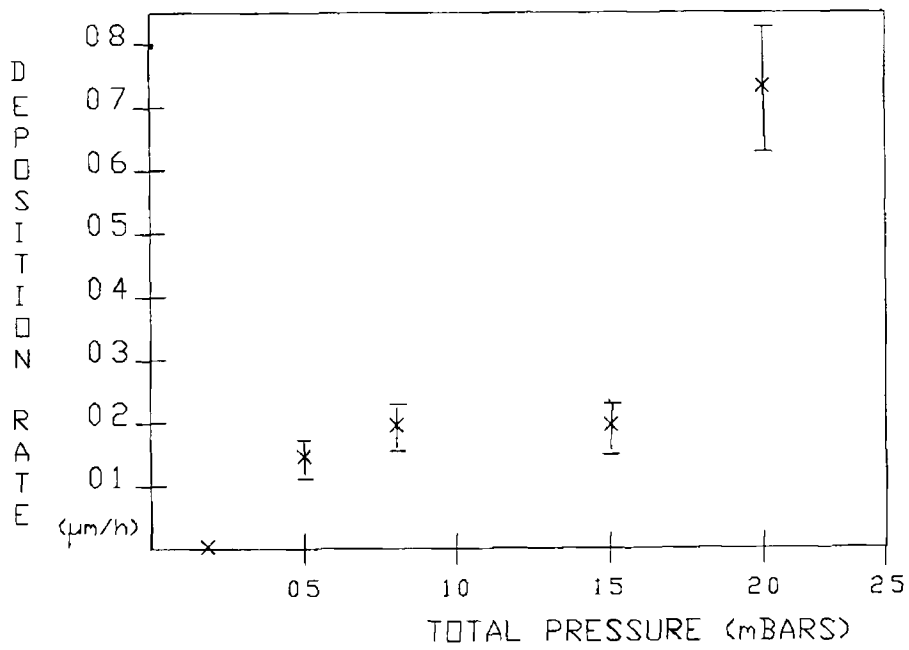


Figure 63 Deposition Rate vs Total Pressure

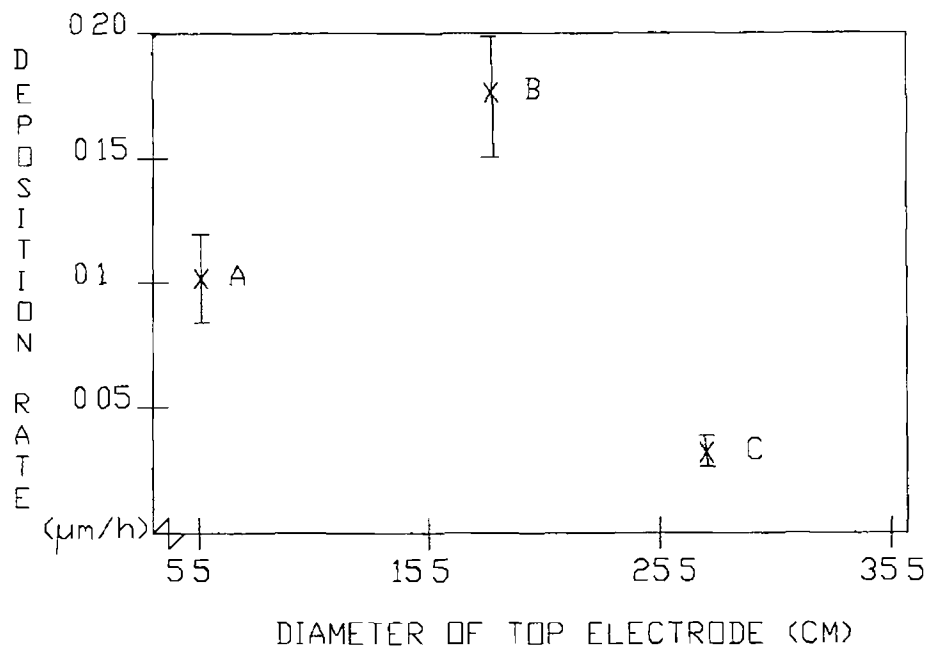


Figure 64 Deposition Rate vs Top Electrode Diameter

## 6.2 Stress of Thin Films

Plasma deposited films are particularly susceptible to intrinsic stress [65]. As will be shown the stress is dependent on many of the deposition parameters such as the induced bias, substrate temperature, pressure, etc. The film stress is the limiting factor in the growth of films to thicknesses greater than around one micron because the forces can be strong enough to exceed the elastic limit of the film or substrate and can cause the film itself or the substrate to shatter. Intrinsic stress is dominant and must be controlled for film applications. Total stress observed  $S$  is given by

$$S = S_{\text{external}} + S_{\text{thermal}} + S_{\text{intrinsic}} \quad (6.1)$$

When a stressed film is deposited upon a thin substrate, it will cause it to bend. Most measuring techniques use this phenomenon. Others utilise x-ray or electron diffraction, but these techniques give the strain and hence the stress in a crystallite lattice. This is not necessarily the same as that measured by substrate bending since the stress at the grain boundaries may not be the same as that in the crystallites.

The mechanical methods for stress measurement are the Disk and Bending Beam methods [65]. The disk method is preferred because of its ease of use. In this method the stress of a film is measured by observing the deflection of the centre of a circular substrate when the film is deposited on it.

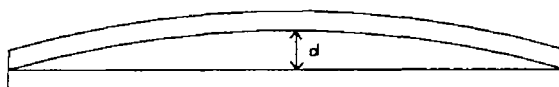


Figure 6.5 Bending of cover-slip under deposited film

The approach taken was to use an optical microscope with a travelling stage. The fine focus was used to determine the deflection from the middle of the disk to the edge. The disks were glass cover slips of 19 mm diameter and 0.6 mm thick. From the centre shift  $d$  and the properties of the glass cover slip the stress  $S$  was calculated [95]

$$S = \frac{d}{(D/2)^2} \frac{Y(g) T(g)^2}{3(1-\nu) T(f)} \quad (6.2)$$

where  $D$  = diameter,  $T(g)$  = thickness of glass,  $Y(g)$  = Young's modulus of glass,  $\nu$  = Poisson ratio,  $T(f)$  = Thickness of film.

All the films exhibited compressive stress. The films were limited to thicknesses of below  $1\mu\text{m}$  to avoid film shattering off and so avoid confusing film adhesion and film stress. Figure 6.6 is a photograph of a stressed film taken with an optical microscope. It shows clearly the buckling of the surface under compressive stress.

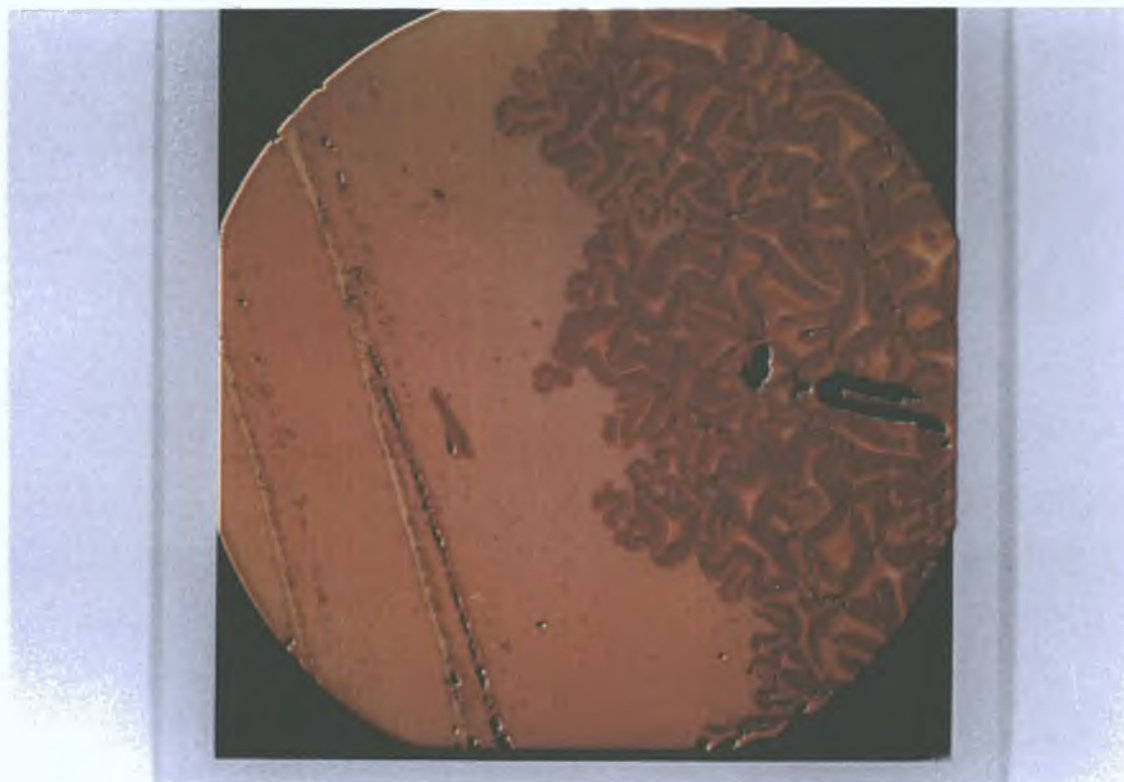


**Figure 6.6 Photograph of stressed film**

Figure 6.7 shows the effect of bias on film stress. Increasing the negative bias causes the stress to increase.

Figure 6.8 shows the decrease in stress with increasing pressure. This is due to the fact that at higher pressures more polymer-like films are produced.

Figure 6.9 illustrates the surprising result that as the substrate temperature is increased the stress of the films is also increased. Higher temperature would be expected to increase the surface mobility of adatoms and facilitate their incorporation into optimum bonding configuration and hence reduce film stress. A possible explanation is that at higher temperatures the film is less polymer-like with fewer graphitic carbon bonds and more tetrahedral bonds which provide less scope for stress relief due to the greater average number of interatomic bonds per atom.

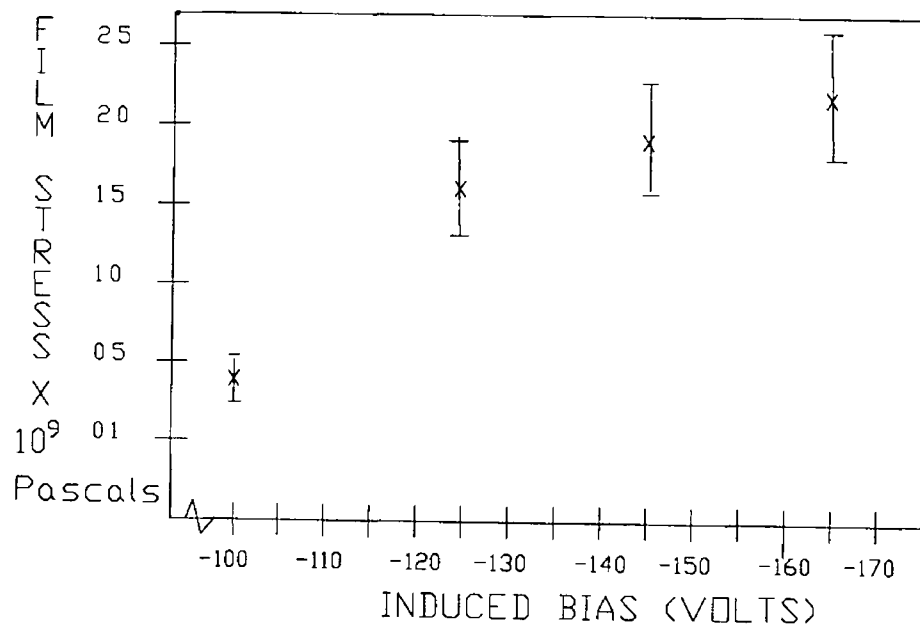


Figure 67 Film Stress vs Induced Bias

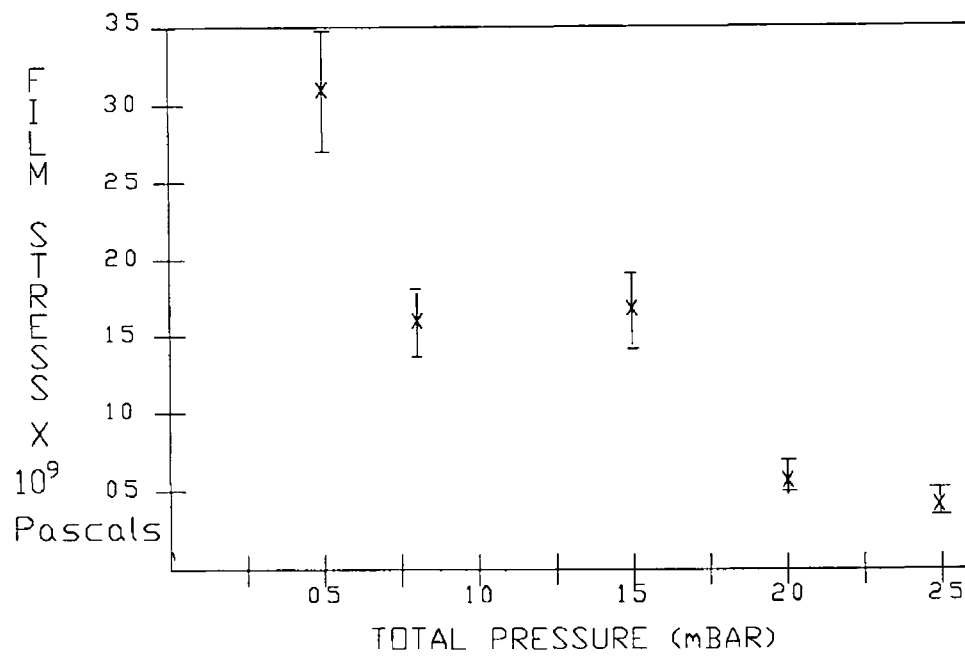


Figure 68 Film Stress vs Total Pressure

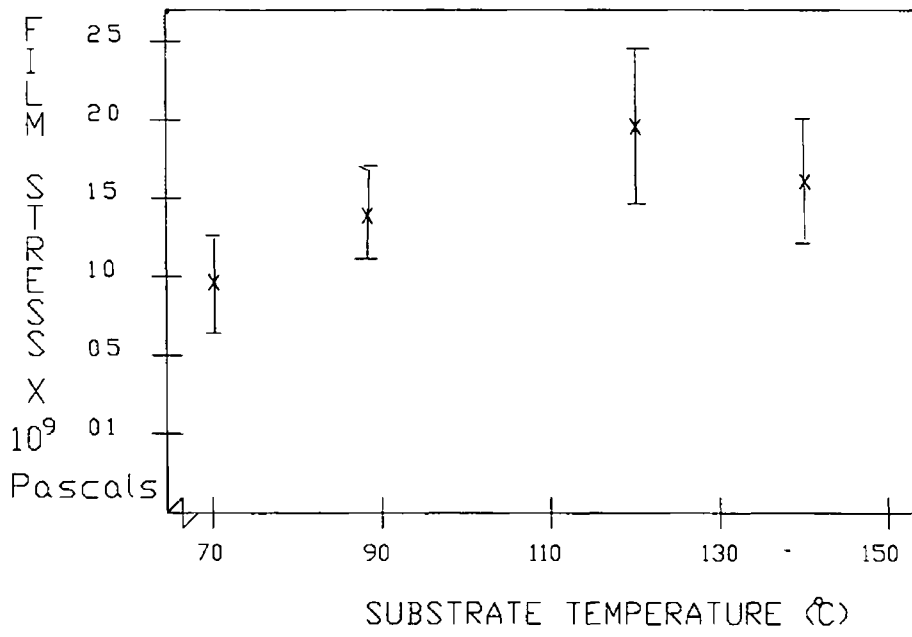


Figure 69 Film Stress vs Substrate Temperature

### 6.3 Adhesion of Films

This is the most important attribute of a deposited film without which all other film characteristics [113] are meaningless. If the adhesion of films is adequate, the main obstacle to their use in mechanical components is overcome. Many parameters affect the adhesion such as temperature of the substrate, induced bias, cleanliness of the substrate, surface finish and pressure.

Tape measurements were used because of ease of use, quickness and availability. In this technique adhesive tape is stuck to the film and pulled off, removing the film partially or wholly. This method is only qualitative and gives no indication of the relative magnitudes of the adhesive forces if the adhesion of the film to the substrate exceeds the adhesion of the tape to the film. A standard masking tape was used. This allowed easy viewing of stripped film as results were stored on acetate sheets. The tape was peeled off at a similar angle and speed by the operator.

A series of experiments were conducted to determine the effect of substrate temperature, pressure, bias and electrode area upon adhesion of the film to the substrate.

The temperature did not have a drastic effect but adhesion increased with substrate temperature. It was necessary to have a minimum substrate temperature for best deposits. The coverage and smooth finish of the film were also improved by heating. Figure 6.11 shows the percentage improvement in adhesion as a function of the substrate temperature.

The adhesion of the film was greatly enhanced by increased negative bias. Low bias (<100V) films peeled off substrates. These films were also soft and resembled a sort of polymer film. There would seem to be an optimum bias for adhesion as at high bias rates the film was powder-like. This may be as a result of high stress. Figure 6.12 shows the percentage improvement in adhesion as a function of the induced bias. The graph is divided into two parts, as it was found that above a negative bias of 160 volts the film removed from substrate due to stress factors.

As the pressure is increased the adhesion of the film improves. At very low pressures of less than 0.4 mBar film removed totally from substrate. Figure 6.13 shows the percentage improvement in adhesion as a function of the pressure.

The area of the top electrode could be easily changed. This meant that a series of experiments could be conducted to investigate its effects on film properties. From

this it was seen in figure 6 4 an optimum ratio was achieved This was probably due to the fall-off in plasma density with large electrode area Figure 6 11 shows the percentage improvement in adhesion as a function of electrode diameter

In an effort to improve the adhesion of carbon films to the steel Polished steel samples were coated with 2  $\mu\text{m}$  of tungsten As can be seen, in figure 6 10, the adhesion was dramatically improved This was attributed to the formation of tungsten carbides [32] at the interfacial layer This result also suggests a possible reason for the good adhesion of the films on silicon and glass substrates due to the formation of silicon carbides The dark areas of the photograph are the removed film



Figure 6 10 Effect of coating the steel with tungsten, before deposition of carbon film

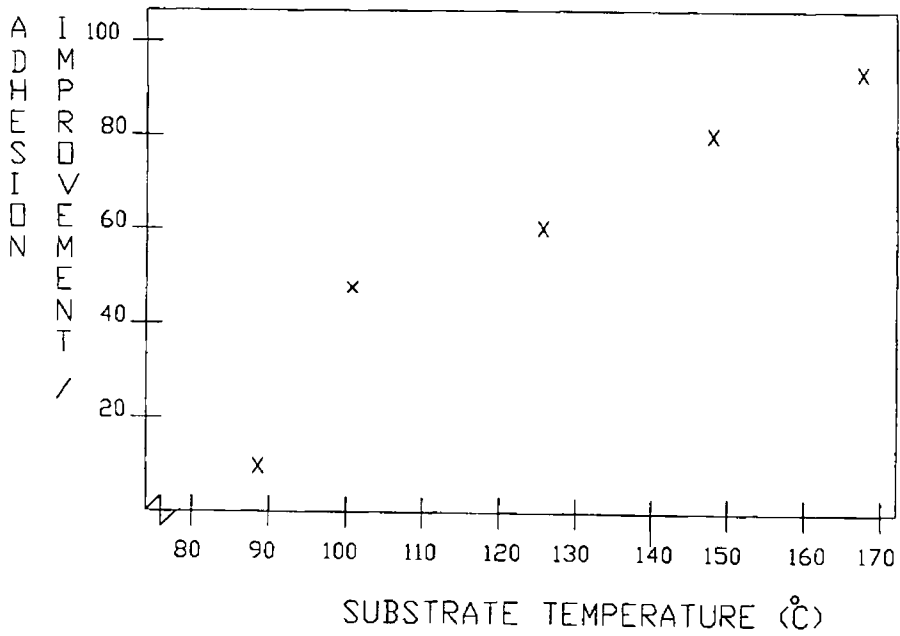


Figure 6 11 Adhesion Improvement % vs Substrate Temperature

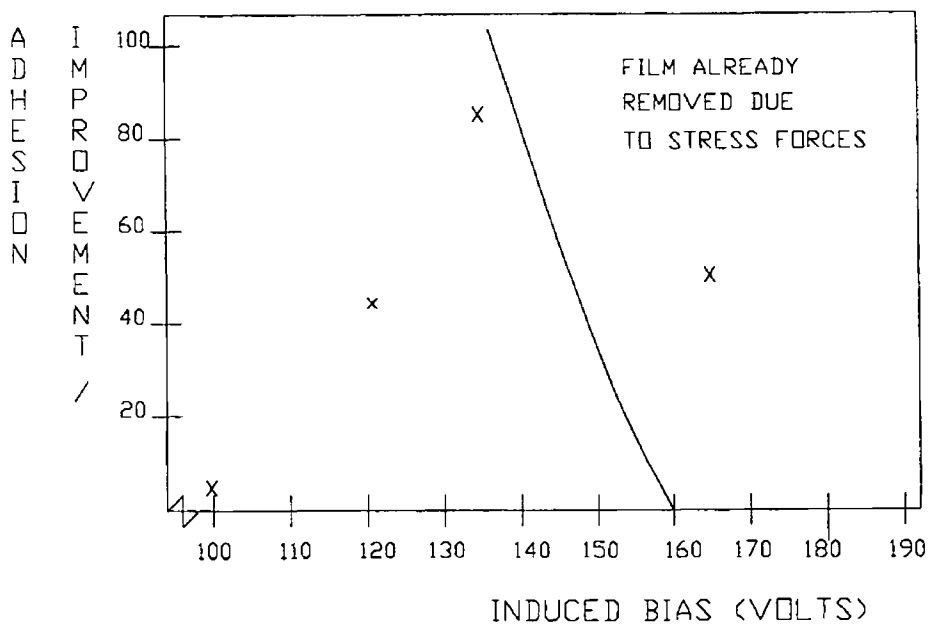


Figure 6 12 Adhesion Improvement % vs Induced Bias

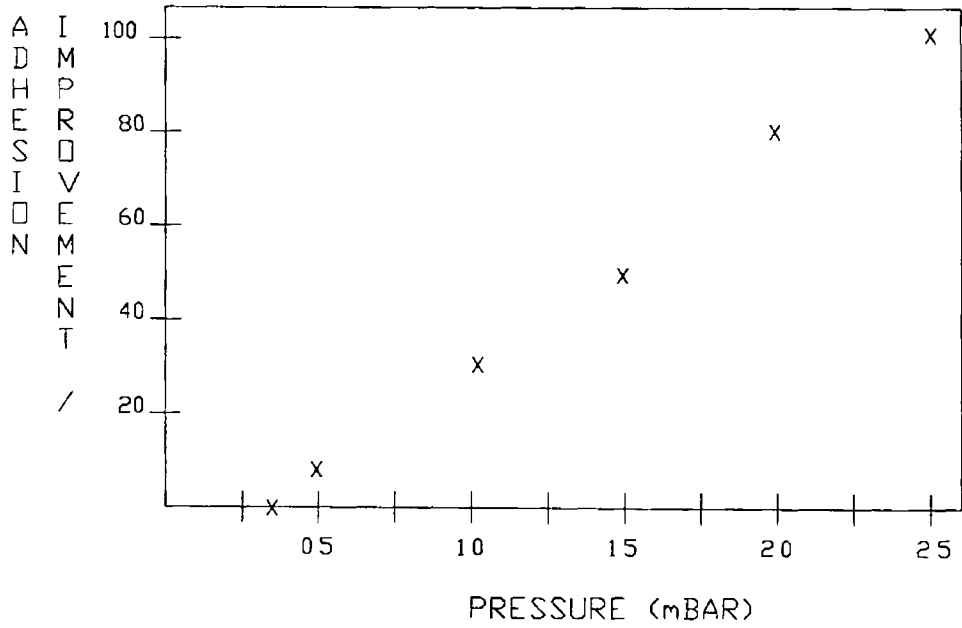


Figure 6 13 Adhesion Improvement % vs Pressure

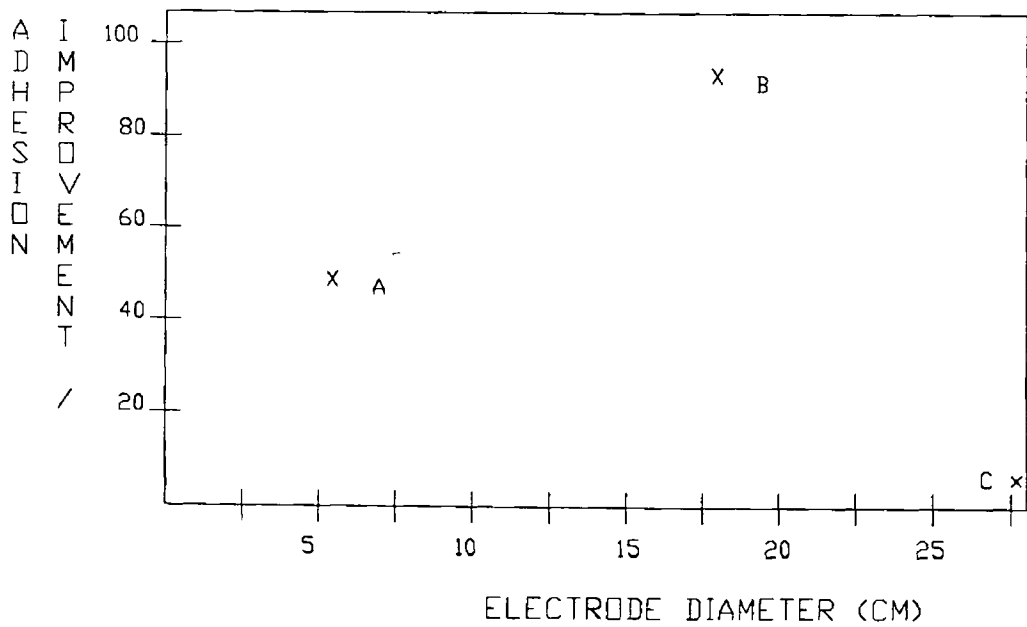


Figure 6 14 Adhesion Improvement % vs Electrode Diameter

## 6.4 Effect of Deposition Parameters on the Mechanical Properties of Thin Carbon Films

Accurate measurement of the hardness of thin films is extremely difficult. Diamond tipped indentors commonly used for such measurements should not indent more than one tenth of the film thickness [115] otherwise the measurement is substrate dependent. Films may also demonstrate elastic properties giving misleadingly high hardness values. Qualitatively, one finds the films difficult to scratch with a steel point.

A Leitz Mini-Load 2 indenter was used to obtain hardness values on films of several micron thickness. These hardness values were approximately 3000 Vickers, uncorrected for film elasticity. Films of this thickness are very highly stressed and disintegrate in a short period. It is difficult to grow hard carbon films greater than one micron thickness for this reason. It was decided to produce films of thickness less than one micron and to test these films for their wear resistant properties.

Available for the wear abrasion test was a rubber wheel abrasion tester built to ASTM 665 specifications [116]. The purpose of this machine is to reproducibly rank different coatings in order of their resistance to abrasion. From these wear measurements in revolutions per micron, approximate hardness values can be extrapolated by knowing wear amounts for materials of known Vickers hardness.

In wear applications the hardness of the wear coatings is naturally of prime interest. For abrasive wear applications the hardness of the coating has to be higher than the hardness of the abrasive particles themselves. The abrasive wear rate decreases very fast with increased coating hardness and even small hardness increases have significant effects.

The procedure involved mounting the sample in the arm of the machine. The specimen is immersed in a slurry of abrasive particles ( $\text{Al}_2\text{O}_3$  particles) and pressed against the rotating wheel at a specified force by means of a lever arm and weight system, as shown in figure 6.15.

Wear is inversely proportional to the hardness of the abraded material [117,118]

$$\text{Wear} \propto 1/\text{Hardness} \quad (6.3)$$

Figure 6.16 shows the wear resistance in revolutions of abrasion wheel per micron ( $\text{rev}/\mu\text{m}$ ) of film plotted as a function of substrate temperature. A linear increase in wear resistance is found with substrate temperature. At the lower

temperatures the adhesion of the films is poor Hence it is difficult in this region to separate poor adhesion with wear resistance Low wear rates signify a failure in the adhesive force of the film rather than the cohesive wear which is obvious at high wear rates

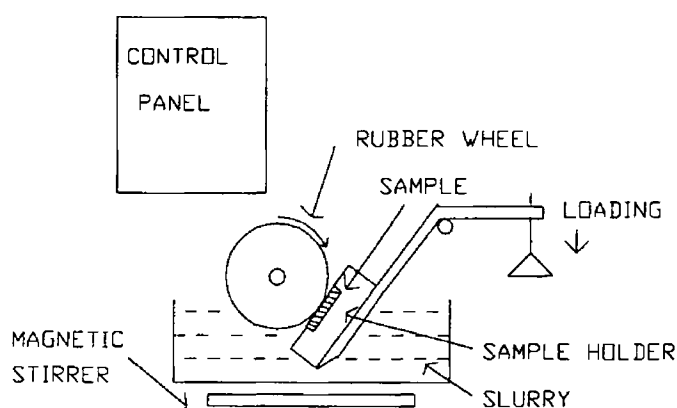
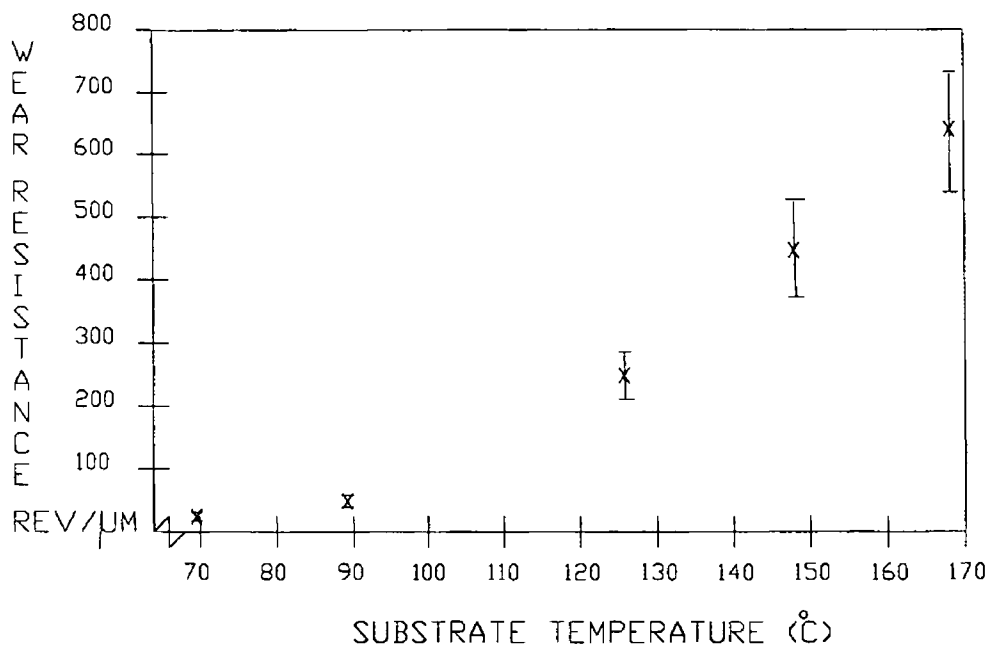


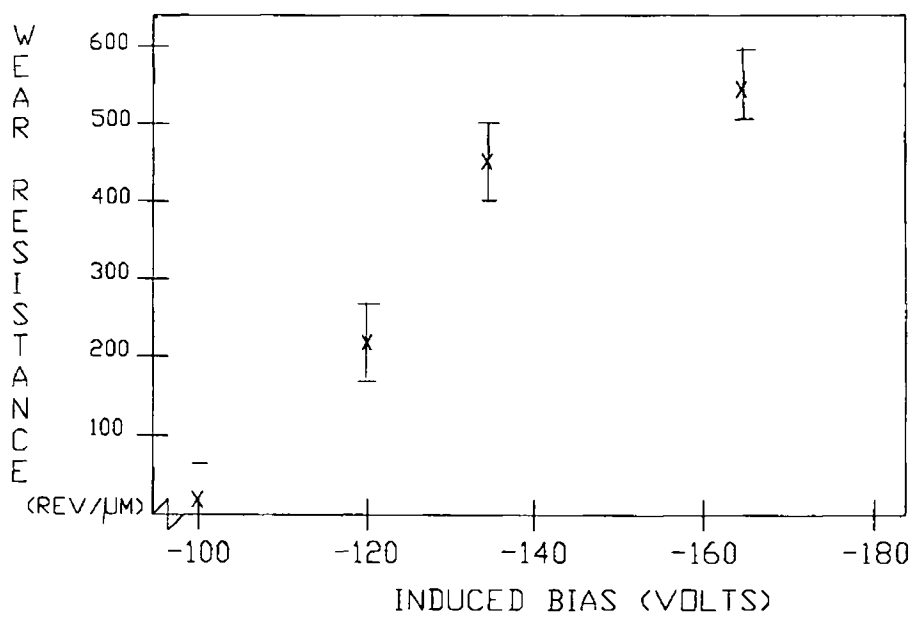
Figure 6 15 Schematic Drawing of Wear Abrasion Tester

Figure 6 17 shows the wear resistance as a function of the induced bias, a dramatic increase in wear resistance is observed with increasing bias Again it is difficult to separate poor adhesion and wear as it was found from adhesion tests that below -120 volts induced bias, adhesion was very poor and the films were soft and dusty like in appearance

Figure 6 18 shows the wear resistance as a function of total pressure of the deposition system It reveals a sudden increase in film wear rate above 1 5 mBar The films in this region were found to be polymer-like Bunshah [59] found that films produced at high pressures and low power were polymer-like in structure



**Figure 6 16 Wear Resistance vs Substrate Temperature**



**Figure 6 17 Wear Resistance vs Induced Bias**

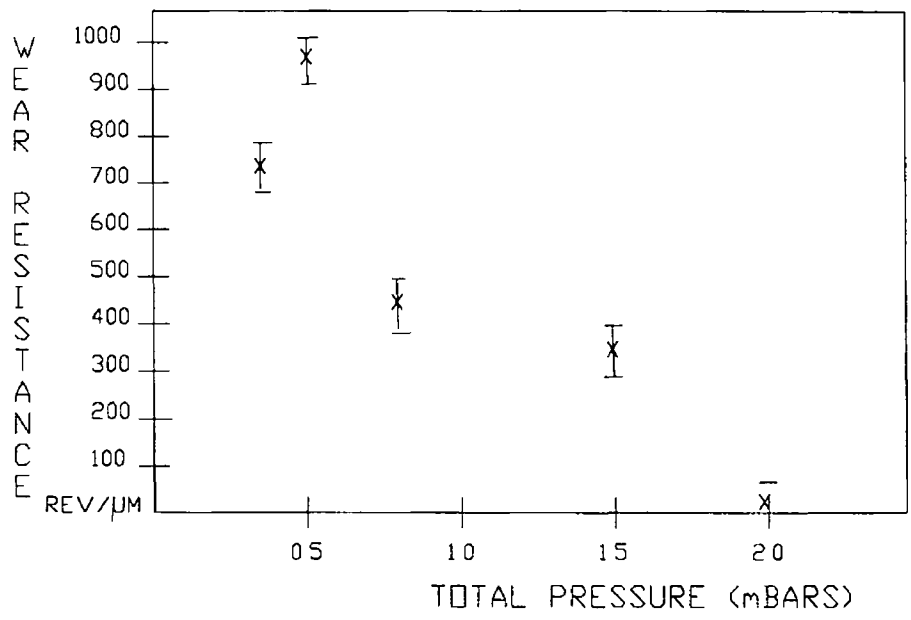


Figure 6 18 Wear Resistance vs Total Pressure

## 6.5 Summary of Results of the Mechanical Properties of Thin Carbon Films

For any large throughput of coated items it is necessary to have a high deposition rate. Clearly by increasing the bias the ion flux is increased which produces a significant increase in the deposition rate. The process and resultant film characteristics are interdependent in a complex way. Optimising the film growth along with the properties is extremely difficult. The properties required for a particular application dictate the process parameter values. For example, although the deposition rate is increased by increasing the bias so also is the intrinsic stress of the film. A summary of the effects of increasing the three main parameters on film properties is given below.

<u>Parameter</u>	<u>Dep./rate</u>	<u>Stress</u>	<u>Adhesion</u>	<u>Wear Resistance</u>
<b>Bias</b>	Increase	Increase	Improved	Increased
<b>Pressure</b>	Increase	Decrease	Improved	Decreased
<b>Substrate Temperature</b>	Decreased	Increased	Improved	Increased

Table 6.1 Effect of Deposition Parameters on the Film Properties

The intrinsic stress is the main disadvantage of carbon films. This stress must be minimised during the film growth. It is thought to be caused by the high hydrogen content of the films. It has been found that the addition of hydrogen to the plasma actually reduced the hydrogen content of the films [75]. All the above deposits were done at a methane to hydrogen ratio of 5:1. This is not to suggest that this is an optimum ratio, but was one which produced high quality hard films.

## 6.6 Composition and Structure of Carbon Films

Important criteria for the understanding of the films unusual properties is their bonding and structure, and their variation depending on the deposition parameters

### 6.6.1 IR Spectroscopy

Infra-red spectrometry [119] works upon the principle of exciting molecules at the resonant frequency of the molecular bonds. This instrument scans through the wavelength range from  $4000\text{ cm}^{-1}$  to  $250\text{ cm}^{-1}$ . The resultant transmission spectrum shows the absorption peaks of the various molecular species interactions. This phenomena is similar to the simple harmonic oscillator, where it can be shown through quantum mechanics, that the vibrational energies, like all other molecular energies are quantized, and the allowed vibrational energies for any particular system may be calculated from the Schrodinger equation. For the simple harmonic oscillator these turn out to be

$$E_{\nu} = (\nu + 1/2) h W_{\text{OSC}} \quad \text{Joules} \quad (6.4)$$

Where  $\nu$  is called the vibrational quantum number. An extension of this theory into three dimensions and polyatomic molecules allows an understanding of the spectra. There are many possible vibrational modes of the molecules. As an example, the water molecules three fundamental vibrations are shown in figure 6.19

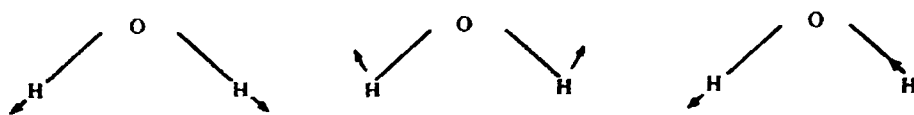


Figure 6.19 a) Symmetric Stretching b) Symmetric Bending c) Antisymmetric Stretch

The bonding structures of many molecules can be observed by their absorption peaks in IR analysis

Functional group spectroscopy provides information on the existence of CH, CH<sub>2</sub>, or CH<sub>3</sub> groups [22,120]. This can yield information on the reduction of carbon-carbon cross-linking by hydrogen decorated atoms can be inferred

In order to determine the effect of deposition parameters upon the film bonding, a piece of silicon wafer was included with the substrates as the various systematic

parameter changes were conducted. The silicon samples were then placed in a dual beam Perkin-Elmer 983 infra-red spectrometer.

A typical spectrum is shown in figure 5 20. Strong absorption bands were observed near the 2900 and 1450  $\text{cm}^{-1}$  lines and are unambiguous evidence for C-H bonds, most probably in methyl and methylene groups. Other peaks were observed with the addition of oxygen, as shown in figure 6 20 it increased the C=O absorption peak at 1785  $\rightarrow$  1755  $\text{cm}^{-1}$ , or nitrogen to the system [121]. The broad O-H near 3300  $\text{cm}^{-1}$ , the N-H or  $\text{NH}_2$  bands between 3200 and 3500  $\text{cm}^{-1}$  all appeared depending on the gas mixture. In general these contaminants had detrimental effects on the film growth.

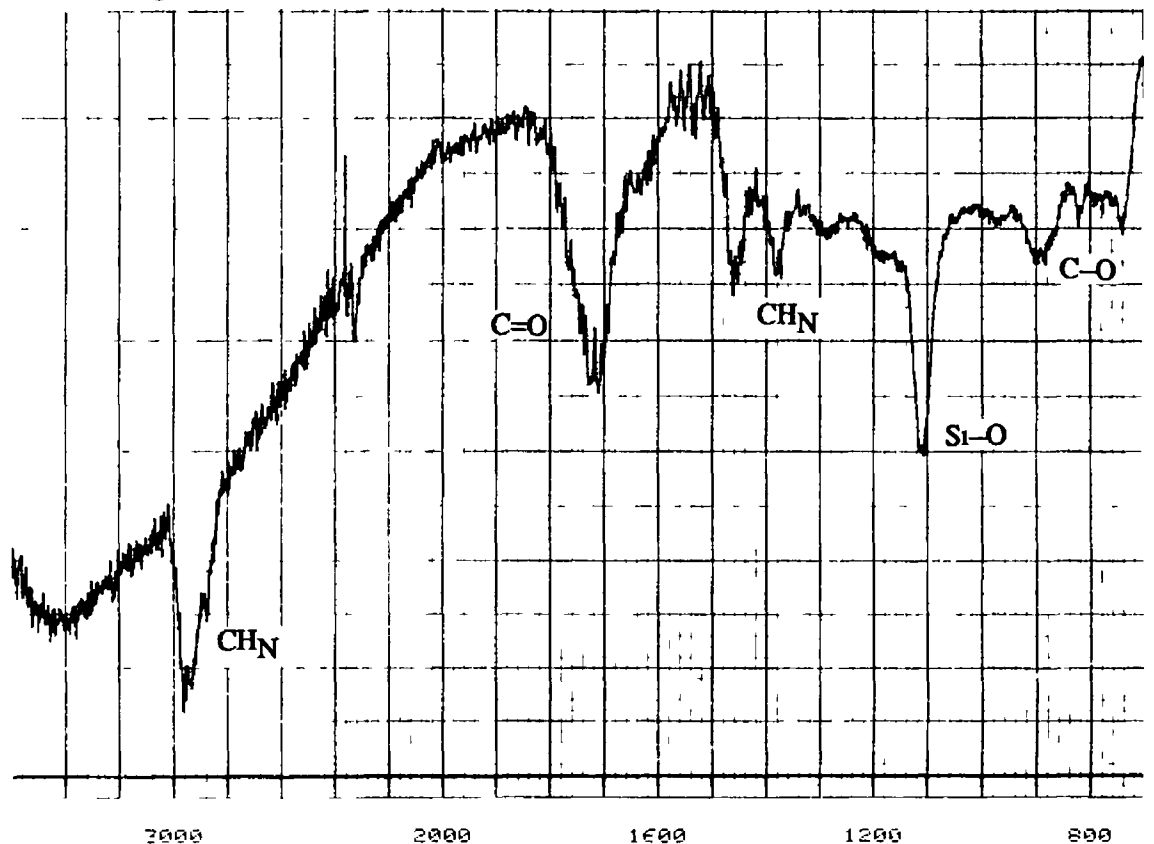


Figure 6 20 Typical I.R. Absorption Spectrum of a Carbon Film

The IR spectrograph's features did not vary substantially with variations in the deposition parameters. In order to determine the the parameters effect upon the bonding within the film. The absorption coefficient for the C-H peak at 3000  $\text{cm}^{-1}$  was plotted as a function of the main deposition parameters.

The transmitted intensity  $I'$ , is given by the equation [122]

$$\text{Film (1) } I_1' = I_0 \text{ Exp } -(\alpha + \beta) X_1 \quad (6.5)$$

where  $\alpha$  is the absorption coefficient for the substrate material

$\beta$  is the absorption coefficient of the absorption mode of interest

$X$  is the thickness of the film

$$I_1 = I_0 \text{ Exp } -\alpha X_1 \quad (6.6)$$

$$\frac{I_1'}{I_1} = \text{Exp } -\beta X_1 \quad (6.7)$$

Hence,

$$\beta = 1/X \text{ Ln. } I_0/I' \quad (6.6)$$

This coefficient will be proportional to the amount of C-H bonds present at a particular wavelength. This equation also takes into consideration the thickness of the deposited film.

In figure 6.21 the absorption coefficient is shown as a function of the applied substrate temperature. A linear fall-off with substrate temperature is observed. This suggests that there is a decrease in the proportion of C-H bonds in the film. This is as expected, more hydrogen is expelled from the film at high temperatures.

The absorption coefficient as a function of the induced bias is shown in figure 6.22. The proportion of C-H bonds is found to decrease with the applied bias. This is evidence that the gas molecules are being dissociated more effectively at higher bias voltages. It is important to note that the deposition rate and wear resistance also increased at higher bias voltages.

The absorption coefficient as a function of the total pressure is shown in figure 6.23. As was predicted from the films mechanical properties, there was a large increase in the proportion of C-H bonds with pressure. These films are certainly polymer-like in nature.

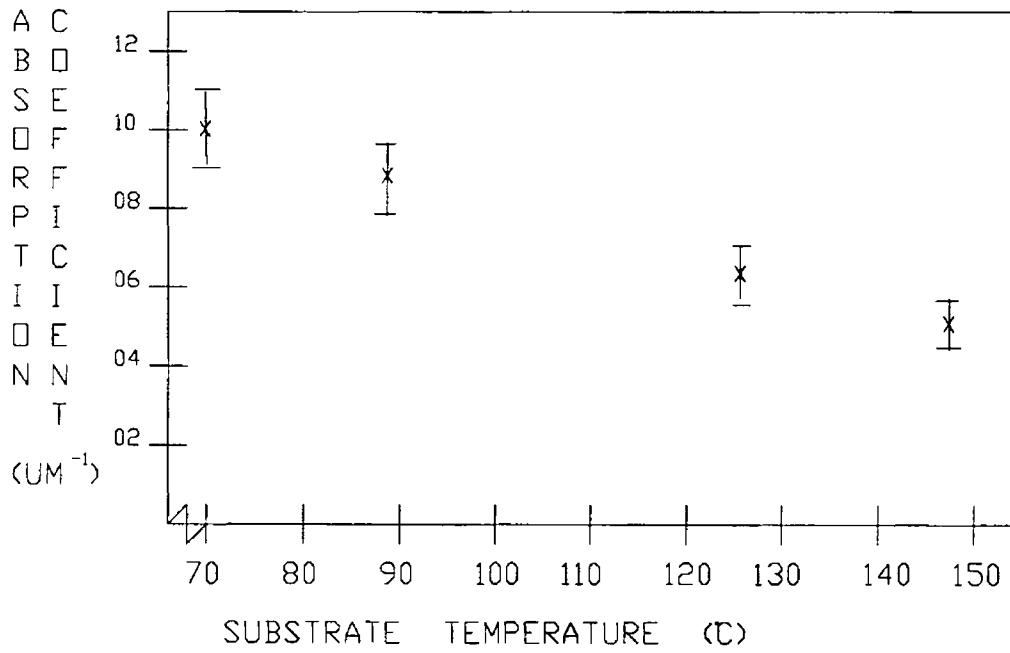


Figure 6 21 Absorption Coefficient vs Substrate Temperature

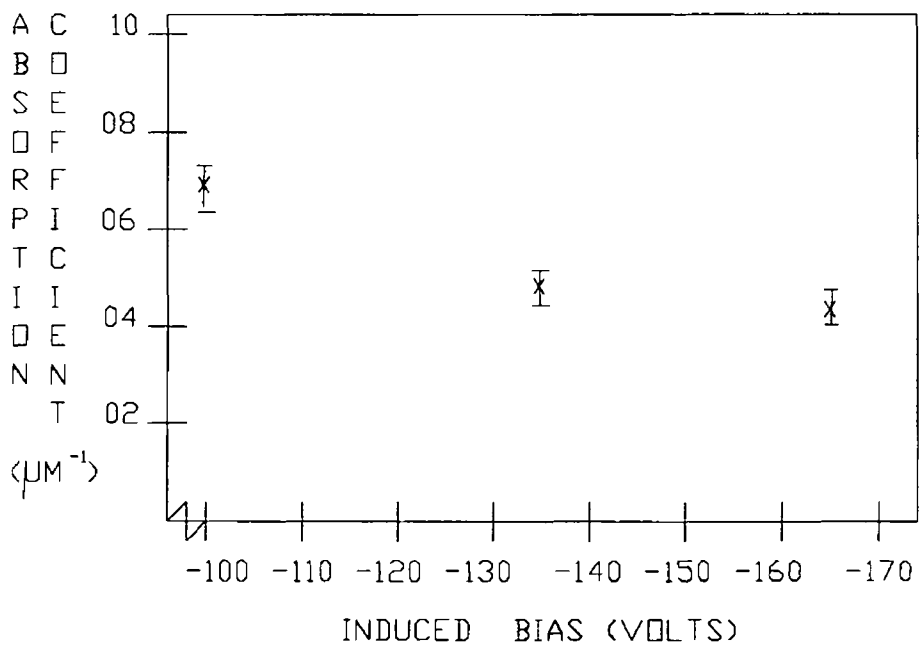


Figure 6 22 Absorption Coefficient vs Induced Bias

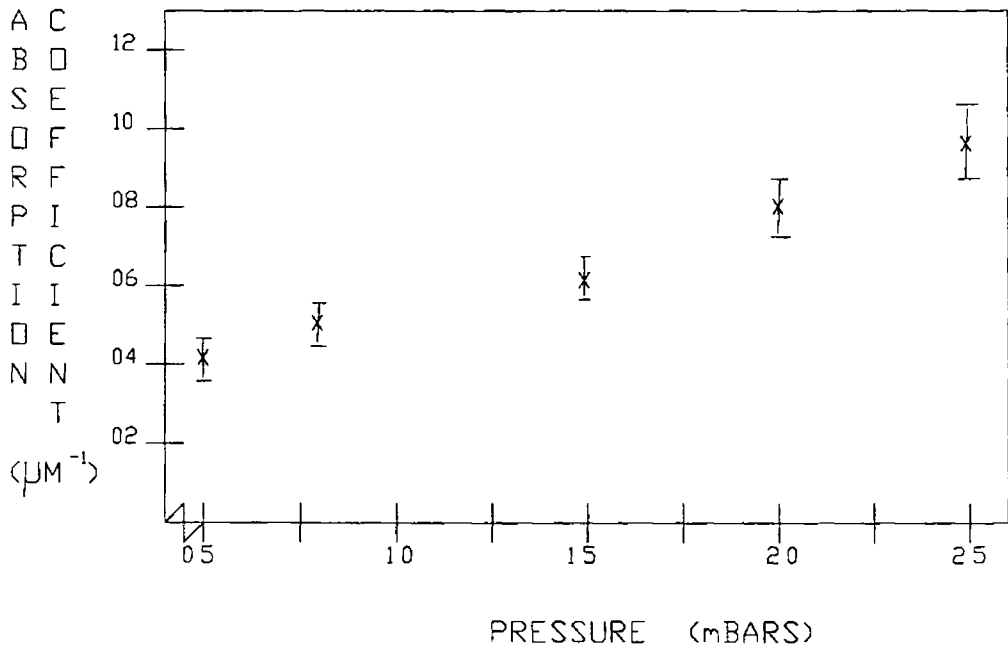


Figure 6 23 Absorption Coefficient vs Pressure

## 6 6 2 X-Ray Diffraction

A selection of films were also subjected to tests of X-Ray Diffraction XRD [123] This technique utilises the phenomena of diffraction of light waves as they pass through gaps in a crystal lattice Using the Bragg equation for the diffraction of light, the lattice spacing  $d$ , which is a unique property of every crystalline material can be found

$$\text{Bragg Equation} \quad n\lambda = 2d \sin \theta \quad (6.7)$$

where  $n$  = Fringe Number

$\lambda$  = Wavelength of X-rays

$\theta$  = Angle of Diffraction

This instrument consists of a sample stage at the centre of a circular drum, which has a travelling X-ray detector around its circumference The instrument rotates the detector about the drum yielding a plot of light intensity versus diffraction angle

From the XRD tests no crystal structure was observed This itself is a result in that now an amorphous structure is identified The IR and XRD results would together suggest that an amorphous carbon structure, consisting of mainly C-H bonds is present The structure was described as a network of random covalently bonded molecules by Angus [83,84] This could explain their unusual strength, being a closely packed structure of strong C-H bonds

Graphitic like films were easily recognisable because of their ease of wear and soot like appearance It is more difficult to separate amorphous and polymer-like films, but certainly at high pressures and low power a polymer was formed This polymer had very good coverage and surface finish and exhibited very little film stress Unfortunately these films were soft and easily removed The amorphous type were very hard and wear resistant, but very highly stressed and could be not grown to thicknesses greater than 1  $\mu\text{m}$  without film shattering-off the substrate There was a vast difference in the wear abrasive properties of these two films but their deposition conditions were quite similar This suggests that at critical level the films change from a hard amorphous to a soft polymer-like with increasing pressure This can be seen in figure 6.18 as the pressure is increased above 15 mbar the wear resistance falls off sharply

## 67 Plasma Gas Species

A simulation under the typical deposition conditions was performed on another system to which a mass spectrometer was attached. This instrument tells the atomic mass units of the various gas species present and the proportion of these in a plasma gas [57,95,124]

The spectrum was taken with the rf power turned on and with the same conditions but with the rf turned off. This was done to identify the ionization effect of the gas caused by the analyser itself.

Shown in figure 6.24 is a spectrogram of methane without rf plasma activation. The peaks of  $\text{CH}_x$  derivatives at 13 and 16 amu can be clearly seen. When the plasma is activated the spectrogram changes too that of figure 6.25, here the methane derivatives are clearly visible between 13 and 15 amu. A large hydrogen peak is also observed at 2 amu. These spectrographs confirm the results from the IR that the films contain carbon-hydrogen bonded molecules and the methane gas is not being dissociated into pure carbon atoms. The intensities of the  $\text{CH}_x$  peaks were substantially increased due to the extra ionization caused by the plasma. All the C-H derivatives are present in the plasma, with a noticeable increase in the proportion of  $\text{CH}_2$  and CH peaks in the activated gas.

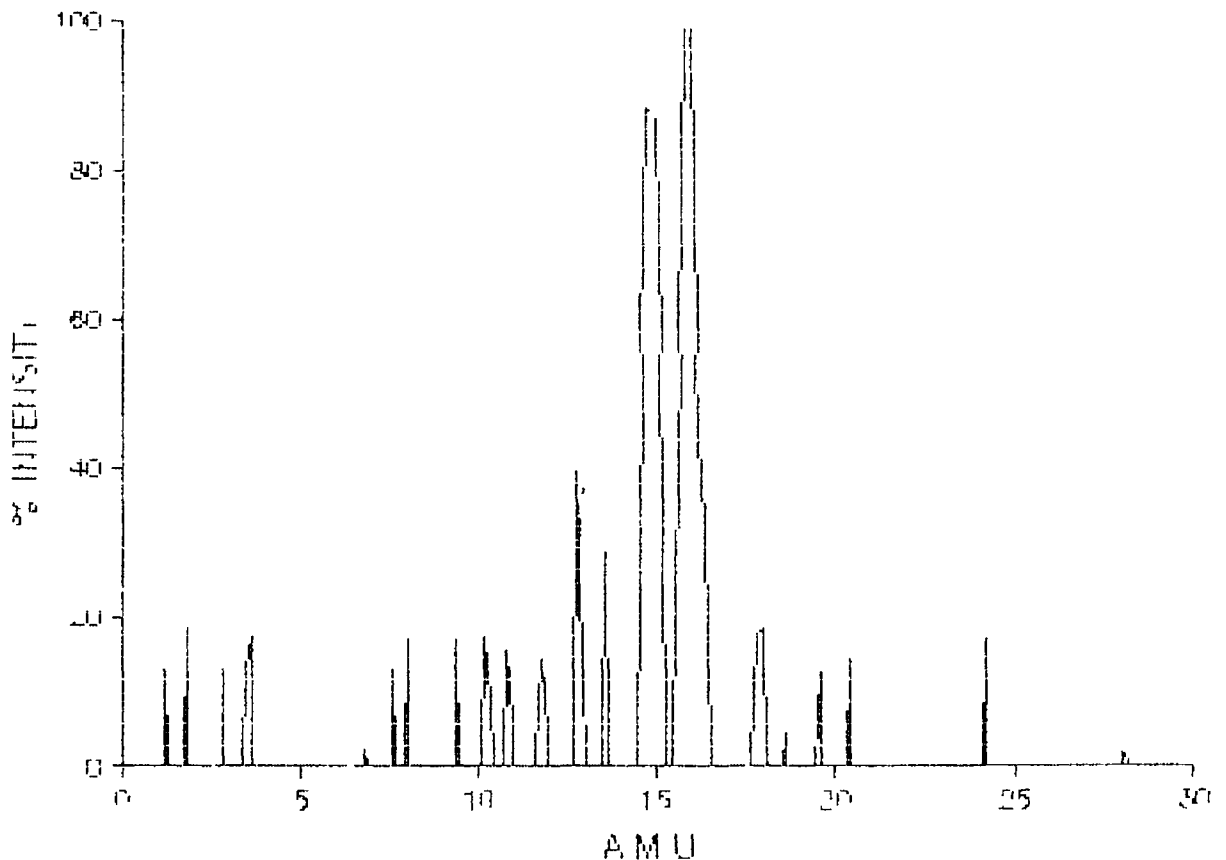


Figure 6.24 Mass Spectrogram of Methane

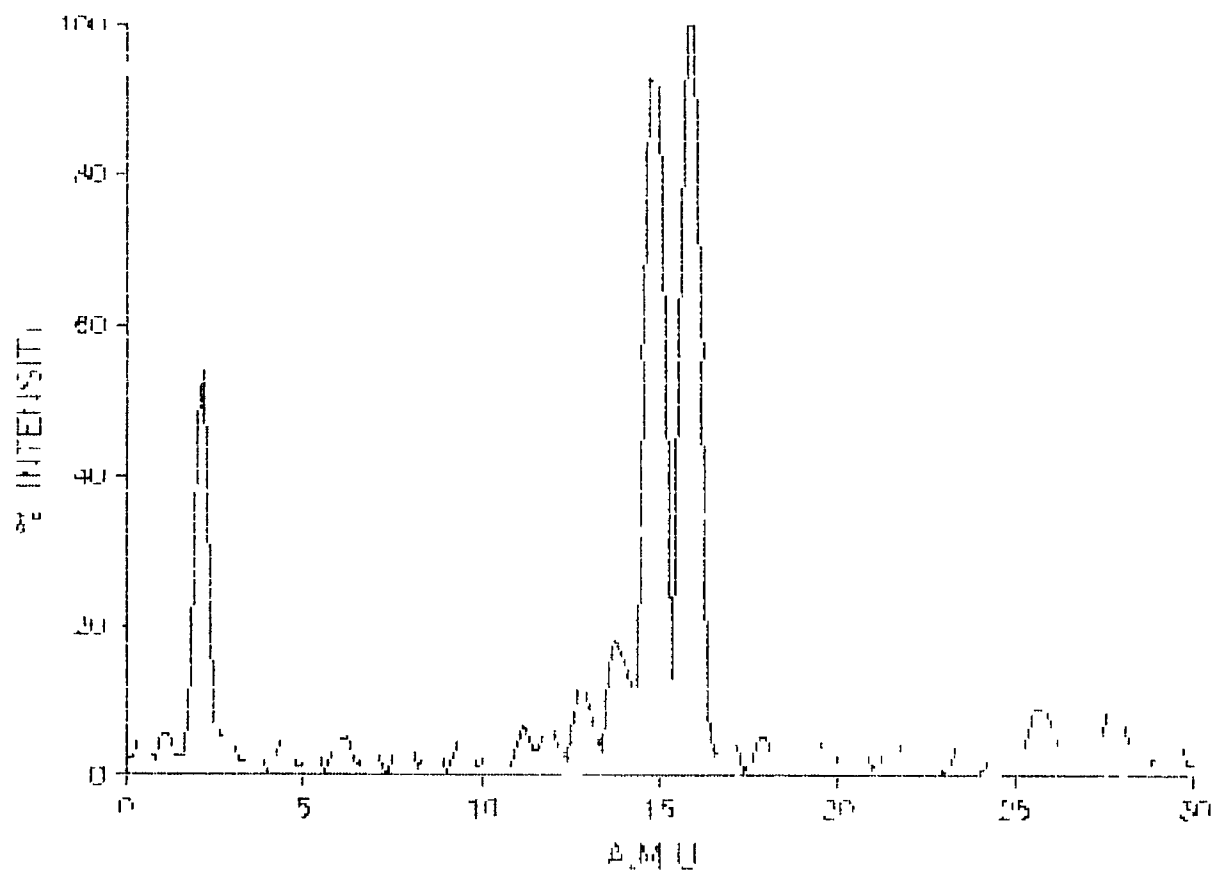


Figure 6.25 Mass Spectrogram of RF Activated Methane Discharge

## CHAPTER 7

### DISCUSSIONS

#### 7.1 Introduction

A range of films were deposited under various experimental conditions. The range of film properties and their complex dependence on deposition parameters make specialising in certain fundamental properties necessary. The three parameters of substrate temperature, induced bias and pressure were identified as the most important, the other variables such as electrode area or reactor geometry etc are peculiar to any one system, hence their effects, although important, cannot be generalised.

The optimisation of film qualities is extremely difficult. Many of the effects of the varying parameters are inter-dependent, so conclusive results are impossible. Presented here are the process trends, which identify clearly the areas of difficulty in the process and properties of carbon films.

#### 7.2 Effect of Substrate Temperature

In order to achieve good adhesion of the film to the substrate, the substrate must be heated to a certain level. This increases the surface adatom mobility, which leads to a better coverage on the surface and a more densely packed structure. It is extremely difficult to separate the effects of the various parameters from each other, as increasing the induced bias will also increase surface adatom mobility.

Assuming all other parameters are held constant and only the parameter of interest is changed then we can analyse the effect of this one parameter change.

As shown in figure 6.1 the deposition rate falls off linearly with the substrate temperature. This is due to the reduction in sticking coefficient with increasing temperature. It can be shown that the mass condensed at time  $t$  is given by [65]

$$M(t) = \frac{M \cdot t + \exp(-I^* D \tau_a t) - 1}{I^* D \tau_a} \quad (7.1)$$

It is seen that the mass deposited  $M(t)$  strongly depends on the total impingement time  $t$ , the substrate temperature  $T_x$ , the diffusion coefficient of monomers on the substrate  $D$ , the mean residence time of adsorbed monomers  $\tau$ , and the impingement rate  $I^*$ . This is shown graphically in figure 7.1

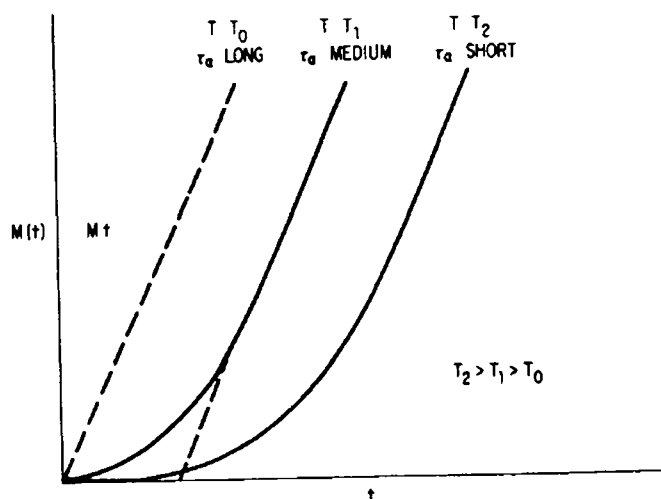


Figure 7.1 Mass deposited vs. time at various substrate temperatures

All the samples were deposited for the same length of time, hence at higher temperatures, less film material was laid down

It can also be shown that there is an exponential dependence of the nucleation frequency on  $\Delta G^*$  (free energy). The rate at which supercritical aggregates are created will decrease rapidly with increasing temperature. This means that at higher substrate temperatures it will take longer before a continuous film is produced [72]

$$[\delta \Delta G^* / \delta T] > 0 \quad (7.2)$$

The film's physical properties are of utmost importance. As stated already substrate heating was necessary for good adhesion. As can be seen in figure 6.8 a minimum substrate temperature of 100 °C is needed, and above this level adhesion improves with temperature. Without good adhesion it is impossible to determine such properties as wear resistance or film stress. In performing the range of tests a compromise must be made with the substrate temperature, that is to have good adhesion and yet good deposition rate.

The film stress was found to increase with increasing substrate temperature. The increased stress can be attributed to two effects. Firstly, the hydrogen content of the films was reduced with increasing temperature. This is seen in figure 6.21 that the absorption coefficient of C-H peaks decreases with substrate temperature. Less C-H bonds are formed at high temperature adding to the evidence that a surface reaction was incorporating more carbon atoms and expelling volatile hydrogen in atom and molecular form. This leads to a purer carbon content film, which does not have the

bonded hydrogen to relieve stress. Secondly, as the substrate temperature is increased the microstructure will be more densely packed as was shown in figure 4.11. This compacting of the carbon structure with substrate temperature will cause increased stress of the film. The wear resistance as a function of substrate temperature would indicate that these films were more resistant and therefore harder.

### 7.3 Effect of Induced Bias

The induced bias is found to be determined by the rf power to the chamber, the gas pressure and the gas type. It reflects the ionization state of the plasma and is a measure of ion energy arriving at the surface. By knowing the induced bias and the peak to peak voltage of the rf the important parameter of plasma potential can be found which is typically of the order of about 20 volts.

The higher the induced bias the more ionization, hence more dissociation of the gas molecules which leads to a higher deposition rate as seen in figure 6.2. The gas molecules are being broken up more effectively, so one would expect that the deposited film would contain less C-H bonds. Figure 6.22 confirms this showing that the absorption coefficient of the C-H peak decreases with increasing bias voltage.

Although increasing the bias voltage helps the adhesion, this has a threshold level and because the film stress increased with bias, a stage was reached when the film spontaneously shattered off the substrate. This limited the thickness of the films to less than one micron, so that adhesion tests could be conducted without the effect of stress. This bias effect on the adhesion is shown in figure 6.12. It is clear that a critical level is reached where film adhesion falls off dramatically.

As the induced bias is increased so also is the wear resistant property of the film. This is seen in figure 6.17. At low bias levels the film was soft, polymer-like. This, as stated, can be summarised as follows. Low bias voltage gives bad dissociation of the hydrocarbon molecules, hence incorporation of many polymer-like structures and a low deposition rate. At high bias a high ion flux is achieved, deposition rate is higher, dissociation of the molecules is more efficient, hence the film is of a higher carbon content. This is shown by the IR data that the absorption coefficient of the C-H peak decreases as a function of bias voltage in figure 6.22. Unfortunately, at high deposition rates and ion flux energies, more impurity atoms are incorporated and defects in film structure occur, which lead to highly stressed films.

## 7.4 Effect of Total Pressure

The chamber pressure directly affects the deposition process and the film properties. Increasing the pressure reduces the adatom surface mobility, just as lowering the substrate temperature will do. The pressure of the chamber was changed by increasing or decreasing the flow-rates. Yasuda [125] suggested the parameter of  $W/FM$  where  $W$  is the power,  $F$  is the flow rate and  $M$  is the molecular mass. Hence, the effect of pressure is related to power and type of gas dissociation. Practically the approach taken was to adjust the power to repeat the same deposition conditions such as the induced bias. Increasing the pressure also caused a higher substrate temperature to be achieved. This was due to heat convection effects within the chamber. In order to compensate for this effect the substrate heater power was reduced at high pressures.

By increasing the flow rates the "residence time" of active species at the substrate and the supply of fresh monomer to the discharge are increased. Which means that there are more species and they have a longer time to be incorporated into the film growth. As was seen in figure 6.3 the deposition rate increased with pressure. Above a pressure of approximately 1.5 mbar the deposition rate was three times that of the low pressure region. The process at high pressure is a plasma polymerization phenomena [126].

Several models have been proposed to explain plasma polymerization. In early studies of a.c. discharges the main emphasis was on the process of monomer adsorption on the substrate, but in later work the effects in the gas volume were taken into account [127].

Lam et al [128] analysed four main possibilities in the case of r.f. discharge in styrene and again found that the adsorption of monomers on the substrate is very important. They claimed that the best description of the behaviour was that the monomers were activated in the gas phase by electron bombardment and were diffused to the substrate where they propagated and terminated. Yasuda [125] suggested a new terminology, and accordingly proposed that, in general, polymerization in a glow discharge comprises both of plasma-induced polymerization (essentially conventional polymerization triggered in an electric discharge) and plasma (atomic) polymerization. In the latter case the original monomer molecules serve as the source of the reactive species (fragments or even atoms) which form large molecules by repeated stepwise reactions. In the former case, plasma-induced polymerization, this proceeds via utilisation of polymerizable structure and no gaseous byproduct is created. The formation of the polymer and the properties of the coatings are controlled by the

balance between plasma-induced polymerization, plasma polymerization and ablation of the polymer [129]

Further, justification for describing the films at high pressures as polymers, is given by the very low stress levels of these films, shown in figure 6 8, and the extremely poor wear resistant properties, shown in figure 6 18. In fact, these films resembled a polythene-like coverage and adhesion to the substrates

The IR spectrograph showed a significant change in the absorption coefficient as a function of the pressure, indicating an increase in the incorporation of C-H bonded molecules in the film. The adhesion of these films improved linearly with pressure. This is misleading in that these films resembled a polymer coating rather than a hard film

In conclusion, at higher pressures polymer-like films were produced. These had good coverage and adhesion and were virtually stress-less. The structure showed a large incorporation of H bonded molecules. These films were soft and easily scratched away. In fact, some were so soft they were below wear resistant measurement on the abrasion tester

Three distinct film types were observed: 1) Hard carbon type, 2) Graphite carbon-like and 3) Polymer-like film

## 7.5 Chamber Geometry

The specific deposition results are dependent on the chamber geometry and design. It has been discussed in section 2.6 that the induced bias is dependent on the relative electrode areas by equation (2.31)

A series of experiments were conducted using different top plates to investigate this effect. The resultant films can be best explained in terms of plasma ion density. An optimum region exists where the deposition rate is high, stress is not excessive, adhesion is good and films exhibit good wear resistant properties. In this region a net film deposition occurred, the induced bias was high enough for hard carbon films to be formed and not the polymer-like which occur at low bias voltages

## 76 Formation of Carbides

The adhesion of the films in general was better on silicon and glass, than on steel. This was attributed to the formation of silicon carbides at the interfacial layer. The adhesion was very bad on the polished steel samples, when hard carbon films were deposited.

Polished steel samples were coated with a tungsten layer of approximately 2  $\mu\text{m}$  thick and coated with carbon. For comparison polished steel samples without a tungsten coating were included with these samples in the deposition system. The result was conclusive. Carbon films of up to one micron could be grown on the tungsten coated steel. These showed excellent adhesion as seen in figure 6.10 and the wear resistant properties of the film went from virtually none, to one which was capable of resisting more than 300 revolutions per micron on the abrasion tester.

Other workers [32] have found similar characteristics coating the substrate with titanium or tungsten helps carbide formation and also produces a thermal expansivity coefficient matching layer.

## 77 Optimum Conditions

The requirements of a particular film determine the deposition conditions. There is a wide range of "carbon" films, having very different properties from very hard diamond-like to soft polymer-like films. Although these soft films were thought to be a nuisance, new applications such as refractive index matching within optical instruments have meant that these films may be of use.

The most desirable film property for this project was the wear resistive aspect of the films. The process is one of a compromise between the various film properties such as a high bias produces hard films but also increases the film's intrinsic stress.

The three main variables are substrate temperature, induced bias and pressure. By adjusting these, other parameter effects such as geometry, or electrode design, can be compensated for. The optimum conditions for a hard carbon film would seem to be an environment as active as possible, that is high bias, high substrate temperature and low pressure. It is the practical factors that limit this such as high stress and low deposition rate.

## CHAPTER 8

### CONCLUSIONS

#### 8.1 Conclusions

Rf plasma deposition is an adaptable and reliable way of producing hard thin carbon films. The process parameters have a complex relationship with each other and their effects on the resultant film properties.

The three most important process parameters are substrate temperature, induced bias and system pressure. In terms of the film's growth environment, these affect the adatom surface mobility, dissociation efficiency of the gas, ion impact energy on the surface and the residence time of atoms or molecules in the reaction zones.

The resultant carbon films varied dramatically depending on the deposition settings. They ranged from soft polymer-like to hard films of a strong amorphous structure, which demonstrated hardness qualities of 3000 Vickers.

The deposition rates and properties of these films were graphically related to the deposition parameters in order for the advantages and disadvantages of each parameter to be examined. It is believed that optimum deposition conditions will depend on the desired film properties.

Experimentation was concentrated on the three most important parameters to effect the film properties. Some other parameters such as electrode area, gas mixture and interfacial layers were also investigated in an effort to achieve hard carbon film growth on steel samples.

The effect of increased bias voltage can be summarised as causing an increase in the gas dissociation leading to increased deposition rate and an increase in the wear resistant properties of these films. The disadvantage of high biased conditions was found to be the increase in the film stress. The film stress was so high in some cases that the forces exceeded the elastic limit of the films and caused them to shatter off the substrate. This intrinsic stress was found to be the limiting aspect in the growth of thin carbon films. Due to this stress, the thickness of the films was limited to less than one micron, so that analysis could be conducted.

Film induced defects and the higher carbon content of the films are the main cause of this intrinsic stress. For a particular film morphology, it has been recognised

that substrate temperature and bias voltage play inverse roles. High temperature deposits may be obtained at low temperatures provided that substrate bias is employed. These high biased produced films were much more wear resistant than low bias films. This was attributed to the purer carbon content of these films as was observed by the IR analysis. These films may be classified as "hard amorphous thin carbon films".

The main consequences of increasing the substrate temperature was the improvement in film adhesion to the substrate and the increased wear resistive properties of the films. Increased temperature deposits caused the deposition rate to fall off below practical deposition levels. The nucleation rate is a function of the substrate temperature and falls off according to equation (7.1). Intrinsic film stress increased with increasing temperature. This result was unexpected, but has been observed in other deposition systems [61] and suggests that a surface chemical reaction is involved in the surface phase of the deposition.

The effect of the deposition pressure on the properties of the films was investigated by varying the gas flow rates to the chamber but keeping the gas ratios constant. The induced bias is a function of gas type and pressure, so in order to keep conditions as reproducible as possible from deposit to deposit while varying only one parameter the rf power to the chamber was increased with increasing gas pressure.

The deposition rate was found to increase with increasing pressure. These films were found to be of very low stress and good coverage. Unfortunately, they were soft, with virtually no wear resistant properties whatsoever. These films were certainly polymer-like in structure. This was confirmed by the IR analysis which showed the increase in C-H bonding present in the films. This film formation was attributed to a "plasma polymerization" [127] process. The increased pressure, caused the "residence time" of the molecules to increase, thus more molecules were available for film growth on the surface. The increased pressure would also cause the dissociation of the hydrocarbon gas to be less efficient so that a higher proportion of the surface molecules have a higher amount of hydrogen atoms bonded to the carbon atoms.

The tests conducted on the relative areas of the top electrode to bottom electrode, indicate clearly the effect of plasma density on film depositions. An optimum ratio was found where net deposition of the film occurred. Basically, with large surface areas, the plasma is dispersed so a lower concentration of dissociated species arrive at the surface. With very small areas, the plasma density is high and the film is being sputtered off the surface as quickly as it is being deposited. For any particular ratio of electrode areas, the film characteristics can be understood in terms of ion flux and surface adatom mobility. A range of thin film properties can be produced by varying

the three primary parameters. But for any particular system an optimum condition will exist.

It was extremely difficult to deposit carbon films upon steel substrates. In an effort to improve this adhesion, samples were coated with a 2  $\mu\text{m}$  thick coating of tungsten, which readily forms tungsten carbide bonds with the deposited film. This proved most successful, achieving adhesion rates as good as those deposited upon glass and silicon. The importance of this interfacial layer is likely to be more beneficial for the practical application of these carbon films on to steel drill bits. These tungsten layers could be used through the coating in a layering process to help reduce the film's intrinsic stress.

## CHAPTER 9

### RECOMMENDATIONS

#### 9.1 Introduction

In any new and innovative technological research field, there are always improvements and modifications to be made both to the deposition system and process. Some of the following recommendations were not possible due to limitations in time or resources available. The recommendations have been divided up into three sections: 1) Deposition System - pieces of equipment that would enhance the system or possible improvements to the existing apparatus; 2) Deposition Process - possible new deposition techniques or ideas on achieving various types of films, and 3) Film Analysis - a brief suggestion as to analytical techniques that would be very useful in determining film properties.

#### 9.2 Deposition System

The present system is lacking two pieces of important equipment. Firstly, the rf generator and tuning mechanism, although capable of producing hard films at current operating pressures, if lower pressures are desired, which may well be when one considers the Thornton diagram in section 4.5.2, it will be unsuitable for these low pressures and will not be able to strike a plasma. Also, the literature would suggest that higher powered plasmas produce hard diamond-like films. This range of different powers is yet to be explored. As important as the power source, a commercial rf tuning mechanism would also be necessary, as this would couple more power into the chamber and reduce the risk of back power spikes destroying the generator.

Secondly, the gas flow control into the chamber. In order to achieve low chamber pressures a very low flow rate is required. This flow must also be reproducible and accurately measurable. To this end, mass flow controllers, calibrated for low flow rates, i.e. less than 50 sccm are necessary for all inlet gas lines. It is also important to mix the gases before entry into the chamber. There are several commercially available steel drum-like apparatus for this use.

One cannot speculate on other additions to the system, such as a mass spectrum analyser, or ion beam gun. These developments are dependent on the area of interest of the project and on the resources available.

### 9.3 Deposition Process

The main obstacles in carbon thin film growth have been clearly identified as intrinsic stress and adhesion of the films to the substrate. Many researchers have tried various techniques to reduce this stress. They include the addition of hydrogen to plasma in large amounts, addition of other gases to selectively etch the surface as the film grows, to produce a hard pure carbon form. The addition of interfacial layers showed very significant improvement to the adhesion of the film. This may require a modification on the system for in situ coating of the samples, with tungsten for example, which would chemically bond the carbon in a carbide form to the surface.

The film may also be grown in a layered structure of composite materials or by changing the deposition parameters so as to create layered structures of stress-free regions. The above may be applied together or in various combinations. As can be seen, the list of possible techniques for deposition films is virtually endless. This would prompt the use of an experimental technique such as the Taguchi Method [130] to help in optimising the growth conditions.

### 9.4 Film Analysis

There are an endless variety of possible tests that could be conducted on the films. In selecting several of these one has to ask which tests will yield the most information. The tests can be divided up into two categories: 1) Characteristically, such as hardness, adhesion, wear resistance, etc., and 2) Structurally and Compositionally.

The thickness of thin films is extremely difficult to measure. The interferometric method used here depends on measuring the line spacings on the resultant photograph. This can be extremely difficult to gauge as often the lines are very close and faint. A better technique would be to use an ellipsometer or a profilometer for this important measurement.

The hardness of thin films is usually done on a microindenter using a Knoop or Vickers diamond indenter. If the indentation is more than a 1/10 of thickness of the film, the measurement is substrate dependent. Knoop indentors do not indent as deeply into the surface so are often used in thin film applications.

A summary of possible thin film characterisation techniques [131] is shown in table 9.1.

## Thin Film Characterisation

### Structure Determination

X-Ray Diffraction

### Morphology

Scanning Electron Microscopy

### Stress

Newton's Rings

Microscope

Bending Beam

### Adhesion

Tape Methods

Scratch Methods

### Hardness

Indentation Tests

### Compositional Analysis

Auger Electron Spectroscopy AES

Auger Depth Profiling ADP

X-Ray Photoelectron Spectroscopy XPS

Electron Probe Microanalysis EPM

Secondary Ion Mass Spectroscopy SIMS

Rutherford Back-Scattering RBS

Table 9 1

## REFERENCES

- [1] M Ishikawa et al, "'Dual-Carbon", a new surface protective film for thin film hard disks', *IEEE Transactions on Magnetics*, Vol Mag-22, No 5, pp 999-1001, Sept 1986
- [2] M Simpson, 'Materials with the diamond touch', *New Scientist*, pp 50-53, March 1988
- [3] H Tsai and D B Bogy, 'Critical review characterization of diamond-like carbon films and their application as overcoats on thin film media for magnetic recording', *J Vac Sci Technol*, Vol A5, No (6), pp 3287-3312, Nov/Dec 1987
- [4] L P Andersson, 'A review of recent work on hard  $\text{sp}^3\text{-C}$  films', *Thin Solid Films*, Vol 86, pp 193-200, 1981
- [5] K Hashimoto et al, 'Physical properties of carbon films produced by plasma CVD', *Proc Int'l Ion Eng Cong - ISIAF'83 & IPAT'83*, pp 1125-1148, 1983
- [6] Chr Weissmantel and C Schurer, 'Mechanical properties of hard carbon films', *Thin Solid Films*, Vol 61, pp L5-L7, 1979
- [7] J J Hauser, 'Electrical, structural and optical properties of amorphous carbon', *J Non-Cryst Solids*, Vol 23, pp 21-41, 1977
- [8] L Holland and S M Ojha, 'Deposition of hard and insulating carbonaceous films on an rf target in a butane plasma', *Thin Solid Films*, Vol 38, pp L17-L19, 1976
- [9] S M Ojha and L Holland, 'Some characteristics of hard carbonaceous films', *Thin Solid Films*, Vol 40, pp L31-L32, 1977
- [10] B V Spitsyn et al, 'Vapor growth of diamond on diamond and other surfaces', *J Cryst Growth*, Vol 52, pp 219-226, 1981
- [11] D S Whitmell and R Williamson, 'The deposition of hard surface layers by hydrocarbon cracking in a glow discharge', *Thin Solid Films*, Vol 35, pp 255-261, 1976
- [12] M Kamo et al, 'Summary abstract synthesis of semiconductive diamond on diamond substrate from gas phase', *J Vac Sci Technol*, Vol A6(3), pp 1818-1819, 1988
- [13] D J Vitkavage et al, 'Plasma enhanced chemical vapor deposition of polycrystalline diamond and diamond films', *J Vac Sci Technol*, Vol A6(3), pp 1812-1815, May/June 1988
- [14] A Doi, N Fujimori and T Yoshuoka, 'Preparation of  $\text{TiC}$ ,  $\text{TiN}$ , and diamond-like carbon by a glow discharge technique', *Science of hard materials*, pp 743-747, Adam Hilger 1986
- [15] S Matsumoto et al, 'Synthesis of diamond films in a rf induction thermal plasma', *Appl Phys Lett*, Vol 51 No 10, pp 737-739, Sept. 1987
- [16] K Suzuki et al, 'Growth of diamond thin films by dc plasma chemical vapor deposition', *Appl Phys Lett*, Vol 50(12), pp 728-729, March 1987

- [17] H Biedermann and L Martinu, 'Carbon and composite carbon-metal films deposited in an rf glow discharge operated in organic gases', *Vacuum*, Vol 35, No 10-11, pp 447-453, 1985
- [18] K Kitahama et al, 'Synthesis of diamond by laser induced chemical vapor deposition', *Appl Phys Lett*, Vol 49 (11), pp 634-635, Sept. 1986
- [19] A Sawabe and T Inuzuka, 'Growth of diamond thin films by electron assisted chemical vapor deposition', *Appl Phys Lett*, Vol 46, No 2, pp 146-147, Jan. 1985
- [20] A Sawabe and T Inuzuka, 'Growth of diamond thin films by electron-assisted chemical vapour deposition and their characterisation', *Thin Solid Films*, Vol 137, pp 89-99, 1986
- [21] E G Spencer et al, 'Ion beam-deposited polycrystalline diamondlike films', *Appl Phys Lett*, Vol 29, No 2, pp 118-119, July 1976
- [22] L Holland and S M Ojha, 'The growth of carbon films, with random atomic structure from ion impact damage in a hydrocarbon plasma', *Thin Solid Films*, Vol 58, pp 107-116, 1979
- [23] Chr Weissmantel, 'Film preparation using plasma or ion activation', *Thin Solid Films*, Vol. 58, pp 101-105, 1979
- [24] M Kitabatake and K Wasa, 'Growth of diamond at room temperature by an ion-beam sputter deposition under hydrogen-ion bombardment', *J Appl Phys*, Vol 58, No 4, pp 1693-1695, Aug 1985
- [25] M Kitabatake and K Wasa, 'Diamond films by ion-assisted deposition at room temperature', *J Vac Sci Technol*, Vol A6(3), pp 1793-1797, May/June 1988
- [26] C Weissmantel, 'Preparation of hard coatings by ion beam methods', *Thin Solid Films*, Vol 63, pp 315-325, 1979
- [27] D Kerwin et al, 'Thin films of diamond-like carbon', *Mat Res Soc Symp Proc*, Vol 47, pp 195-200, 1985
- [28] A Doi et al, 'Plasma deposition of crystalline carbon and 1-carbon film', *Proc Int'l Ion Engineering Congress -ISIAT '83 & IPAT '83*, pp 1137-1142, 1983
- [29] M Kamo et al, 'Diamond synthesis from gas phase in microwave plasma', *J Cryst Growth*, Vol 62, pp 642-644, 1983
- [30] B Chapman, *Glow Discharge Processes*, Wiley, 1980
- [31] T Sugano, *Applications of Plasma Processes to VLSI Technology*, Wiley, 1985
- [32] J Mort and F Jansen, *Plasma Deposited Thin Films*, CRC Press, 1986
- [33] M Faraday, *Phil Trans Roy Soc London*, 128 125, 1838
- [34] V Doane, 'Abrasive wear - the alloy question!' *Wear and Fracture Prevention*, American Soc for Metals 1981
- [35] A Thomas and P Thomas, 'Performance and wear of TiN coated twist drills', *Proc 6th Int'l Conf IPAT '87*, pp 201-206, 1987
- [36] J C Angus, 'Empirical categorization and naming of "diamond-like" carbon films', *Thin Solid Films*, Vol 142, pp 145-151, 1986

- [37] C Weissmantel et al, 'Plasma deposition of  $\text{sp}^2$ -carbon thin films', *Thin Solid Films*, Vol 96, pp 31-36, 1982
- [38] H V Boenig, *Fundamentals of Plasma Chemistry and Technology*, Technomic, 1988
- [39] R Messier et al, 'From diamond like carbon to diamond coatings', *Thin Solid Films*, Vol 153, pp 1-9, 1987
- [40] W Von Bolton, *Z Elektrochem*, Vol 17, pp 971, 1911
- [41] F P Bundy et al, *Nature (London)*, Vol 197, pp 51, 1955
- [42] P Bridgeman, *Sci Americ* Vol 193, pp 42, 1955
- [43] W Eversole, U S Patent 3,030, 188, July 23, 1958
- [44] J C Angus et al, 'Growth of diamond-like film in a reactive plasma', *J Appl Phys* Vol 39 pp 2915-1918, 1968
- [45] B V Derjaguin and D V Fedoseen, *Growth of Diamond and Graphite from the Gas Phase*, Nauka, Moscow, 1977 (in Russian)
- [46] R Mania et al, 'Deposition of thin carbon films in a A C plasma', *Cryst Res Technol* Vol 16, pp 785-800, 1982
- [47] S Matsumota, 'Carbon thin films produced by heated tungsten filament chemical vapour deposition', *J Mater Sci*, Vol 18, pp 1785, 1983
- [48] S Aisenberg and R W Chabot, *J Appl Phys* Vol 42, pp 2953, 1971
- [49] J C Angus, 'Composition and properties of the so called "diamond-like" amorphous carbon films', *Thin Solid Films*, Vol 118, pp, 311-320, 1984
- [50] Z Has et al, 'Electrical properties of thin carbon films obtained by R F methane decomposition on an R F powered negatively self-biased electrode', *Thin Solid Films*, Vol 136, pp 161-166, 1986
- [51] H Ferber and G Wolf, 'Chemical properties of ion bombarded thin carbon surface layers', *Radiation Effects*, Vol 99, pp 89-96, 1986
- [52] B Meyerson and F Smith, 'Electrical and optical properties of hydrogenated amorphous carbon films', *J Non-Cryst Solids*, Vol 35 & 36, pp 435-440, 1980
- [53] N Fujimori et al, 'Characterization of conducting diamond films', *Vacuum*, Vol 36, no 1-3, pp 99-102, 1986
- [54] B Dischler et al, 'Hard carbon coatings with low optical absorption', *Appl Phys Lett*, Vol 42 (8), pp 636-638, April 1983
- [55] K Enke, 'Some new results on the fabrication of and the mechanical, electrical and optical properties of  $\text{sp}^2$ -carbon layers', *Thin Solid Films*, Vol 80, pp 227-234, 1981
- [56] L P Andersson, S Berg et al, 'Properties and coating rates of diamond-like carbon films produced by rf glow discharge of hydrocarbon gases', *Thin Solid Films*, Vol 63, pp 155-160, 1979
- [57] D Nir et al, 'Diamond-like carbon films of low hydrogen content made with a mixture of hydrocarbon and reactive gas', *Thin Solid Films*, Vol 117, pp 125-130,

1984

- [58] Bubenzer et al, 'R F plasma deposited amorphous hydrogenated hard carbon thin films preparation, properties and applications', *J Appl Phys*, Vol 54, pp 4590-4595, 1983
- [59] R F Brunshah (ed), *Deposition Technologies for Films and Coatings*, Noyes, 1982
- [60] J J Thompson, *Wiedemann's Ann d Physik* 32 321, 1889
- [61] K J Klabune, *Thin Films from Free Atoms and Particles*, Academic Press, 1985
- [62] F Cotton and G Wilkinson, *Advanced Inorganic Chemistry*, Wiley, 1972
- [63] F Chen, *Introduction to Plasma Physics*, Plenum Press, 1974
- [64] M Burden and K Cross, 'Radio frequency plasma excitation, *Vacuum*, Vol 29, no 1, pp 13-14, 1975
- [65] L Maissel and R Glang, *Handbook of Thin Film Technology*, McGraw-Hill, 1970
- [66] K Tachibana, 'Diagnostics and modelling of a methane plasma used in the chemical vapour deposition of amorphous carbon films', *J Appl Phys*, Vol 17, pp 1727-1742, 1984
- [67] A R Reinberg, US Patent 3,757, 733, Nov 1973
- [68] A T Bell & J R Hollahan (eds), *Techniques and Applications of Plasma Chemistry*, Wiley, 1974
- [69] J J Wagner and S Veprek, *Plasma Process*, Vol 2, pp 95, 1982
- [70] K Hiroka et al, 'Radio frequency glow discharge plasma of methane reaction mechanisms', *Proc Int'l Ion Eng Cong - ISAT '83 & IPAT '83*, pp 1503-1506, 1983
- [71] D McLachlan, 'The basics of materials', *The Book of Basics*, Materials Research Corporation, 1983
- [72] L Maissel and R Glang, *Handbook of Thin Film Technology*, Part 2, Chapter 8, McGraw-Hill, 1970
- [73] D W Pashley, 'The nucleation, growth, structure and epitaxy of thin surface films', *Adv Phys* Vol 14, pp 327-416, 1965
- [74] L Holland and S Ojha, 'Infra-red transparent and amorphous carbon, grown under ion impact in a butane plasma', *Thin Solid Films*, Vol 48, pp L21-L23, 1978
- [75] S Berg and L P Andersson, 'Diamond-like carbon films produced in a butane plasma', *Thin Solid Films*, Vol 58, pp 117-120, 1979
- [76] L P Andersson and S Berg, 'Initial etching in an rf butane plasma', *Vacuum*, Vol 28, No 10-11, pp 449-452, 1978
- [77] H Norstrom et al, 'Substrate sputtering during plasma deposition of diamond-like carbon films', *Vide Suppl*, Vol 196 pp 11-19 1979
- [78] E Spencer et al, 'Preferential sputtering of graphite by high ion flux densities', *Appl Phys Lett*, Vol 29, pp 118-122, 1976

- [79] J Mori and N Namba, 'Hydrogen content of plasma deposited carbon films', *J Vac Sci Technol*, Vol A1 No 23, pp 655-667, 1983
- [80] O Matsumoto et al, 'Effect of dilution gases in methane on the deposition of diamond-like carbon in a microwave discharge', *Thin Solid Films*, Vol 128, pp 341-351, 1985
- [81] O Matsumoto and T Katagiri, 'Effect of dilution gases in methane on the deposition of diamond-like carbon in a microwave discharge II Effect of hydrogen', *Thin Solid Films*, Vol 146, pp 283-289, 1987
- [82] K Montasser et al, 'Transparent B-C-N-H thin films formed by plasma chemical vapour deposition', *Thin Solid Films*, Vol 117, pp 311-317, 1984
- [83] J C Angus and F Jansen, 'Dense "diamond-like" hydrocarbons as random covalent networks', *J Vac Technol*, Vol A6, No 3 pp 234-239, 1988
- [84] J Phillips, 'Thin carbon films as random covalent networks', *J Non-Cryst Solids*, Vol 34, pp 153-159, 1979
- [85] M F Thorpe, 'Continuous deformations in random networks', *J Non-Cryst Solids*, Vol 57, pp 355-370, 1983
- [86] W L Hsu, 'Chemical erosion of graphite by hydrogen impact A summary of the database relevant to diamond film growth', *J Vac Sci Technol*, Vol A6, No 3, pp 1803-1811, 1988
- [87] J Jansen et al, *J Vac Sci Technol*, Vol A3, pp 605-610, 1985
- [88] G M Jenkins and K Kawamura, *Polymeric Carbons-Carbon Fibre, Glass and Char*, Cambridge Univ Press, 1976
- [89] R Morrison and R Boyd, *Organic Chemistry*, Allyn and Bacon, 1979
- [90] M Shen, *Plasma Chemistry of Polymers*, Marcel Dekker, 1976
- [91] S Praver et al, 'Ion beam conductivity and structural changes in diamond-like carbon coatings', *Appl Phys Lett*, Vol 49, No 18, 1986
- [92] J Gonzalez-Hernandez et al, 'Graphitization of amorphous diamond-like carbon films by ion bombardment', *J Vac Sci Technol*, Vol A6, No 3, pp 1798-1802, 1988
- [93] J A Thornton, 'High rate thick film growth', *Ann Rev Mater Sci*, Vol 7, pp 239-260, 1977
- [94] R Meisner and J Yehoda, 'Geometry of thin film morphology', *J Appl Phys*, Vol 58, No 10, pp 3739-3746, 1985
- [95] D Nir, 'Intrinsic Stress in diamond-like carbon films and its dependence on deposition parameters', *Thin Solid Films*, Vol 146, pp 27-43, 1987
- [96] W H Class, *Basics of Plasmas*, Materials Research Corp, 1983
- [97] M Laugier, 'Stress characterisation of thin films', *Thin Solid Films*, Vol 79, pp 15-19, 1981
- [98] J F Smith, *The Basics of Thin Films*, Materials Research Corp 1983
- [99] J A Thornton, 'Plasma-assisted deposition processes Theory, Mechanisms and

- Applications', *Thin Solid Films*, Vol 107, pp 3–19, 1983
- [100] H Ritchey, 'Turner Topics', Application Notes, *Advanced Energy Industries*, U S A, 1988
- [101] G Bunyard et al, Vacuum and reaction gas monitoring in thin film deposition', *Proc 7th Intern Vac Congr & 3rd Intern Conf Solid Surfaces*, Vienna, pp 185–188, 1977
- [102] *Edwards Vacuum Coating System*, Users Manual, 1982
- [103] W L Johnson, 'Design of plasma deposition reactors', *Solid State Technology*, pp 191–195, April 1983
- [104] C Bowick, *R F Circuit Design*, H W Sams & Co, 1982
- [105] P Bletzinger and M J Flemming, 'Impedance characteristics of an r f parallel plate discharge and the validity of a simple circuit model', *J Appl Phys* Vol 62, No (12), pp 4688–4695, Dec 1987
- [106] W Hayward and D De Maw, *Solid State Design for the Radio Amateur*, American Radio Relay League, 1977
- [107] J F O'Hanlon, *A User's guide to Vacuum Technology*, Wiley, 1980
- [108] P Horowitz and W Hill, *The Art of Electronics*, Cambridge Univ Press, 1980
- [109] J W Coburn and M Chen, 'Optical emission spectroscopy of reactive plasmas A method for correlating emission intensities to reactive particle density', *J Appl Phys* Vol 51, No (6), pp 3134–3136, June 1980
- [110] B E Cherrington, 'The use of electrostatic probes for plasma diagnostics – A review', *Plasma Chemistry and Plasma Processing*, Vol 2, No 2, pp 113–140, 1982
- [111] M Rand, 'Plasma promoted deposition of thin inorganic films', *J Vac Sci Technol*, Vol 16, No 2, pp 420–427, 1979
- [112] *Metals Handbook Vol II, Non-destructive Inspection and Quality Control, 8th Edition*, The American Soc for Metals, 1976
- [113] H E Hintermann et al, 'Adhesion of PVD and CVD Hard Coatings', *Proc Int'l Ion Eng Cong – ISIAT'83 & IPAT '83*, pp 115–117, 1983
- [114] M Ahern, *Private Communication*, 1988
- [115] E Almond et al, 'Mechanical testing of hard materials', *Proc of the Int'l Conf on the Science of Hard Materials*, pp 155–177, British Crown 1986
- [116] D Brown, *Intra-report*, NIHE Dublin 1988
- [117] I V Kragelsky et al, *Friction and Wear Calculation Methods*, Pergammon Press, 1982
- [118] F P Bowden and D Tabor, *The Friction and Lubrication of Solids*, Oxford Univ Press, 1964
- [119] C N Banwell, *Fundamentals of Molecular Spectroscopy*, Chap 3, McGraw-Hill, 1972
- [120] G Socrates, *Infrared Characteristics Group Frequencies* Wiley, 1980
- [121] R Olaison et al, 'Optical absorption edges in hydrogenated 1-carbon films',

*Vide Suppl*, Vol 201, pp 332–335, 1980

[122] H J Pain, *The Physics of Vibrations and Waves*, Wiley, 1983

[123] F J Bueche, *Introduction to Physics for Scientists and Engineers*, pp 675–678, McGraw–Hill, 1981

[124] *Vacuum Analyst Instruction Manual*, V S W Scientific Instruments, 1985

[125] H Yasuda, *Glow Discharge Polymerization in Thin Film Processes*, Academic Press, 1978

[126] M Shen and A T Bell (eds), *Plasma Polymerisation*, ACS Symposium, 1978

[127] H Biederman, 'Deposition of polymer films in low pressure reactive plasmas', *Thin Solid Films*, Vol 86, pp 125–135, 1981

[128] D K Lam et al, in M Shen (ed), *Plasma Chemistry of Polymers*, Dekker, New York, 1976

[129] S Morita, 'Functional Organic thin film by plasma polymerization', *Proc Int'l Eng Cong – ISIAT '83 & IPAT '83*, pp 1423–1434, 1983

[130] P Johnson, *Design of Experiments*, Perry Johnson Inc, 1987

[131] J Smith and D Hinson, 'Thin film characterization', *Solid State Technol*, pp 135–140, 1986

**APPENDIX A.**

Paper Presented to the 6<sup>th</sup> Irish Manufacturing Conference  
August 1989 entitled  
"Plasma Deposition of Hard Carbon Films as Wear Protective Coatings"

Plasma Deposition of Hard Carbon Films  
as Wear Protective Coatings

P W Carey & D C Cameron

School of Electronic Engineering,  
Dublin City University,  
Glasnevin,  
Dublin 9

Abstract

Hard carbon thin films have been investigated intensively in the past decade. They show properties of extreme hardness, chemical inertness and optical transparency and their use has been suggested for wear protective coatings. This paper describes the deposition of such films by PECVD and details the effects of the most important deposition parameters on their mechanical properties.

Films were produced which exhibited extreme hardness of up to 3000 Vickers. Their deposition rate was found to decrease with substrate temperature and increase with induced bias and pressure. The intrinsic stress and wear resistance were found to increase with the induced bias and substrate temperature but decreased as the pressure was increased. The film adhesion was found to improve at higher temperature and bias and also at higher pressure but films in this region were found to be of reduced hardness.

The deposition conditions which must be maintained in any scaling-up of the system to commercial size were identified.

## 1 INTRODUCTION

The wearing and corrosion of machine parts is the main cause of mechanical breakdown. This costs tens of millions of pounds every year in replacements and lost production. Ways to reduce this wear loss include coating the surface with an extremely hard material to improve wear and corrosion resistance. The unusual combination of density, hardness, chemical inertness and electrical insulation make hard carbon films a possible contender for such coatings<sup>1</sup>

There has been a large and continual increase over the past sixteen years in interest in carbon films since the work of Aisenberg and Chabot<sup>2</sup>. Over five thousand articles have been published in the past ten years alone. The produced films are called 1-carbon, diamond-like carbon, a-C H, carbonaceous carbon or plasma polymers carbon, according to their properties or the techniques by which they are produced<sup>3</sup>. These films have been produced by many varied experimental techniques including DC and RF plasma, ion beam, laser induced and microwave plasma.

The method of Plasma Enhanced Chemical Vapour Deposition PECVD is employed in this study. This allows a chemical process to be conducted at relatively low temperatures compared to normal CVD. The process involves dissociating methane gas ( $\text{CH}_4$ ) in a capacitively coupled RF plasma operating at 13.56 MHz.

A description of the experimental apparatus and the effects of the deposition parameters on the process and film characteristics is given. The implications of the important aspects of carbon film deposition with regard to the manufacturing industry are discussed.

## 2 EXPERIMENTAL APPARATUS

The Carbon thin films were deposited by the dissociation of methane in an rf plasma. A schematic diagram of the deposition system is shown in figure 1. The chamber was borosilicate glass pumped by diffusion and rotary pumps. The rf power was supplied by an 13.56 MHz generator with an output of 100 Watts.

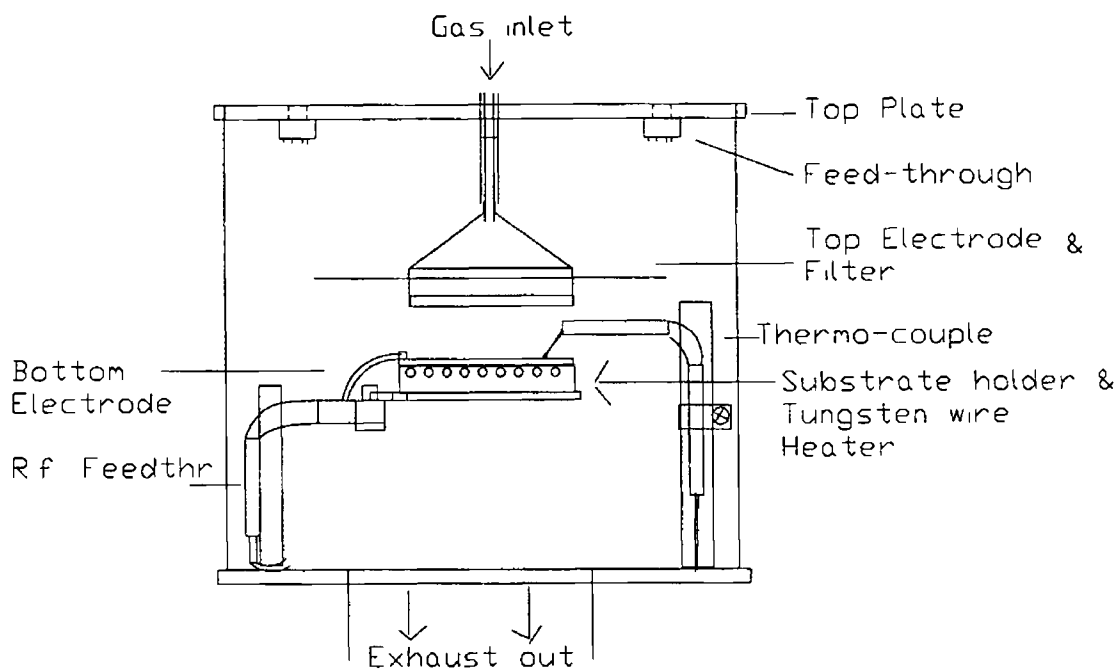


Figure 1 Deposition Chamber

The power was supplied to the bottom electrode and the top electrode was normally earthed but could be floated to any desired potential. The reactant gas was fed in via a "shower head" arrangement which incorporated a sintered glass filter to ensure even gas flow over the substrate. The methane flow was controlled by a Tylan mass flow controller and the other gases were controlled by flowmeters. The substrate temperature was measured by contacting the surface with a moveable thermocouple.

A rf capacitively coupled reactor is advantageous in the manufacturing situation from the viewpoint of both coating distribution and high productivity<sup>4</sup>. The arrangement is intended to compensate for the electric field gradient from the centre of the electrode toward the edge by the gas concentration distribution, and thus to obtain a uniform film. The gas mixture used during deposition was a mixture of methane and hydrogen in the ratio of 5:1. The addition of hydrogen was found necessary to improve the film properties in agreement with other studies<sup>10</sup>. Before loading the steel substrates were polished to a 3 micron finish and ultrasonically cleaned in dichloromethane. Before deposition the substrates underwent an argon bombardment for at least 40 minutes to reduce surface contamination.

## 3 RESULTS

### 3.1 Growth Rate of Films

The growth rate of films is an important process parameter from the manufacturing point of view. It may also affect the structural and compositional properties of the film due to the variations in the ion flux arriving at the substrate surface.

Figure 3.1 shows the effect of substrate temperature on deposition rate. A monotonic decrease with increasing temperature was observed. Above 190°C no film growth whatsoever occurred. This indicates that a surface reaction is taking place whereby volatile species from the gas phase condense on the substrate surface and are then incorporated into the growing film with desorption of by-products. Increase in substrate temperature decreases the residence time of these species on the surface and thus reduces the likelihood of their incorporation into the film.

Figure 3.2 shows the effect of substrate bias voltage on the deposition rate. Bias voltage is related to the rf power supplied to the plasma - increasing rf power increases the substrate bias voltage. Increasing power will increase ionization and therefore increase the active species in the discharge. Increase in bias will also increase the energy of ions arriving at the substrate and thus will probably increase the reaction rate of adsorbed species.

Figure 3.3 shows that the deposition rate increases linearly with gas pressure. A higher gas pressure will provide a higher concentration of reactant materials.

Figure 3.4 shows the effect of top electrode diameter upon deposition rate. At point (A) on the graph the deposition rate is low because of high power density which leads to a large sputtering effect, therefore the net deposition is low. At point (C) there is a low power density hence the gas is not being dissociated effectively in the plasma. This leads to a low deposition rate. At point (B) conditions are optimal and a good net deposition rate is achievable.

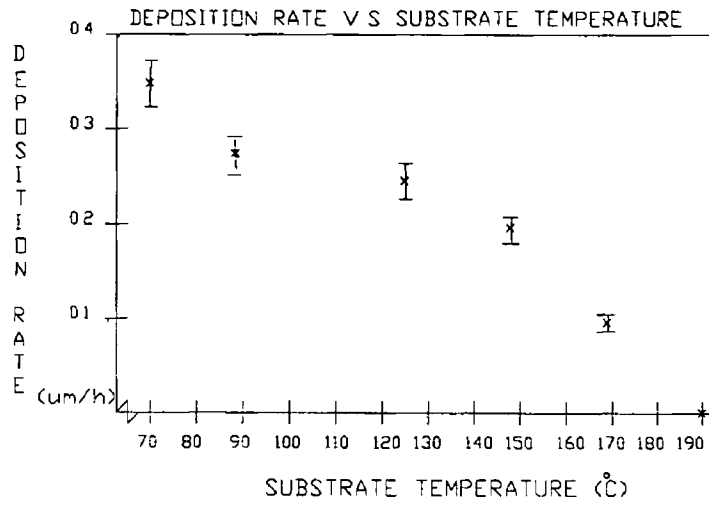


Figure 3 1 Deposition Rate vs Substrate Temperature

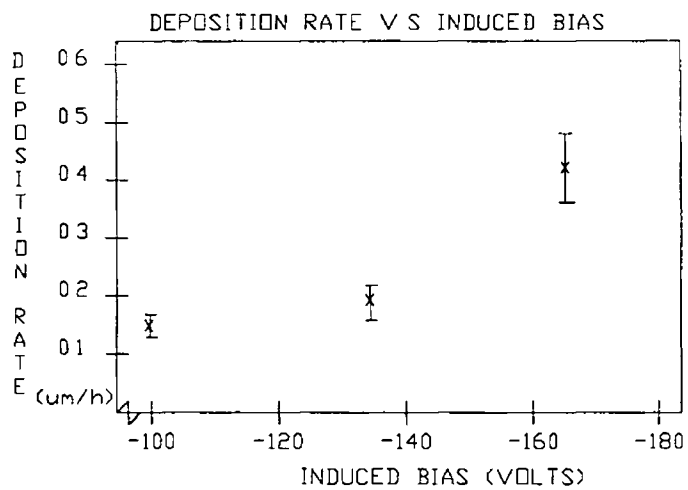


Figure 3 2 Deposition Rate vs Induced Bias

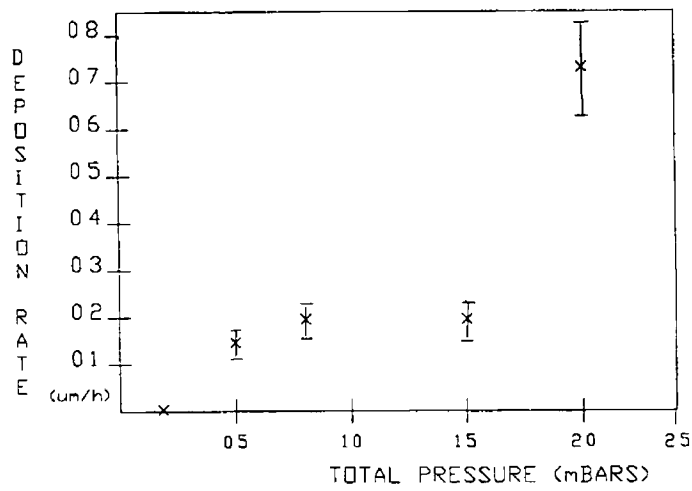


Figure 33 Deposition Rate vs Total Pressure

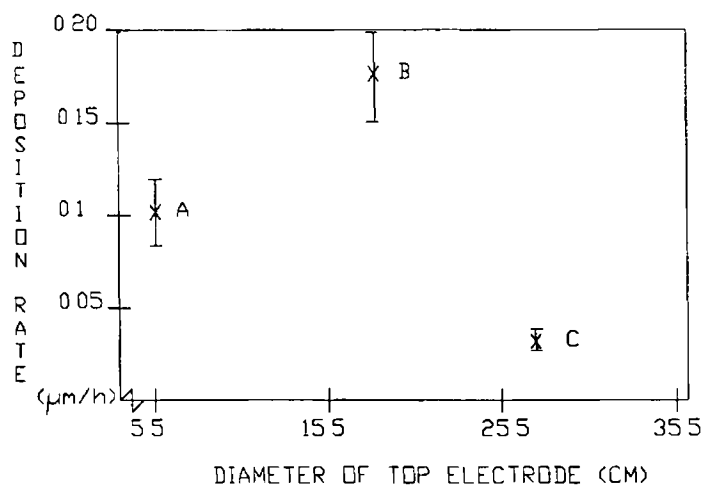


Figure 34 Deposition Rate vs Top Electrode Diameter

### 3.2 Stress of Thin Films

Plasma deposited films are particularly susceptible to intrinsic stress<sup>5</sup>. As will be shown, the stress is dependent on many of the deposition parameters such as the induced bias, substrate temperature, pressure, etc. The film stress is the limiting factor in the growth of films to thicknesses greater than around one micron because the forces can be strong enough to exceed the elastic limit of the film or substrate and can cause the film itself or the substrate to shatter. The stress may be compressive or tensile in nature.

Stress can be caused when the coefficients of thermal expansion of the film and its substrate are not the same. This contribution is known as thermal stress. Even accounting for this, many films have a residual stress known as intrinsic stress. Intrinsic stress is dominant and must be controlled for film applications. Total stress observed  $S$  is given by

$$S = S_{\text{external}} + S_{\text{thermal}} + S_{\text{intrinsic}}$$

When a stressed film is deposited upon a thin substrate, it will cause it to bend. Most measuring techniques use this phenomenon. Others utilise x-ray or electron diffraction, but these techniques give the strain and hence the stress in a crystallite lattice. This is not necessarily the same as that measured by substrate bending since the stress at the grain boundaries may not be the same as that in the crystallites.

The mechanical methods for stress measurement are the Disk and Bending Beam methods<sup>5</sup>. The disk method is preferred because of its ease of use. In this method, the stress of a film is measured by observing the deflection of the centre of a circular substrate when the film is deposited on it.

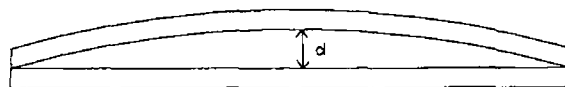


Figure 4 Bending of Cover-slip under deposited film

The approach taken was to use a optical microscope with a travelling stage. The fine focus was used to determine the deflection from the middle of the disk to the edge. The disks were glass cover slips of 19 mm diameter and 0.6 mm thick. From the centre shift  $d$  and the properties of the glass cover slip the stress  $S$  was calculated<sup>6</sup>

$$S = \frac{d}{(D/2)^2} \frac{Y(g) T(g)^2}{3(1-\nu) T(f)}$$

where  $D$  = diameter,  $T(g)$  = thickness of glass,  $Y(g)$  = Young's modulus of glass,  $\nu$  = Poisson ratio,  $T(f)$  = Thickness of film

All the films exhibited compressive stress. The films were limited to thicknesses of below  $1\mu\text{m}$  to avoid film shattering off and so avoid confusing film adhesion and film stress.

Figure 3.5 shows the effect of bias on film stress. Increasing the negative bias causes the stress to increase.

Figure 3.6 shows the decrease in stress with increasing pressure. This is due to the fact that at higher pressures more polymer-like films are produced.

Figure 3.7 illustrates the surprising result that as the substrate temperature is increased the stress of the films also is increased. Higher temperature would be expected to increase the surface mobility of adatoms and facilitate their incorporation into optimum bonding configuration and hence reduce film stress. A possible explanation is that at higher temperatures the film is less polymer-like with fewer graphitic carbon bonds and more tetrahedral bonds which provide less scope for stress relief due to the greater average number of interatomic bonds per atom.

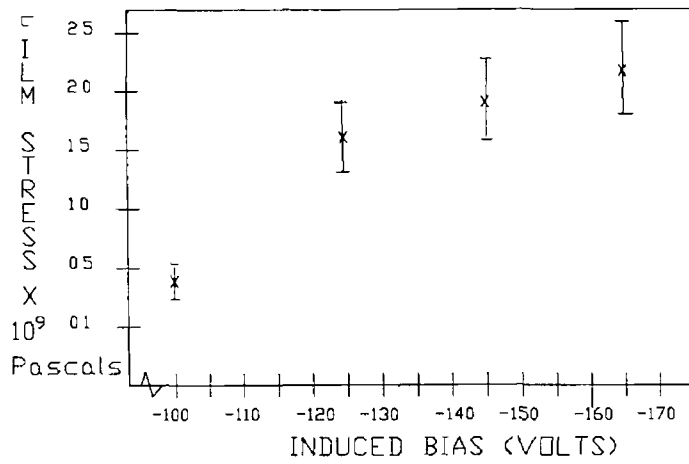


Figure 35 Film Stress vs Induced Bias

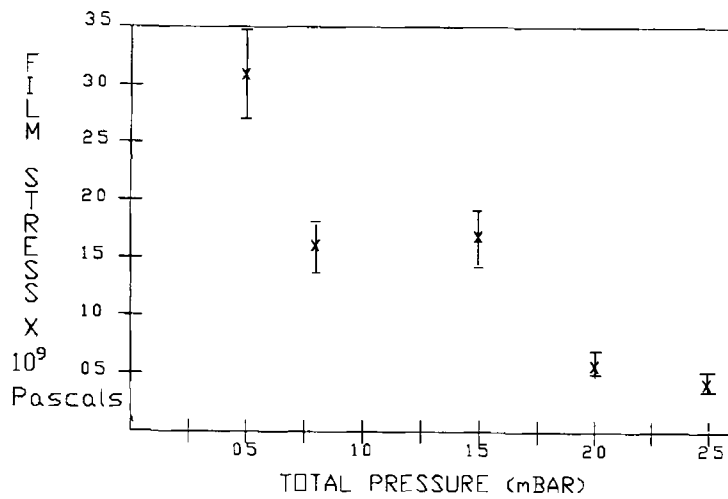


Figure 36 Film Stress vs Total Pressure

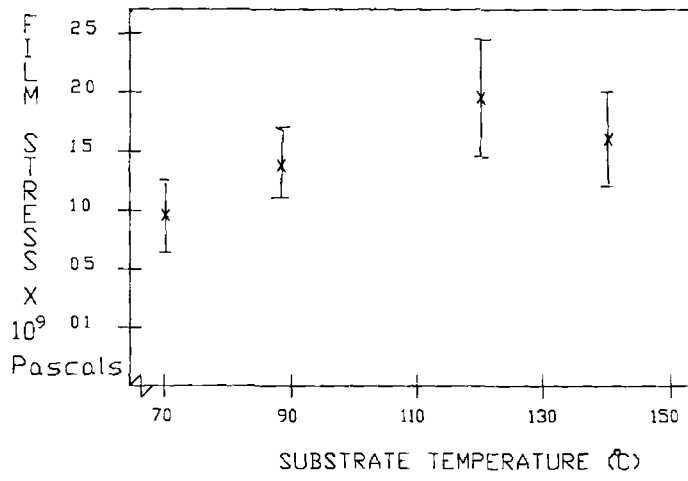


Figure 37 Film Stress vs Substrate Temperature

### 3.3 Adhesion

This is the most important attribute of a deposited film without which all other film characteristics are meaningless. Adhesion is defined as the sum of all the intermolecular interactions between two different juxtaposed materials.

If the adhesion of films is adequate, the main obstacle to their use in mechanical components is overcome. Many parameters affect the adhesion such as temperature of the substrate, induced bias, cleanliness of the substrate, surface finish and pressure.

Tape measurements were used because of ease of use, quickness and availability. In this technique adhesive tape is stuck to the film and pulled off, removing the film partially or wholly. This method is only qualitative and gives no indication of the relative magnitudes of the adhesive forces if the adhesion of the film to the substrate exceeds the adhesion of the tape to the film. A standard masking tape was used. This allowed easy viewing of stripped film as results were stored on acetate sheets. The tape was peeled off at a similar angle and speed by the operator.

A series of experiments were conducted to determine the effect of substrate temperature, pressure, bias and electrode area upon adhesion of the film to the substrate.

The temperature did not have a drastic effect but adhesion increased with substrate temperature. It was necessary to have a minimum substrate temperature for best deposits. The coverage and smooth finish of the film were also improved by heating. Figure 3.8 shows the percentage improvement in adhesion as a function of the substrate temperature.

The adhesion of the film was greatly enhanced by increased negative bias. Low bias (<100V) films peeled off substrates. These films were also soft and resembled a sort of polymer film. There would seem to be an optimum bias for adhesion as at high bias rates the film was powder-like. This may be as a result of high stress. Figure 3.9 shows the percentage improvement in adhesion as a function of the induced bias. The graph is divided into two parts, as above a negative bias of 160 volts the film removed from substrate due to stress factors.

As the pressure is increased the adhesion of the film improves. At very low pressures of less than 0.4 mBar film removed totally from substrate. Figure 3.10 shows the percentage improvement in adhesion as a function of the pressure.

The area of the top electrode could be easily changed. This meant that a series of experiments could be conducted to investigate its effects on film properties. From this it was seen that the film adhesion was best with a smaller top electrode area. This was

probably due to the fall-off in plasma density with large electrode area. This was probably due to the fall-off in plasma density with large electrode area. Figure 3.11 shows the percentage improvement in adhesion as a function of electrode diameter.

In an effort to improve the adhesion of carbon films to steel, polished steel samples were coated with 2  $\mu\text{m}$  of tungsten. As can be seen, in figure 5, the adhesion was dramatically improved. This was attributed to the formation of tungsten carbides<sup>7</sup> at the interfacial layer. This result also suggests a possible reason for the good adhesion of the films on silicon and glass substrates due to the formation of silicon carbides. The dark areas of the photograph are the removed film.



Figure 5 Effect of Coating the steel with tungsten, before deposition of carbon film

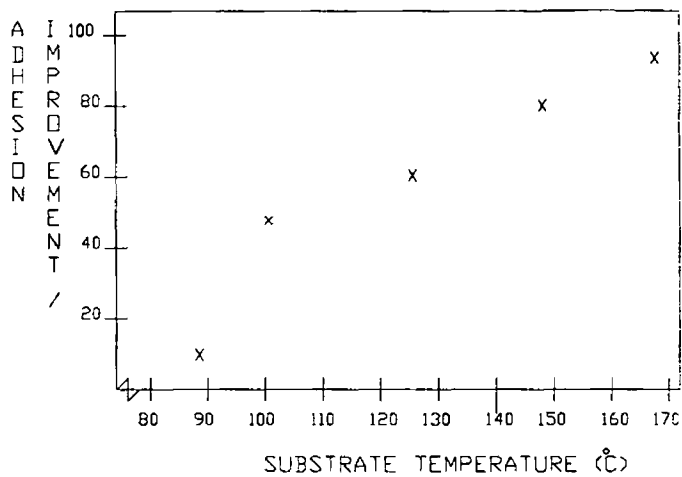


Figure 38 Adhesion Improvement % vs Substrate Temperature

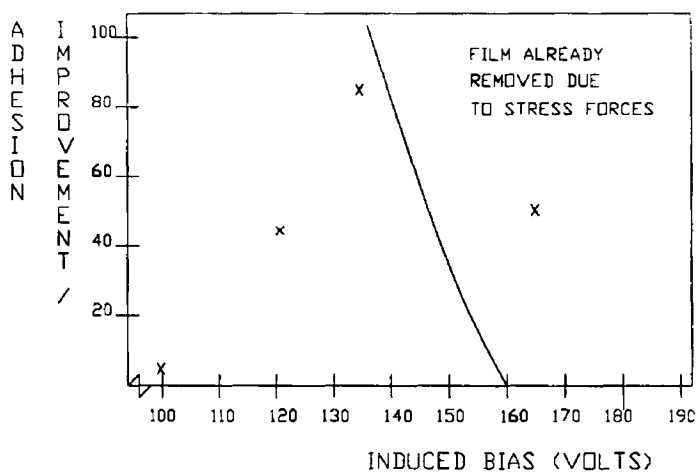


Figure 39 Adhesion Improvement % vs Induced Bias

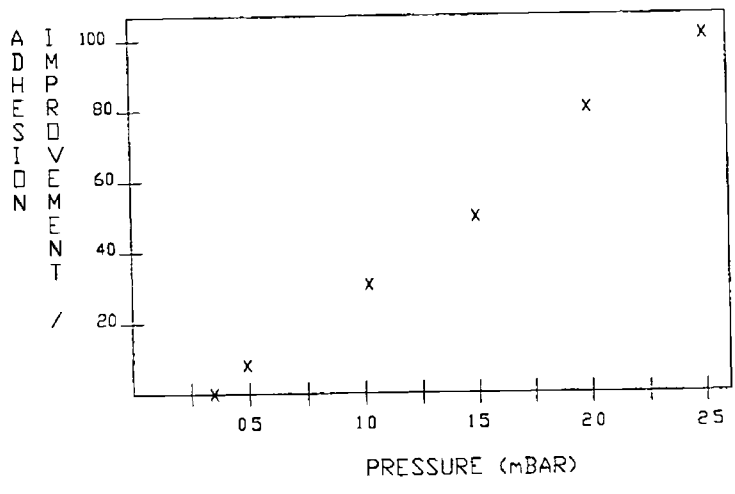


Figure 3 10 Adhesion Improvement % vs Pressure

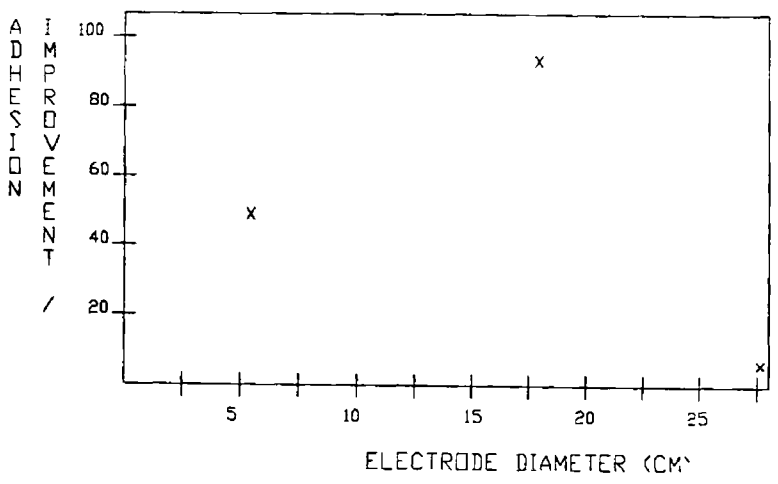


Figure 3 11 Adhesion Improvement % vs Electrode Diameter

### 3.4 Effect of Deposition Parameters on the Mechanical Properties of Thin Carbon Films

Accurate measurement of the hardness of thin films is extremely difficult. Diamond tipped indentors commonly used for such measurements should not indent more than one tenth of the film thickness<sup>5</sup> otherwise the measurement is substrate dependent. Films may also demonstrate elastic properties giving misleadingly high hardness values. Qualitatively, one finds the films difficult to scratch with a steel point.

A Leitz Mini-Load 2 indenter was used to obtain hardness values on films of several micron thickness. These hardness values were approximately 3000 Vickers, uncorrected for film elasticity. Films of this thickness are very highly stressed and disintegrate in a short period. It is difficult to grow hard carbon films greater than one micron thickness for this reason. It was decided to produce films of thickness less than one micron and to test these films for their wear resistant properties.

Available for the wear abrasion test was a rubber wheel abrasion tester built to ASTM 665 specifications. The purpose of this machine is to reproducibly rank different coatings in order of their resistance to abrasion. From these wear measurements in revolutions per micron, approximate hardness values can be extrapolated by knowing wear amounts for materials of known Vickers hardness.

In wear applications the hardness of the wear coatings is naturally of prime interest. For abrasive wear applications the hardness of the coating has to be higher than the hardness of the abrasive particles themselves<sup>6</sup>. The abrasive wear rate decreases very fast with increased coating hardness and even small hardness increases have significant effects.

Today a large range of various coatings can be grown by PVD and CVD processes and some of the most commonly used materials are listed in table 1 below<sup>8</sup> pgs(1-15). Of these carbides and nitrides are the most used ones, but other refractory compounds such as oxides and borides are being increasingly used.

Coating	Thermal Coeff 10 <sup>-6</sup> k <sup>-1</sup>	Hardness Kg mm <sup>-2</sup>	Decomposition Temp °C
TiC	7.4	2900	3067
HfC	6.6	2700	3928
TaC	6.3	2500	3983
WC	4.3	2100	2776
Cr <sub>3</sub> C <sub>2</sub>	10.3	1300	1810
Al <sub>2</sub> O <sub>3</sub>	9.00	2000	2300
TiN	9.35	2000	2949
<b>Substrate</b>			
H S Steel	12-15	800-1000	
Al	23	30	658

Table 1 Some Commonly Used Hard Coatings

The procedure involved mounting the sample in the arm of the machine. The specimen is immersed in a slurry of abrasive particles (Al<sub>2</sub>O<sub>3</sub> particles) and pressed against the rotating wheel at a specified force by means of a lever arm and weight system, as shown in figure 6.

Wear is inversely proportional to the hardness of the abraded material<sup>9</sup>

$$\text{Wear} \propto 1/\text{Hardness}$$

Figure 3.12 shows the wear resistance in revolutions of abrasion wheel per micron (rev/μm) of film plotted as a function of substrate temperature. A linear increase in wear resistance is found with substrate temperature. At the lower temperatures the adhesion of the films is poor. Hence it is difficult in this region to separate wear resistance from adhesion. Low wear rates signify a failure in the adhesive force of the film rather than the cohesive which is obvious at high wear rates.

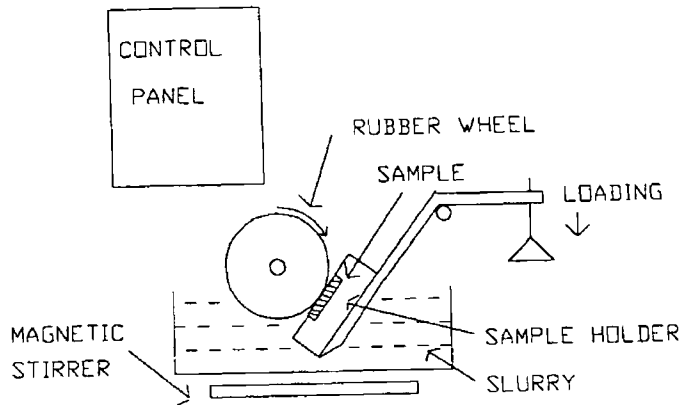


Figure 6 Schematic Drawing of Wear Abrasion Tester

Figure 3 13 shows the wear resistance as a function the induced bias shows a dramatic increase with bias Again it is difficult to separate poor adhesion and wear as it was found from adhesion tests that below -120 volts induced bias, adhesion was very poor and the films were soft and dusty like in appearance

Figure 3 14 shows the wear resistance as a function of total pressure of the deposition system It reveals a sudden increase in film wear rate above 15 mBar The films in this region were found to be polymer-like Bunshah<sup>14</sup> found that films produced at high pressures and low power were polymer-like in structure

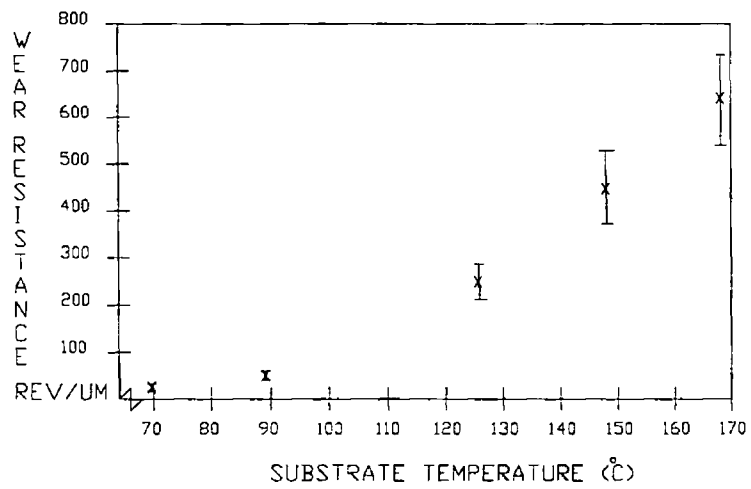


Figure 3 12 Wear Resistance vs Substrate Temperature

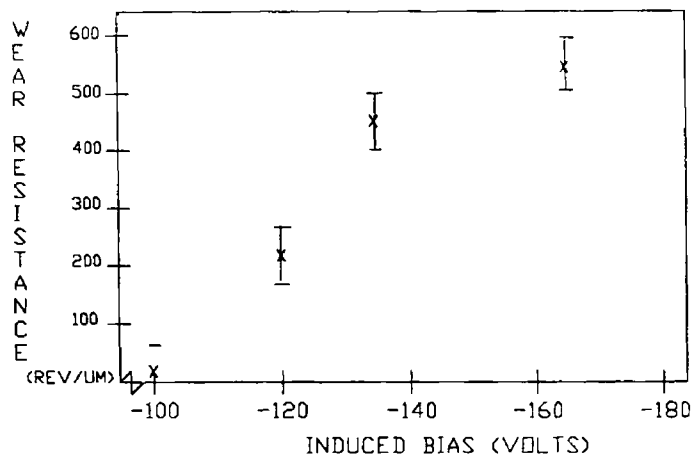


Figure 3 13 Wear Resistance vs Induced Bias

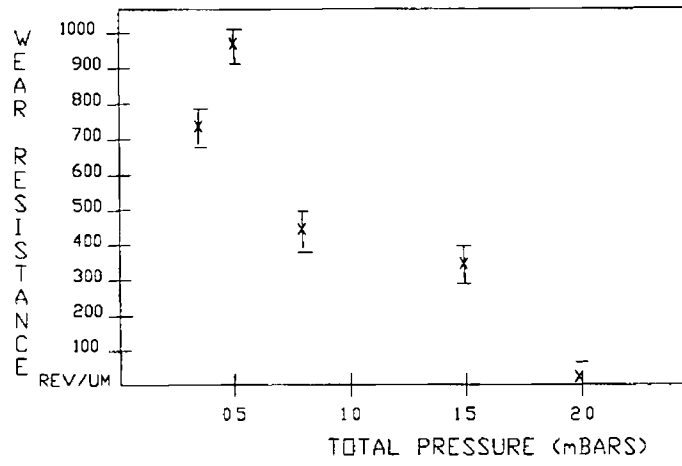


Figure 3 14 Wear Resistance vs Total Pressure

#### 4 DISCUSSION

If carbon films are to be of use to the manufacturing industry, several intrinsic difficulties with their deposition process and characteristics must be over-come. For any large throughput of coated items it is necessary to have a high deposition rate. Clearly by increasing the bias the ion flux is increased which produces a significant increase in the deposition rate. The process and resultant film characteristics are interdependent in a complex way. Optimising the film growth along with the properties is extremely difficult. The properties required for a particular application dictate the process parameter values. For example, although the deposition rate is increased by increasing the bias so also is the intrinsic stress of the film.

A summary of the effects of increasing the three main parameters on film properties is given below

<u>Parameter</u>	<u>Dep./rate</u>	<u>Stress</u>	<u>Adhesion</u>	<u>Wear Resistance</u>
Bias	Increase	Increase	Improved	Increased
Pressure	Increase	Decrease	Improved	Decreased
Substrate Temperature	Decreased	Increased	Improved	Increased

Table 2 Effect of Deposition Parameters on the Film Properties

The intrinsic stress is the main disadvantage of carbon films. This stress must be minimised during the film growth. It is thought to be caused by the high hydrogen content of the films. It has been found that the addition of hydrogen to the plasma actually reduced the hydrogen content of the films<sup>10</sup>. All the above deposits were done at a methane to hydrogen ratio of 5:1. This is not to suggest that this is an optimum ratio, but was one which produced high quality hard films.

## 5 IMPORTANT ASPECTS FOR THE MANUFACTURING PROCESS

### 5.1 Plasmas in Industrial Processes

Plasma Enhanced CVD<sup>11,12</sup> offers the facility of unique processing applications to very many ready established chemical processes. Plasmas offer clean efficient coating or etching of materials. Various low temperature materials can now be processed in a highly active chemical process that hitherto were exclusively high temperature procedures. Rf plasmas offer the facility of coating insulating materials, which can enhance their properties to a standard of material which would be very much more expensive. In a world of ever increasing raw materials costs, new materials or prolongment of the useful lifetime of old will be needed as we enter the 21<sup>st</sup> century.

### 5.2 Usefulness to Manufacturers

Although initial costs and development are expensive plasma processing is cheap and has very high throughput. Raw materials for carbon films are methane, hydrogen gas and electrical power. This high technological area is especially important in the Irish industrial environment, since being small and adaptable to world trends Ireland could act in a specialist service capacity in the world of materials processing.

Plasma deposition methods have found widespread acceptance as a technique for the deposition of thin films with electrically, mechanically and optically desirable characteristics. The process spans from dielectric low temperature coating in the micro-electronics industry to the expanding area of macro-electronic device fabrication. The plasma deposition process enables the sophisticated materials and device engineering which is required by this emerging technology.

From a process point of view, major challenges exist if the requirements posed by different technology applications are to be met. Carbon film deposition onto materials to enhance their wear resistant properties must compete with other established technologies or coatings, e.g. TiN. Definite advantages such as cost or reliability have to be established before hard carbon technology can successfully compete. In all cases, the challenge is to fabricate relatively defect free films with uniform properties over large areas.

### 5.3 Scale-up Issues

In order that plasma deposition can be profitable and economically viable a transformation must be made from the laboratory to the production line<sup>7</sup>. All deposition reactors are expensive, therefore, it is necessary to ensure that the scaled-up version will produce the desired results. It is important to understand to first order how a volumetric enlargement of the reaction space requires other externally controlled parameters to change. Obviously substrate temperature will be similar if the kind of reactive species and their condensation rate are the same as for the small scale process. The primary question is therefore, how the gas flow rates, the pressure and electrical power have to be changed to assure that the scale-up does not affect the plasma chemistry significantly.

The deposition can be viewed as two separate stages. Firstly, the formation of condensable species and secondly the mass transport, by convective diffusion, of these radicals to the surface of the growing film. For the former process it has been theoretically proven that the rate coefficients for the reactions caused by electrons in a gas pressure  $P$ , subjected to electrical excitation by a source of effective electric field strength  $E$ , depend only on the value  $E/P$ <sup>13</sup>. To first order, molecular dissociation rates by electron impact are therefore a function of this ratio.

The molecular transport is also, through diffusion coefficient  $D$ , a function of the pressure, since  $DP$  is a constant for any gas. Therefore pressure and effective field strength should be similar for small and large scale reactors. The only parameter left to vary is the gas flow rate which can be scaled by imposing the requirement that the average gas flow velocity be the same in a small and a large reactor. Alternatively it can be required that the average gas residency time be the same for both reactors. When the interelectrode distance of the large and small reactor are the same, the requirements of the same gas velocity and gas residency time are equivalent.

In any case, the problem of scaled-up parameter optimisation is reduced to the adjustment, by linear extrapolation, of the electrical power and the flow rate. However, it would be a mistake to think life is so simple since other factors would be changed in reactor geometry, e.g. wall temperature effects, and practical design considerations such as easy cleaning and automation will affect the plasma environment.

Finally the efficiency of the reactor is crucial for it to be a viable commercial operation. High material efficiency is usually associated with low deposition rates. This is especially important for the case where a large throughput of devices is necessary or thick films ( $>10\mu\text{m}$ ) are needed.

## 6 CONCLUSION

Hard carbon films were obtained which showed varying characteristics depending on the deposition parameters. The three most critical parameters from a deposition viewpoint were identified as being substrate temperature, pressure and induced bias, and the effect of these parameters on the mechanical properties of the resultant films was shown. The limiting factor was identified as film stress and the effect of this stress on other characteristics was discussed.

From a manufacturer's viewpoint carbon films are a possible area of material processing waiting to be explored with new products. The scaling-up of the process is possible provided the required film properties are clearly defined in the initial stages of the design.

## 7 REFERENCES

- (1) "A Review of Recent Work on Hard  $sp^3$ -C Films"  
L P Andersson, Thin Solid Films, 86 (1981) pg 93
- (2) S Aisenberg and R Chabot, J Vac Sci Tech, 10 (1973) 104
- (3) "Empirical Categorisation and naming of "Diamond-like" Carbon Films" John C Angus Thin Solid Films 142 (1986) pg 145
- (4) "Applications of plasma processes to VLSI technology"  
T Sugano, John Wiley and Sons Inc NY 1985
- (5) "Handbook of Thin Solid Films" Maissel & Glang  
McGraw Hill USA 1970
- (6) "Intrinsic stress in diamond-like carbon films and its dependence on deposition parameters"  
Dan Nir Thin Solid Films 146 (1987) 27
- (7) "Plasma Deposited Thin Films", Mort & Jansen  
CRC Press Inc Florida 1986
- (8) "Proceedings of Continuing Education Institute Vapour Deposited Wear Resistant Coatings"  
Oct 6-9,1986 Frankfurt W Germany
- (9) "Friction & Wear Calculation Methods"  
Kragelsky & Dobyshin Pergamon Press 1986
- (10) O Matsumoto and T Katagiri, Thin Solid Films, 146 (1987) 283
- (11) "Glow discharge processes, sputtering and plasma etching", Brian Chapman  
John Wiley and Sons Inc NY 1980

- (12) "Fundamentals of Plasma Chemistry and Technology"  
Herman V Boenig Technomic Publishing Co Inc PA 1988
- (13) W L Johnson, Solid State Tech 3 (1983) 191
- (14) "Deposition Technologies for Thin Films and Coatings"  
R F Bunshah et al Noyes Publication NJ 1982